Technische Universität Braunschweig

HELMHOLTZ ZENTRUM FÜR INFEKTIONSFORSCHUNG

Elucidating the impact of c-di-AMP-induced IL-17 in the generation of antigen-specific immunity

Von der Fakultät für Lebenswissenschaften

der Technischen Universität Carolo-Wilhelmina zu Braunschweig

zur Erlangung des Grades

einer Doktorin der Naturwissenschaften

(Dr. rer. nat.)

genehmigte

D i s s e r t a t i o n

von Shiwani Agarwal
aus Raxaul, Indien

1. Referentin: Professorin Dr. Petra Dersch
2. Referent: Professor Dr. Stefan Dübel

Eingereicht am: 16.08.2017

Mündliche Prüfung (Disputation) am: 9.11.2017

Druckjahr 2017

Acknowledgments

The project was carried out in the period from 15th of May 2013 to 14th of December 2016. The work was performed at the Department of Vaccinology and Applied Microbiology at the Helmholtz Centre for Infection Research in Braunschweg, Germany. The accomplishment of this thesis would not have been possible without the help and support of many people who directly or indirectly supported this fruitful project. First of all I would like to express my sincere gratitude to my supervisors, Prof. Dr. Carlos A. Guzmán and Dr. Peggy Riese. Dear Carlos and Peggy, I am grateful for your continuous support, constructive discussions, challenging environment, motivation, and fruitful advice, as well as your patience that allowed me to develop as an independent scientist, yet a beginner. Thank you for giving me the opportunity to work with you and for supporting me in every aspect that concerned this thesis. I feel extremely lucky and honored to have been guided by such brilliant scientists. Besides my supervisors, I would also like to thank my thesis committee members, Prof. Dr. Dunja Bruder and Dr. Till Strowig for the invested time, efforts and valuable scientific input supporting the development of the project presented here. I would also like thank Prof. Dr. Petra Dersch, Prof. Dr. Stefan Dübel and Prof. Dr. Dieter Jahn for acting as the referees for my thesis. I would like to express my gratitude to Prof. Dr. ImmoPrinz and Prof. Dr. Andrea Bleich for the collaboration by providing some of the animal models used in this thesis. I would like to say a big thank you to my working group - VAC. Dr. Thomas Ebensen and Dr. Kai Schulze thanks a lot for your advice and the help with animal experiments. Thank you Sebastian Weissmann and Stephanie Trittel for teaching me all that I know about flow cytometry. I would also like to thank Dr. Christine Rückert and Dr. Dario Lirussi for interesting scientific discussions. I would like to thank my fellow labmates - Ivana Skrnjug, Neha Vashist and Simon Delandre for the stimulating scientific and non-scientific discussions, sleepless nights working together before deadlines and for all the fun we have had in the last four years. Elena Reinhard, Hanna Shkarlet, Matthias Neumeyer and Ulrike Bröder thank you for the valuable support in the lab. Cornelia Senske and Dr. Blair Prochnow thank you very much for being so helpful and collaborative. The team spirit that I experienced with you all was a driving force for my work.Last but not the least; I would like to express my infinite gratefulness to my family and the closest friends: Nanno, Kevin, Hanna, Simu, Aarti, Bahar, Marina, Priya, Niharika, Urmi and Bishnu for your unrestricted love, support and your constant reassurance. Kevin - thank you for being my family away from home, for your support and for giving me the strength to carry on.

To my parents

Table of Contents

Acknowledgments i
Table of Contents iv
Table of figures viii
Table of tables xi
Abbreviations xii
1. Abstract 1
2. Introduction 5
2.1. The immune system 5
2.1.1. The innate immune system 6
2.1.2. The adaptive immune system 7
2.1.2.1. T cell-mediated immunity 7
2.1.2.2. B cell-mediated immunity 9
2.2. Viral infections 12
2.2.1. Influenza A virus 12
2.3. Mucosal Vaccination 15
2.3.1. Basic principles of the mucosal immune response 15
2.3.2. Mucosal vaccines 16
2.3.3. Challenges of mucosal vaccines 17
2.3.4. Adjuvants 18
2.3.4.1. Mucosal adjuvants 19
2.4. IL-17 ‘a proinflammatory cytokine’ 22
3. Aim of the thesis 27
4. Materials and methods 29
4.1. Materials 29
4.1.1. Technical equipment 29
4.1.2. Chemical and reagent 30

4.1.3. Antibodies for flow cytometry 33
4.1.4. Antibodies for Enzyme-linked immunospot Assay (ELISPOT) 35
4.1.5. Antibodies for Enzyme-linked immunosorbent Assay (ELISA) 36
4.1.6. Solutions and buffers 36
4.1.7. Antigen and adjuvants 38
4.1.8. Cell line used in experiments 38
4.1.9. Cell Culture Media 38
4.1.10. Influenza virus 39
4.1.11. Mice 39
4.1.12. Primers for genotyping IL-17a/f$^{-/-}$ mice 39
4.1.13. Primers for assessing gene expression 40
4.1.14. PCR cycle 40
4.1.15. Kits used for cytokine and antibody detection 40
4.2. Methods 42
4.2.1. IL-17a/f$^{-/-}$ genotyping by PCR 42
4.2.2. c-di-AMP induced Th17 differentiation 43
4.2.2.1. Generation of BMDCs 43
4.2.2.2. *In vitro* assessment of Th17 differentiation 43
4.2.3. c-di-AMP induced plasma B cell differentiation 45
4.2.3.1. *In vitro* activation of B cell upon treated with c-di-AMP 45
4.2.3.2. *In vitro* assessment of plasma B cell differentiation 45
4.2.4. Mouse immunization experiments 46
4.2.5. Sample collection 47
4.2.6. Preparation of single cell suspension 47
4.2.6.1. Spleen 47
4.2.6.2. Cervical Lymph Nodes 47
4.2.6.3. Lung 48
4.2.7. Cell counting 48

4.2.8. Detection of cytokine production in spleen cells from immunized mice by ELISPOT 49
4.2.9. Re-stimulation of cells for multifunctional T and B cell analysis 49
4.2.10. Preparation of samples for flow cytometry analysis 50
4.2.11. Cell proliferation for cytokine assay 51
4.2.12. Cytometric bead array (CBA) 52
4.2.13. In vivo Cytotoxic T Lymphocyte (CTL) assay 52
4.2.14. ELISA measurement of antigen-specific IgG, IgG1 and IgG2c titers 53
4.2.15. ELISA measurement of total IgA and antigen-specific IgA 54
4.2.16. Microbial 16S analyses 54
4.2.17. Immunofluorescence staining 55
4.2.18. Gene expression assessment by RT PCR 55
4.2.18.1. RNA extraction by TRIZOL 55
4.2.18.2. cDNA generation and gene expression assessment by qPCR 56
4.2.19. Propagation and titration of influenza virus 56
4.2.19.1. Virus propagation in embryonated hen's eggs 56
4.2.20. Hemagglutination assay 57
4.2.21. Microneutralization (MN) assay 57
4.2.22. Challenge of immunized mice 58
4.2.23. Statistical analysis 58
5. Results 59
5.1. Distribution of immune cells in WT and IL-17a/f deficient mice 59
5.2. Comparison of two different adjuvants for their potential to induce IL-17 secreting cells 60
5.3. Mechanism of c-di-AMP-induced Th17 differentiation 63
5.3.1. BMDCs derived from IL-17a/f$^{-/-}$ mice display reduced maturation upon treatment with c-di-AMP 63
5.3.2. BMDCs derived from IL-17a/f$^{-/-}$ mice are defective in driving Th17 differentiation upon c-di-AMP stimulation 64

5.3.3. Identification of secreted mediators contributing to c-di-AMP-induced Th17 differentiation 65

5.3.4. IL-6 is required for c-di-AMP-induced Th17 differentiation 69

5.4. Impact of c-di-AMP-induced IL-17 secretion on the elicitation of antigen-specific adaptive immune response 71

5.4.1. c-di-AMP-induced IL-17 secretion enhances OVA-specific Th2 and humoral responses 72

5.4.1.1. The contribution of c-di-AMP-induced IL-5 secretion to the induction of humoral immune responses 77

5.4.1.2. T_{FH} cells contributes to the c-di-AMP-induced antibody response by supporting plasma B cell differentiation 79

5.4.2. Influence of the microflora on c-di-AMP-induced IL-17-mediated antigen-specific immune responses 83

5.4.3. Influenza vaccine elicits Th17 dependent local antigen-specific IgA response 90

5.4.4. Mechanisms favoring c-di-AMP-induced mucosal IgA response in an influenza vaccine model 96

5.4.4.1. c-di-AMP-induced IL-17 secretion results in the co-localization of T_{FH} cells and GC B cells in GCs thereby promoting plasma B cell differentiation 96

5.4.4.2. Impact of c-di-AMP-induced mucosal IL-17 secretion on pIgR expression by lung epithelium 100

5.5. Assessment of c-di-AMP-induced protective immune responses in an acute influenza challenge 103

6. Discussion and Outlook 105

7. Summary 115

Reference 118

Table of figures

Figure	Description
Figure 1:	Components of the immune system
Figure 2:	T cell activation by APCs
Figure 3:	CD4 T cell subset differentiation
Figure 4:	Formation of germinal center reaction
Figure 5:	Structure of the Influenza A virus
Figure 6:	A schematic representation of the mucosal immune system indicating inductive and effector tissues for antigen-specific immune response post i.n. administration
Figure 7:	Chemical structures of bacterial cyclic di-nucleotides
Figure 8:	Functions of innate IL-17 secreting cells
Figure 9:	Differentiation of Th17 cells
Figure 10:	PCR temperature cycles for IL-17a/f genotyping
Figure 11:	Scheme of *in vitro* experiments to evaluate the mechanism of c-di-AMP-induced Th17 differentiation
Figure 12:	Scheme of *in vitro* experiments to evaluate the mechanism of c-di-AMP-induced plasma B cell differentiation
Figure 13:	A schematic overview of mouse immunization experiments
Figure 14:	Gating strategy
Figure 15:	Distribution of immune cell populations in WT and IL-17a/f$^{-/-}$ mice
Figure 16:	IL-17 secretion byγδ T cells and NKT cellsupon adjuvant treatment
Figure 17:	c-di-AMP-induced IL-17 secretion by CD4^{+} T cells

Figure 18:	Expression of maturation markers and IL-17RA by BMDCs upon *in vitro* stimulation
Figure 19:	Th17 differentiation upon c-di-AMP stimulation *in vitro*
Figure 20:	Cytokine secretion upon *in vitro* stimulation of BMDCs
Figure 21:	IL-12/IL-23p40 expression by BMDCs upon *in vitro* stimulation
Figure 22:	Impact of IL-6 and IL-23 blocking on c-di-AMP-induced Th17 differentiation
Figure 23:	Experimental design for the evaluation of antigen-specific immune responses: WT and IL-17a/f$^{-/-}$
Figure 24:	Impact of c-di-AMP-induced IL-17 secretion on antigen-specific Th2 responses
Figure 25:	Impact of c-di-AMP-induced IL-17 secretion on antigen-specific Th1 responses
Figure 26:	Impact of c-di-AMP-induced IL-17 secretion on activation of cytotoxic T lymphocytes
Figure 27:	Impact of c-di-AMP-induced IL-17 secretion on antigen-specific IgG secretions
Figure 28:	Contribution of c-di-AMP-induced IL-17 secretion to antigen-specific IgA secretions
Figure 29:	Immunization-induced serum cytokine pattern
Figure 30:	Frequencies of T_{FH} cells, GC B cells and plasma B cells upon immunization of WT and IL-17a/f$^{-/-}$ mice
Figure 31:	B cells activation upon *in vitro* stimulation
Figure 32:	Restoration of plasma B cells differentiation by supplementing IL-17a/f$^{-/-}$ cultures with rIL-17A
Figure 33:	Impact of microbiota on c-di-AMP-induced antigen-specific humoral responses
Figure 34:	Impact of microbiota on c-di-AMP-induced antigen-specific Th2

	responses
Figure 35:	Impact of microbiota on c-di-AMP-induced antigen-specific Th1 and Th17 responses
Figure 36:	Microbial composition in WT and IL-17a/f$^{-/-}$ mice
Figure 37:	Impact of SFB on the outcome of c-di-AMP-induced antigen-specific humoral response
Figure 38:	NIBRG-14-specific neutralizing antibody response
Figure 39:	Mucosal IgA concentrations and sIgA titers upon immunization
Figure 40:	c-di-AMP-induced IL-17 secretion by CD4^{+} T cells
Figure 41:	Impact of c-di-AMP-induced IL-17 secretion on NIBRG-14-specific Th1 responses
Figure 42:	Impact of c-di-AMP-induced IL-17 secretion on NIBRG-14-specific Th1 responses
Figure 43:	Co-localization of T_{FH} cells and GC B cells mediated by c-di-AMP-induced IL-17 secretion
Figure 44:	c-di-AMP-induced plasma B cell differentiation
Figure 45:	Immunization-induced serum cytokine pattern
Figure 46:	Impact of c-di-AMP-induced IL-17 secretion on pIgR expression by lung epithelial cells
Figure 47:	c-di-AMP-induced IFNγ and TNFα secretion in the airways
Figure 48:	Weight development of immunized mice after i.n. H5N1 virus challenge
Figure 49:	Schematic overview illustrating the possible mechanism of c-di-AMP-induced Th17-mediated response in the generation of antigen-specific mucosal IgA response

Table of tables

Table	Description
Table 1:	Adjuvants licensed for use in human vaccines
Table 2:	Technical equipment
Table 3:	Chemicals and reagents
Table 4:	Antibodies used in flow cytometry analysis
Table 5:	Antibodies used in ELISPOT
Table 6:	Antibodies used in ELISA
Table 7:	Solutions and buffers
Table 8:	Antigen and adjuvant
Table 9:	Cell line used in experiments
Table 10:	Cell culture media
Table 11:	Influenza virus strains used for challenge studies
Table 12:	Mice used in the experiments
Table 13:	Primers used in PCR for genotyping (provided by Eurofins)
Table 14:	Primers used in qPCR for gene expression (provided by Eurofins)
Table 15:	PCR cycle used for the SybrGreen program
Table 16:	Kits used for cytokine and antibody detection

Abbreviations

Abbreviation	Full name
ABTS	2,2´-azino-bis (3-ethylbenzthiazoline-6 sulfonic acid) diammonium salt
ACK	Ammonium chloride-potassium
ADCC	Antibody-dependent cell mediated cytotoxicity
AEC	3-amino-9-ethyl-carbazole (AEC substrate kit)
α-GalCer	α-galactosylceramide
APCs	Antigen presenting cells
BAL	Bronchoalveolar lavage fluid
BALT	Bronchus-associated lymphoid tissue
BCR	B cell receptor
BMDCs	Bone marrow-derived dendritic cells
BSA	Bovine serum albumin
CD	Cluster of differentiation
CDs	Cytosolic sensors
c-di-AMP (cAMP)	Bis-(3´, 5´)-cyclic dimeric adenosine monophosphate
c-di-GMP	Bis-(3', 5')-cyclic dimeric guanosine monophosphate
CDNs	Bacterial cyclic di-nucleotides
cGAMP	(3´, 5´)-cyclic (adenosine monophosphate-guanosine monophosphate)
CFA	Complete Freund's adjuvant
cLNs	Cervical lymph nodes
CLR	C-type lectin receptor
CMIS	Common mucosal immune system
Cpm	Counts per minute
CR	Complement receptor

CS	Complement system
CT	Cholera toxin
CTL	Cytotoxic T lymphocyte
CXCL	Chemokine ligand
CXCR	Chemokine receptor
DCs	Dendritic cells
DMSO	Dimethyl sulfoxide
DNA	Deoxyribonucleic acid
DSS	Dextran sodium sulfate
EAE	Experimental autoimmune encephalomyelitis
EDTA	Ethylenediaminetetraacetic acid
e.g.	*Exempli gratia*
ELISA	Enzyme-linked immunosorbent assay
ELISPOT	Enzyme-linked immunospot assay
FACS	Fluorescence activated cell sorting
FasL	Fas Ligand
FCS	Fetal calf serum
FDCs	Follicular dendritic cells
FITC	Fluorescein-isothiocyanate
GALT	Gut-associated lymphoid tissue
GCs	Germinal centers
GC B cells	Germinal center B cells
GM-CSF	Granulocyte-macrophage colony stimulating factor
HA	Hemaglutinin
HEPES	4-(2-hydroxyethyl)-1-piperazineethanesulfonic acid
h.i.	Heat inactivated
HRP	Horseradish peroxidase

iBALT	Inducible bronchus-associated lymphoid tissue
i.e.	*Id est*
IFN	Interferon
Ig	Immunoglobulin
IL	Interleukin
i.n.	Intranasal
IRF3	Interferon regulatory factor 3
ISGs	IFN-stimulated genes
LAIV	Live attenuated influenza vaccine
LPS	Lipopolysaccharide
LT	Heat labile enterotoxin
M cells	Microfold cells
MALT	Mucosa-associated lymphoid tissue
MHC	Major histocompatibility complex
min	Minute
MOG	Myelin oligodendrocyte glycoprotein
MS	Multiple sclerosis
NA	Neuraminidase
NALT	Nose-associated lymphoid tissue
NK	Natural killer
NKT	Natural killer T cells
NLR	NOD-like receptor
NOD	Nucleotide-binding oligomerization domain
n. s.	Non-significant
OVA	Ovalbumin
PAGE	Polyacrylamide gel electrophoresis
PAMP	Pathogen-associated molecular pattern

PBS	Phosphate-buffered saline
PCR	Polymerase chain reaction
pDCs	Plasmacytoid DCs
PE	Phycoerythrin
PerCP	Peridinin-chlorophyll-protein complex
PE-Cy7	Phycoerythrin-cyanin 7
PFA	Paraformaldehyde
pIgR	Polymeric-Immunoglobulin receptor
PMA	Phorbol 12-myrisate 13-acetate
PRR	Pathogen recognition receptor
QIV	Quadrivalent inactivated vaccine
RA	Rheumatoid arthritis
RIG	Retinoic acid-inducible gene
REG	Regenerating proteins
Rgs16	Regulator of G-protein signaling
RLRS	RIG-like receptors
RNA	Ribonucleic acid
rNP	Recombinant nucleoprotein
RORγt	RAR-related orphan receptor gamma
RT	Room temperature
RTPCR	Reverse transcriptase polymeric chain reaction
SC	Secretory component
SFB	Segmented filamentous bacterium
sIgA	Secretory IgA
SEM	Standard error of the mean
STAT	Signal transducer and activator of transcription
STING	Stimulator of interferon genes

TBK	Tank-binding kinase
T_{CM}	Central memory T cell
TCR	T cell receptor
T_{EM}	Effector memory T cell
T_{FH}	Follicular helper T cell
TGF	Transforming growth factor
Th	T helper
Th17	T helper 17
TIR	Toll/interleukin-1 receptor
TIV	Trivalent inactivated vaccine
TLR	Toll-like receptor
TNF	Tumor necrosis factor
TRAIL	TNF-related apoptosis-inducing ligand
T_{reg}	Regulatory T cells
T_{RM}	Tissue-resident memory T cell
UV	Ultraviolet
WT	Wild type

1. Abstract

Respiratory infections represent a major health problem worldwide. Among them infections caused by the influenza virus causes annual epidemics leading to 250,000 to 500,000 deaths worldwide.Vaccination has proven to be an effective tool in controlling and eradicating many infectious diseases including viral infections. However, inadequate protection elicited by current vaccines foster the search for improved or new immune interventions. Implementation of adjuvants represents a key approach to improve immunogenicity and efficacy of mucosal vaccines. One of the striking features of mucosal vaccines is the induction of IL-17 response. The role of IL-17 secreting cells in the fight against mucosa associated bacterial and fungal infections have been emphasized. However, their role in combating viral infections and their significance for mucosal vaccine design remains elusive. Bis-(3',5')-cyclic dimeric adenosine monophosphate (c-di-AMP), a potent IL-17 inducer, was investigated for its potential to induce IL-17-mediated antigen-specific immune responses. *In vitro* blocking experiments illustrated that IL-6 but not IL-23 secreted by c-di-AMP primed bone marrow derived dendritic cells seems to be the crucial mediator for c-di-AMP-induced Th17 differentiation. Furthermore, intranasal immunization with Ovalbumin or NIBRG-14 (inactivated, mouse-adapted H5N1 strain) adjuvanted with c-di-AMP resulted in impaired T helper 2 cell response and IgA concentrations but enhanced Th1 response in mice lacking IL-17. Differences in microbiota composition impacted c-di-AMP-induced IL-17 mediated antigen-specific Th1 and IgG responses, but had no significant influence on IgA responses.This demonstrates the importance of IL-17 responses for the efficient establishment of mucosal immunity. Collectively,the presented data reveals that c-di-AMP-induced IL-17 response contribute to IgA secretion by favoring plasma cell generation in the germinal center (GC) by co-localizing follicular helper T cells and GC B cells and by regulating polymeric-immunoglobulin receptor expression on airway epithelial cells favoring secretory IgA transport into the lumen. In addition, upon challenge, vaccinated mice revealed negligible weight loss, thereby demonstrating that vaccination conferred protection against sublethal influenza challenge. The knowledge emerging from this thesis clearly shows the beneficial influence of c-di-AMP-induced IL-17 responsesin regulating mucosal IgA responses. This paves the road towards the establishment of a rational design for novel intranasal vaccines.

Abstract

Respiratorische Infektionen stellen weltweit ein Gesundheitsproblem dar. Unter ihnen das Influenza Virus, wessen jährlich wiederkehrende Epidemien zu 250.000 bis 500.000 toten weltweit führen. Impfungen haben sich in der Vergangenheit als effektives Mittel in der Kontrolle und Ausrottung von Infektionskrankheiten erwiesen. Dies schließt auch virale Erreger mit ein. Nichtsdestotrotz, der inadäquate Schutz der derzeit verfügbaren Impfungen fördert die Suche nach verbesserten bzw. neuen Immuninterventionen. Die Implementierung von Adjuvantien repräsentiert einen Hauptansatz in der Verbesserung von Immunogenität und Wirksamkeit von Schleimhaut-Impfstoffen. Eine der auffallenden Eigenschaften von Schleimhaut-Impfstoffen ist die Induktion der IL-17 Immunantwort. Die Rolle von IL-17 sekretierenden Zellen im Kampf gegen Schleimhaut assoziierten bakteriellen und fugalen Infektionen wurde hervorgehoben. Ihre Rolle im Kampf gegen virale Infektionen eröffnet jedoch noch Fragen. Bis-(3', 5')-cyclic dimeric adenosine monophosphate (c-di-AMP), ein potentieller IL-17 Induktor, wurde Untersucht um dessen Potenzial in der Induktion einer IL-17 meditierten Antigenspezifischen Immunantwort zu eruieren. *In vitro* Blockierungsexperimente zeigten, das IL-6 jedoch nicht IL-23 sekretiert von c-di-AMP induzierten, Knochenmark abgeleiteten dendritischen Zellen, ein wichtiger Mediator für c-di-AMP induzierte Th17 Differenzierung ist. Zudem resultierte die intranasale Immunisierung mit c-di-AMP adjuvantiertem Ovalbumin oder NIBRG-14 (inaktivierter, Maus adaptierte H5N1 Stamm) in der Beeinträchtigung der T helper 2 Immunantwort und der IgA Konzentrationen. Die Th1 Immunantwort in IL-17 Defizienten Mäusen wurde jedoch erhöht. Unterschiede in der Mikrobiota Zusammensetzung beeinträchtigten c-di-AMP induzierte, IL-17 meditierte, Antigenspezifische Th1 und IgG Immunantworten. Dies hatte jedoch keinen signifikanten Einfluss auf die IgA Immunantwort. Dies demonstriert die Wichtigkeit der IL-17 Immunantwort für die effiziente Etablierung einer Schleimhaut basierten Immunität. Zusammen zeigen die präsentierten Daten, das eine c-di-AMP induzierte IL-17 Antwort die IgA Sekretion beiträgt, indem sie die Generation von Plasma Zellen im germinalen Zentrum (GC) favorisiert. Dies geschieht durch die co-lokalisierung von T_{FH} Zellen und GC B Zellen als wohl durch die Regulierung der polymeric-immunoglobulin Rezeptor Expression auf Epithel Zellen der Lunge welche den sekretorischen Transport von IgA in das Lumen favorisieren. Zudem verloren immunisierte Mäuse nach einer Immunherausforderung kaum an Gewicht. Dies demonstriert den erfolgreichen Impfschutz gegen die sublethale Immunherausforderung mit Influenza. Die Erkenntnisse aus dieser Arbeit zeigen klar den vorteilhaften Einfluss der c-di-AMP

induzierten IL-17 Antwort in der Regulierung der Schleimhaut basierenden IgA Immunntwort. Dies eröffnet den Weg zu dem Design einer neuen intranasalen Impfung.

2. Introduction

2.1. The immune system

The immune system is a host defense system comprised of several structures, cells and mediators, which exert different effector functions that protect the host against disease. The major function of the immune system is to defend the host from dangerous entities, such as infectious pathogens, toxic substances, and transformed cells, as well as to distinguish them from host's healthy self-tissue, thereby preserving the integrity of the body [1]. The detection and elimination of pathogens require the critical interaction between the innate and adaptive immune mechanisms to induce protective immunity. The innate immune system is considered to act in a rapid and unspecific manner, and thereby represents the first line of defense. In contrast, the adaptive immune response takes several days to become activated and results in antigen-specific responses which consist of humoral and cellular components. Another crucial feature of the adaptive immunity is the generation of immune memory, which leads to a more vigorous, rapid and highly specific immune response upon a second encounter with a pathogen [2, 3]. The different innate and adaptive immune mechanisms protect the host from colonization and/or invasion by pathogens, as well as subsequent progression of infections (Figure 1).

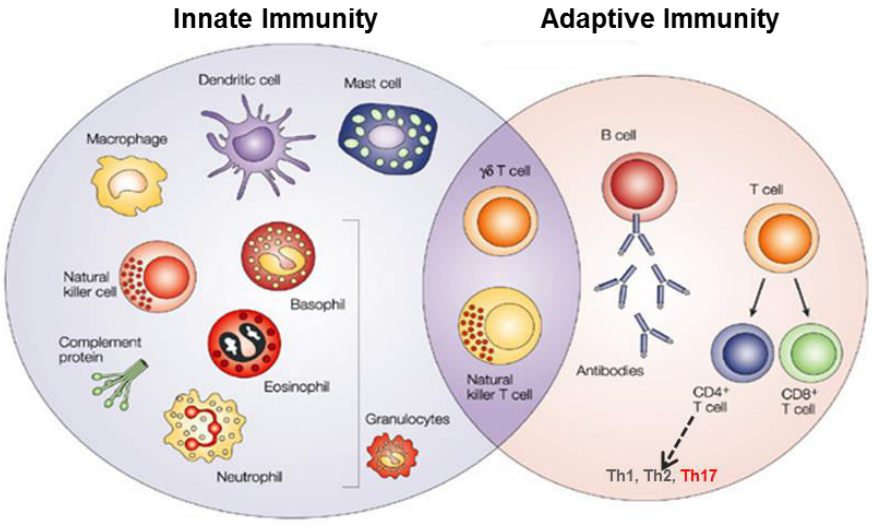

Figure 1: Components of the immune system: The innate and the adaptive immune system comprise specific cell populations which differ in their phenotype and effector functions (adapted from [4]).

2.1.1. The innate immune system

The hallmark of innate immunity is its rapid and unspecific response to pathogens. The innate immune system is an evolutionarily conserved system which is comprised of hematopoietic cells including macrophages, dendritic cells (DCs), mast cells, eosinophils, neutrophils, natural killer (NK) cells, natural killer T (NKT) cells and γδ T cells. Once the pathogen has crossed the physical barrier, different effector mechanisms are activated. Innate immune responses include the secretion of cytokines and chemokines, the induction of antimicrobial peptides, the initiation of cell death and the recruitment of phagocytic cells to the site of infection [4, 5]. Upon sensing of the potentially harmful motifs, a signaling cascade is initiated which leads to the activation of appropriate innate immune cells which results in the clearance of invading pathogens and the stimulation of the adaptive immunity [1].

Most of the innate cells have the ability to take up pathogens via phagocytosis or micropinocytosis [6-8]. Amongst others, macrophages and DCs are antigen-presenting cells (APCs) which are able to capture the encountered antigens, process them and present them either via major histocompatibility complex class II (MHC class II) or MHC I molecules. MHC molecules loaded with pathogen-derived peptides are transported to the cell surface where they present the processed peptide to T lymphocytes thereby inducing a primary immune response. In addition, DCs play a role in the maintenance of B cell function by acting as a delivery vehicle of intact antigens to naive B cells [9, 10].

APCs express pattern recognition receptors (PRR) which are able to recognize highly conserved and specific pathogen-associated molecular patterns (PAMPs) present on pathogens such as viruses, bacteria, parasites and fungi [11, 12]. PRRs are a large group of receptor molecules, including toll like receptors (TLRs), complement receptors, C-type lectin receptors (CLRs), RIG-1-like receptors (RLRS) cytosolic sensors and nucleotide-binding oligomerization domain (NOD) receptors which detect a wide range of non-mammalian structural motifs found in and on pathogens [13, 14]. Upon activation via PAMPs APCs up-regulate the expression of MHC molecules and co-stimulatory molecules like CD80 (B7-1) and CD86 (B7-2). Once activated, APCs further initiate pro-inflammatory responses by the secretion of cytokines and chemokines and migrate to draining lymph nodes to activate antigen-specific T or B cells [13, 15]. The ability of DCs to activate a large variety of different immune cells is the key to bridge innate and adaptive immune responses [16].

2.1.2. The adaptive immune system

The adaptive immune response is characterized by its high specificity and consists of highly specialized cells that participate in the elimination or containment of harmful pathogens, thereby preventing the establishment of infections. The adaptive immune system is composed of T lymphocytes mediating cellular immunity and B lymphocytes mediating humoral immunity. The effector functions of adaptive immune responses are based on the secretion of antibodies, targeting and neutralizing the antigen outside the host cell, cell-mediated killing of the infected cell and the formation of memory cells ensuring long-term protection.

2.1.2.1. T cell-mediated immunity

T cells undergo developmental selection and maturation in the thymus. T lymphocytes consist of two main subsets, T helper lymphocytes (Th) and cytotoxic T lymphocytes (CTL). They are characterized by the surface expression of T cell receptors (TCR) and the variability of the TCR repertoire, which enables the detection of a multiplicity of pathogens, results from the recombination in germline genes during their development [17]. Exposure of antigenic peptides, presented by APCs to naïve T cells residing in secondary lymphoid organs, results in T cells activation. T cell-mediated immunity includes the priming of naïve T cells, the initiation of their effector function and the establishment of long-term persisting memory T cells [18].

Priming of naïve T cells

Naïve T cells are activated by two specific signals provided upon activation of APCs by PAMPs [19]. The first signal is represented by antigen presentation via MHC class I or MHC class II to a corresponding TCR. The second signal is initiated by the interaction of co-stimulatory molecules such as CD80 or CD86 expressed on the surface of activated APCs with their corresponding co-receptor CD28 expressed on the surface of T cells [20] (Figure 2).

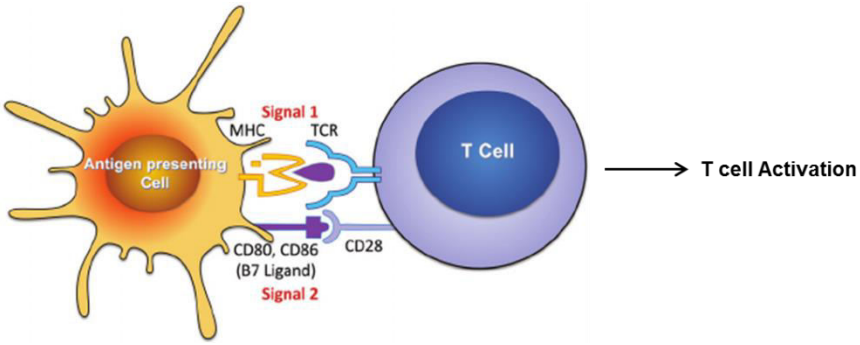

Figure 2: T cell activation by APCs: APCs, such as DCs, efficiently activate T cells via signal 1 (MHC - TCR) and signal 2 (CD80/CD86 – CD28) (adapted from [21]).

The engagement of these signals results in cytokine production including an enhanced IL-2 secretion by T cells leading to T cell proliferation and activation. In addition, the activation of naïve antigen-specific T cells is supported by the surrounding cytokine milieu that promotes the differentiation into different $CD4^+$ effector T cell phenotypes such as Th1, Th2, Th17, regulatory T cells (T_{reg}) and follicular helper T cells (T_{FH}). Presence of IL-12 drives differentiation of naïve T cells into Th1 phenotype and presence of IL-4 differentiates into Th2 phenotype. Naïve T cells differentiate into Th17 cells in presence of IL-6 and TGFβ. T_{reg} differentiation is mediated in presence of TGFβ and IL-10, and IL-6 and IL-21 drives differentiation of naïve T cells into T_{FH} cell phenotype [22] (Figure 3).

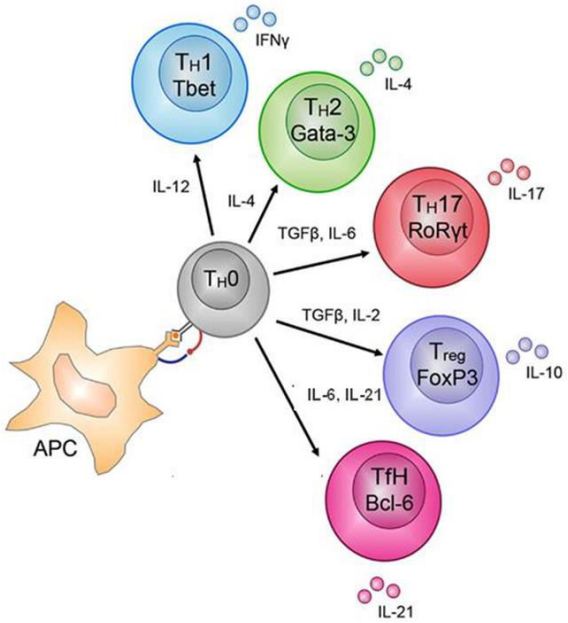

Figure 3: CD4 T cell subset differentiation: $CD4^+$ T cells are able to differentiate into different subsets based on the cytokines secreted during priming of the naïve CD4 cells by APCs (adapted from [23]).

Effector functions of activated T helper cells and CTL

$CD4^+$ T cells, which recognize antigens presented via MHC class II molecules, differentiate into different effector phenotypes. Th1 cells mainly secrete IFNγ, but also IL-2 and TNF-α and thus promote pro-inflammatory cell-mediated immunity. Furthermore, Th1 cells also induce the production of IgG2c antibody secreted by B cells. In contrast, Th2 cells, which primarily secrete IL-4, IL-5, IL-6, IL-10 and IL-13, support non-inflammatory immune responses and provide B cell help thus inducing the production of IgG, IgA, and IgE antibodies [24]. Th17 cells secrete IL-17A, IL-17F and IL-22, and thereby promote pro-inflammatory immune responses [25, 26]. T_{regs} are essential to keep the balance of the immune system and to prevent an excessive immune reaction. They secrete immunesuppressive cytokines such as TGF-β and IL-10 that attenuate immune responses and mediate the maintenance of self thus preventing autoimmune diseases [27]. T_{FH} cells secreting IL-21 are required for the formation of germinal centers (GCs), as well as regulating GC B cell differentiation into plasma B cells and memory B cells [28, 29]. In contrast to $CD4^+$ T cells, $CD8^+$ T cells are activated by antigenic peptides presented via MHC class I and develop into effector CTLs, which mainly secrete IFNγ and the contents of lytic granules, and express death ligands, such as TNF-related apoptosis-inducing ligand (TRAIL) and Fasligand (FasL), thereby promoting the killing of target cells [30-32].

Long-term persistence of memory T cells

Upon encounter with a pathogen a small population of antigen-specific T cells differentiates into memory T cells. $CD4^+$ and $CD8^+$ memory T cells reside in lymphoid organs for a prolonged period of time. Upon a second encounter with a pathogen these memory populations rapidly mediate effector functions, thereby preventing the establishment of an infection [33]. The main memory T cell populations are central memory T cells (T_{CM}), effector memory T cells (T_{EM}) and tissue-resident memory T cell (T_{RM}) [34]. Upon encounter with antigen T_{EM} cells execute effector functions, whereas T_{CM} cells rapidly proliferate, expand and acquire effector functions. On the other hand, T_{RM} cells demonstrate non-migratory phenotype and promote local antigen-independent responses in tissues such as, skin, lungs, gut and vagina.

2.1.2.2. B cell-mediated immunity

B cells are bone marrow-derived lymphocytes that express clonally diverse cell surface immunoglobulin (Ig) receptors that recognize specific antigenic epitopes. The B cell

development involves the combinatorial rearrangement of V, D and J gene segments in the heavy (H) chain locus and the V and J gene segments in the light (L) chain locus thus resulting in the different repertoire of functional VDJ_H and VJ_L rearrangements encoding the B-cell receptor (BCR) [35].

Based on the Fc-part of the heavy chain, antibodies are classified into five different classes namely IgD, IgM, IgA, IgG and IgE [36]. Upon a first antigen encounter with a pathogen, mature naïve B cells expressing either IgD or IgM become activated. The subsequent interaction with Th2 cells via CD40-CD40L engagement and the effect of T cell derived cytokines leads to sequential clonal expansion, isotype-switching, affinity maturation and memory B cell generation. Isotype switching leads to the production of high-affinity IgG, IgA and IgE antibodies [37]. Systemic humoral responses are characterized by IgG and IgE antibodies. Antigen-specific IgG is crucial for the elimination of viral or bacterial pathogens, whereas IgE provides immunity against parasites such as helminths. However, IgE can also mediate allergic response by binding to Fc receptors expressed on mast cells and basophils [38, 39]. In contrast to IgG, which acts on the systemic level, IgA secretion forms the hallmark of mucosal antibody-mediated protection. IgA exists in a dimeric form which is composed of two IgA molecules linked through a short J-chain polypeptide [40, 41]. Dimeric IgA covalently binds to the secretory component (SC) and is transported to the mucosal lumen as secretory IgA (sIgA) mediated by the polymeric-Ig receptor (pIgR) expressed by epithelial cells on the basolateral membrane. Various cytokines such as IL-4, IFNγ, TNFα, IL-6, IL-10 and TGF-β stimulate this process [42]. The sIgA acts as the first line of defense for protecting the mucosa from various pathogenic micro-organisms and it is essential for the maintenance of the mucosal homeostasis. In addition to their essential role in mediating humoral immunity, B cells also contribute to the activation of other immune cells. Thus, they prime CD4 T cells by presenting processed antigens and influence T cell differentiation by producing different cytokines [43].

Germinal center reaction

The induction of T cell-dependent antibody responses including the affinity maturation and generation of memory B cells takes place in GCs which represent transient structures that are formed within the peripheral lymphoid organs - spleen and lymph nodes. The lymph nodes are characterized by follicles mainly comprised of naïve B cells segregated by an inter-follicular region which is surrounded by a T cell-rich zone [44]. GCs form within the center of these follicles, which includes a follicular dendritic cells

(FDCs) network. The GC reaction is initiated by the activation of naïve B cells and pre-T_{FH} cells within the follicle or the T cell zone by exogenous antigen. Subsequently, B cells and pre-T_{FH} cells migrate to the inter-follicular region where they proliferate and interact thus resulting in activated GC B cells (Figure 4). Subsequently, B cells either migrate to the medullary chords termed as extra-follicular B cells where they differentiate into short-lived plasmablasts or they enter the GC pathway resulting in the formation of the early germinal center which consists of B cell blasts surrounded by the mantle zone. The GC rapidly expands due to proliferating B cell blasts and differentiates into dark zones and light zones marking the establishment of mature GCs [45, 46]. The GC B cells subsequently develop into high-affinity long-lived antibody secreting plasma cells as well as memory B cells that migrate and reside in the bone marrow.

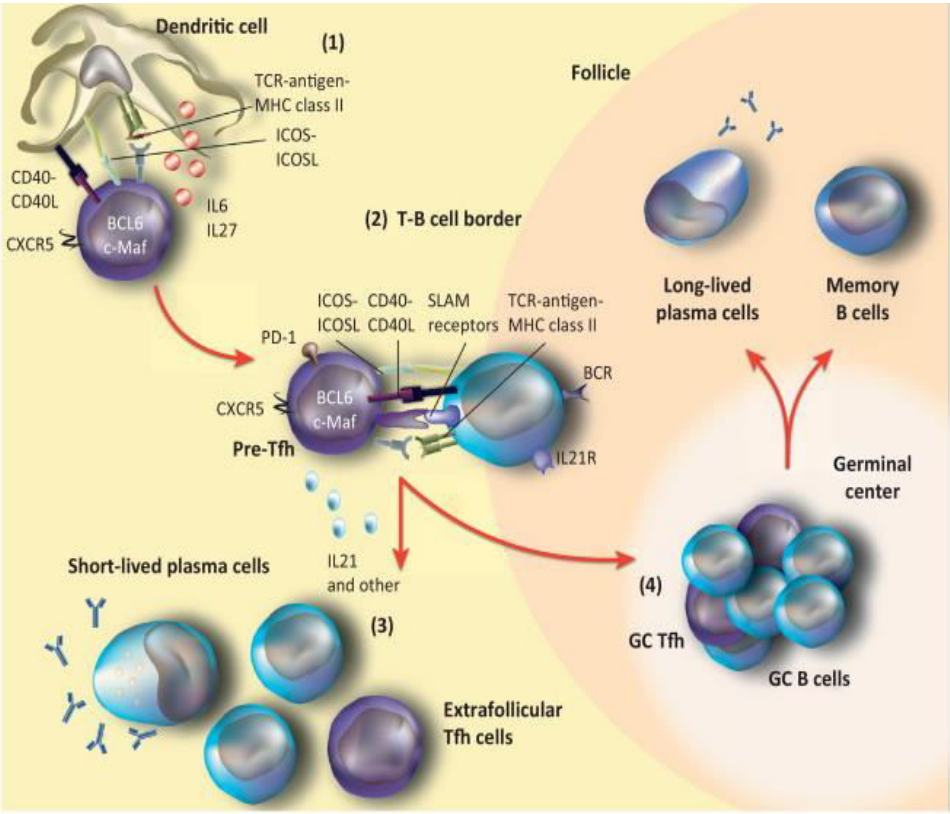

Figure 4: Formation of the germinal center reaction: (1) FDCs present antigen and activate naïve CD4 T cells to differentiate into T_{FH} cells. (2) The migration of pre-T_{FH} cells toward the T–B cell border is facilitated by CXCR5 expression. B cells undergo signals thereby instructing their maturation pathway either to extra-follicular activated B cells or GC B cells. (3) Extra-follicular activated B cells convert to short-lived plasma cells and secrete antibody. (4) In the GC, interactions between GC T_{FH} cell and GC B cells results in GC maintenance and the formation of memory cell and long-lived plasma cells (adapted from [47]).

2.2. Viral infections

Viruses are infectious and obligate intracellular pathogens which depend on the host machinery for replication. The viral genome is either comprised of DNA or RNA. Within an appropriate host cell, the viral genome is replicated and the virions, new infectious virus particles, are the vehicle for transmission of the viral genome to the neighboring cells leading to the beginning of the next infectious cycle. Viral infections have been responsible for quite a few pandemics *e.g.* the 1918 “Spanish flu” pandemic that killed approximately 50 million people worldwide [48] and the ongoing HIV/AIDS pandemic that have killed an estimated 39 million people worldwide [49]. Infectious diseases are still the second leading cause of death worldwide hence preventive measures and an in-depth understanding of the immunological mechanisms essential for pathogen elimination are required to combat infectious diseases.

2.2.1. Influenza A virus

Influenza A virus belongs to the family of *Orthomyxoviruses*. It is roughly spherical in shape and is 80-120 µm in diameter. The viral envelope contains 3 viral transmembrane proteins namely hemagglutinin (HA), neuraminidase (NA) and matrix 2 – ion channel. The central core is surrounded by the M1 protein and contains 7-8 pieces of segmented, single stranded, negative sense viral RNA genome. Influenza A contains 11 genes on 8 pieces of RNA encoding for 11 proteins - HA, NA, M2, M1, NP, NS1, NS2, PA, PB1, PB1-F2 and PB2 [50] (Figure 5). The influenza A virus is classified based on the viral surface proteins HA and NA. Currently, 18 HA and 11 NA serotypes of Influenza A virus have been identified.

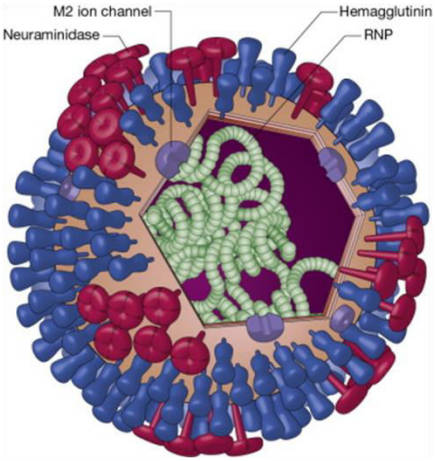

Figure 5: Structure of Influenza A virus (adapted from [51]).

The influenza A virus causes a zoonotic infection and is able to adapt to a wide range of hosts thereby resulting in occasional pandemics causing millions of deaths worldwide. Pandemics and seasonal epidemics are caused due to the emergence of new influenza subtypes caused by “antigen-shift” or “antigen-drift”. Antigen-shift is the process by which two different strains of the virus from two different species combine to form a new subtype. Antigen-drift is the natural mutation occurring over-time of the known influenza strain. In humans, the influenza A virus causes yearly seasonal epidemics resulting in high morbidity (3 to 5 million) and mortality (250,000 to 500,000) worldwide [52]. Generally, the H1, H2 and H3 subtypes are known to commonly infect humans. A new subtype of influenza, H5N1, known as “avian influenza” or “bird flu”, usually does not infect humans but poultry. Rare cases of human infections with the avian virus occurred due toa close contact causing severe pneumonia leading to mortality in 50% of infected individuals [53, 54]. Furthermore, the 2009 outbreak of “swine flu” alarmed the world for a new pandemic threat.

Immune responses initiated upon influenza infection:

The influenza virus enters the host through the oral or nasal cavities and is first countered by the mucus that covers the respiratory epithelium. Upon surpassing the mucus the virus attaches to and invades the respiratory epithelial cells from where it spreads to the immune cells such as DCs and macrophages in the respiratory tract. The viral RNA present within the infected cells is recognized as foreign by various PRRs - TLR3 and TLR7 thus leading to the secretion of type I interferons (IFNs), as well a further proinflammatory cytokines and chemokines. IFNs secreted by macrophages, DCs and plasmacytoid DCs (pDCs) stimulate the expression of IFN-stimulated genes (ISGs) in neighboring cells, which induces an antiviral response. Furthermore, the proinflammatory cytokines cause local and systemic inflammation and initiate the adaptive immune response. Chemokines secreted at the site of infection mediate the recruitment of additional immune cells, including neutrophils, monocytes and NK cells, which contribute to viral clearance and elimination of infected dead cells [55, 56]. However, an excessive production of inflammatory cytokines as well as the infiltration of neutrophilsis a key factor contributing to immunopathology resulting in the acute lung injury observed during influenza infection [57, 58]. In addition to viral clearance by innate cells, the elimination of the virus also requires adaptive immunity mediated by CD4 T cells and CD8 T cells, as well as B cells secreting neutralizing antibodies [59].

Vaccination – a critical tool to prevent influenza infection

Vaccination is the most effective and cost-efficient approaches to prevent influenza infections. Three classes of licensed seasonal vaccines, including inactivated, live attenuated and recombinant HA vaccines, are currently available against influenza infection [60]. The inactivated influenza vaccines (IIV) consist of a split virion or a subunit vaccine that is administered intramuscularly or intradermal, respectively. The trivalent inactivated vaccine (TIV) contains H1N1 and H3N2 subtypes of influenza A along with a dominant influenza B subtype. A recently licensed quadrivalent influenza vaccine (QIV) includes an additional influenza B subtype. The IIVs induces strain-specific systemic IgG antibody response against the viral HA glycoprotein, thus inhibiting virus binding and entry into the host cell. Although these strain-specific antibodies against HA neutralize the virus and prevents infection, HA is under positive selective pressure driving to evolve and thereby circumventing immune recognition. The second classes of the licensed vaccine products are the live attenuated influenza vaccines (LAIV). They contain the similar influenza strains as the QIV but are administered intranasally and thus additionally activate the mucosal components of the immune system, such as IgA antibodies which can neutralize viruses at the portal of entry. In addition, LAIV induce CTL responses efficiently contributing to protection by lysis of infected cells [61]. Despite their great potential to induce protective immunity, the use of LAIV is not always recommended for use in groups at risk for severe infections, such as small children, elderly or patients affected by chronic infections or immunocompromised individuals. The third group of licensed influenza vaccines is represented by the first recombinant HA vaccine (FluBlok), which is currently approved for adults aged between 18 to 49 years who are allergic to eggs [62]. Although the currently licensed influenza vaccines are relatively effective in healthy young individuals, several hurdles such as the need for annual vaccination, the emergence of antigenically novel viruses, the varying degree of immunogenicity and the missing correlates of protection still remain to be addressed [63].

2.3. Mucosal Vaccination

Pathogens such as influenza enter the body through the mucosal membranes. Therefore, vaccines that act already at the entry sites represent an effective tool to control disease development and progression. Mucosal vaccines are demonstrated to improve the prevention of infectious diseases as they are able to trigger cellular and humoral immune protection not only systemically but also at local as well as distal mucosal areas, thereby reducing the risk of disease transmission [64, 65]. Mucosal vaccines have several advantages over parenteral administrations such as being needle-free (*i.e*. painless), an easy way of administration, and a low risk of cross-infection and side-effects, therefore resulting in a high acceptance by the public [66]. In addition, stimulation of an efficient local response can also reduce colonization of pathogens thereby providing protection against both infection and disease. However, to date only a few mucosal vaccines have been approved for humans due to safety concerns derived from the use of some mucosal vaccines in humans and the poor stability and immunogenicity of antigens delivered via mucosal routes [64]. The recent technological advances (*e.g*. the adjuvantation of formulations, use of innovative delivery system) might allow the development of efficacious mucosal vaccines that display an adequate safety profile.

2.3.1. Basic principles of the mucosal immune response

Anatomically, the immune system is divided into functional compartments, of which the two most important are the peripheral lymphoid system and the mucosal lymphoid system. The mucosa-associated lymphoid tissues (MALT) encompassing the nasopharynx-associated lymphoid tissue (NALT), bronchus-associated lymphoid tissue (BALT) and gut-associated lymphoid tissue (GALT) are highly vulnerable to infection and possess a complex array of specific and unspecific mechanisms to combat pathogens [67-69].

The unspecific mucosal defense of the respiratory tract is mediated via physical and chemical barriers. The physical barrier is composed of an epithelium layer which is lined with tiny, hair-like projections called cilia and covered with a layer of mucus which acts as the first line of defense by clearing the pathogen via constant mechanical movement. The integrity of epithelial cells defines the access of APCs to pathogens, which are crucial for initiating a pathogen-specific immune response. Mucosal chemical barriers

are composed of mucins, which are secreted by goblet cells and anti-microbial peptides, such as defensins, which are secreted by epithelial cells [70-72].

The mucosal antigen-specific responses mediated by the local production and secretion of sIgA, which is resistant to degradation in the protease-rich environment at the mucosal surfaces. In humans over 1mg/ml of IgA antibodies are present in the secretions that are associated with the mucosal surfaces [73]. The sIgA has multiple roles in the mucosal defense system as it entraps pathogens in the mucus, thereby preventing the attachment of pathogens to the epithelial layer. It also mediates other functions such as antibody-dependent cell mediated cytotoxicity (ADCC) with leads to the destruction of local infected cells [74].

2.3.2. Mucosal vaccines

The route of vaccination plays an important role in order to evoke immune responses against specific pathogens not only at local but also at distant mucosal sites. Mucosal vaccines against a specific target pathogen delivered either orally or intranasally induce immune response that mimics those observed after natural infections [75]. For example, LAIV administered by the intranasal (i.n.) route was proven effective at protecting against seasonal influenza infections [76]. Additionally due to the compartmentalization within the mucosal immune system oral vaccination usually does not stimulate efficient immue responses in genitourinary tract or respiratory tract, whereas i.n. vaccination evokes immune responses at local (NALT and respiratory tract) as well as distal (vaginal) sites [77].

Following intranasal administration, immune responses are initiated at the inductive site known as NALT. NALT is a key secondary lymphoid structure of the upper respiratory tract which is composed of specialized follicle-associated epithelium which contains microfold (M) cells. M cells act as an accessible trans-membranous transporter and their basolateral surfaces form intraepithelial pockets which are populated with immune cells such as DCs, macrophages, B and T cells. Antigens transcytosed through the M cells are processed and presented by APCs including macrophages, DCs and B cells to naïve lymphocytes. APCs either stimulate lymphocytes locally or migrate to T and B–cell regions in the LN [78-80]. GC formation and antibody class switching occur in the B cell region. This results in the induction of mucosal and systemic immune response characterized by the production of IgA and IgG [81]. Primed immune cells disseminate through the common mucosal immune system (CMIS) that connects inductive mucosal

sites to effector sites, *e.g.* the lung (Figure 6). In parallel, activated T cells and B cells migrate through the body via the bloodstream and contribute to systemic immune response. Mucosal vaccines induce both mucosal and systemic antigen-specific immune responses and thereby provide appropriate defensive responses [82].

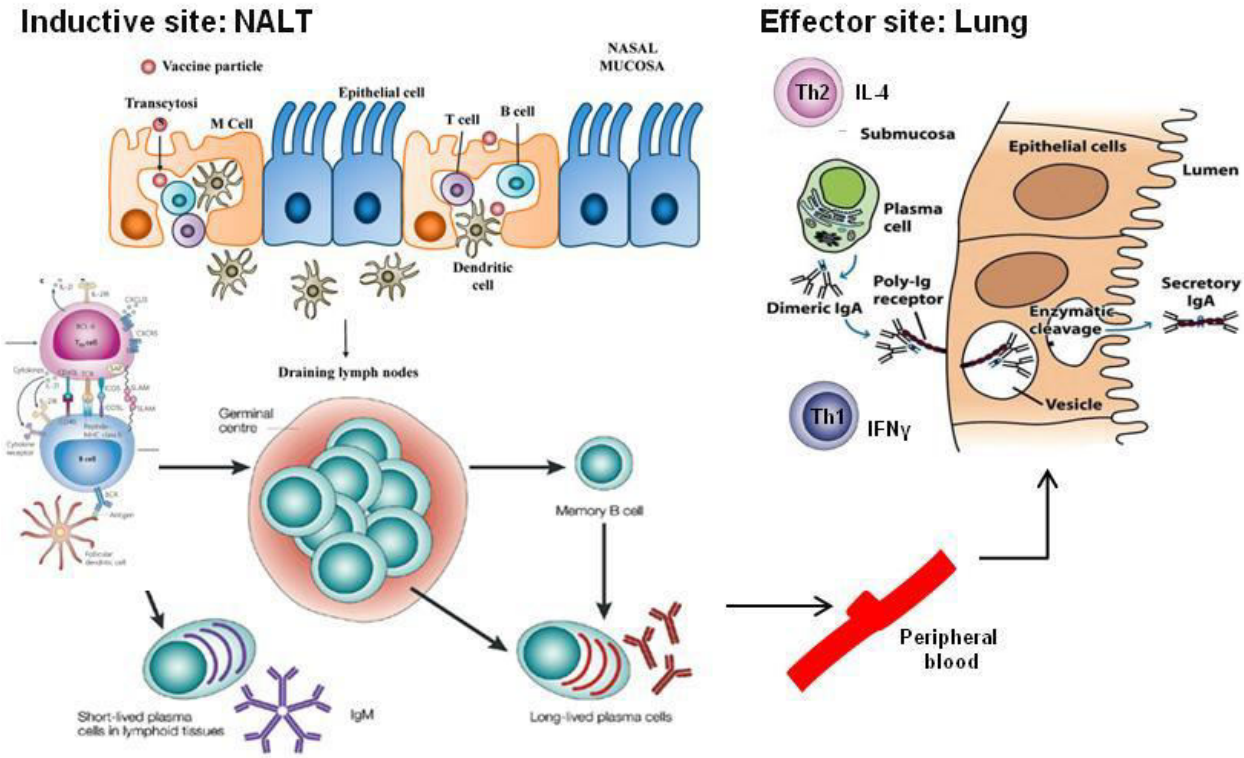

Figure 6: Schematic representation of the mucosal immune system indicating inductive and effector tissues for antigen-specific immune responses post i.n. vaccine administration: I.n. administered antigens are taken up from the lumen of nasal cavities located in the NALT. DCs take up the antigen and present it to Th cells in the draining lymph nodes. Consequent interactions between DCs, CD4 cells and B cells induce GC center reactions resulting in the generation of IgA producing plasma B cells. IgA-committed B cells migrate to the effector site via the peripheral blood and secrete dimeric IgA that binds to pIgR and is transported to apical surfaces where they are cleaved into sIgA (adapted from [83, 84]).

2.3.3. Challenges of mucosal vaccines

Despite the many advantages exhibited by intranasally administered mucosal vaccines compared to parental ones, several obstacles such as a poor permeability of the administered formulation, degradation of the formulations, release and uptake of the vaccine component still needs to be overcome [75, 85]. These obstacles negatively impact vaccine stability, and prevent sufficient antigen delivery and presentation by resident APCs, which in turn hampers the initiation of proper immune response and require higher antigen doses as compared to parental vaccines [86]. The breaching of

the mechanical and physiochemical barriers could be facilitated by the use of delivery systems [87] and the reduced immunogenicity of the antigen and the insufficient induction of systemic humoral and cellular immune responses as compared to parental vaccination strategies might be overcome by adjuvantation [88]. In addition to the above-mentioned challenges, major concerns exist in terms of their safety profile especially in different risk groups, such as immunocompromised individuals, small children, elderly and chronically infected patients (*e.g*. live attenuated vaccines).

2.3.4. Adjuvants

Adjuvants are agents which help to increase the immunogenicity of an antigen. This is facilitated by different mechanisms including the generation of an antigenic reservoir allowing a slow release of antigens. Adjuvants can further improve the delivery of antigens to APCs thereby improving antigen presentation and processing. In addition, adjuvants can be used to tailor the antigen-mediated immune response in a desired direction [89]. An ideal adjuvant should not exhibit antigenic properties by itself but promote well-defined immune responses and improve antigen-specific immunity. The different classes of adjuvants that are used for the implementation in vaccines are either immunostimulators, such as TLR ligands and bacterial toxins, or vehicles such as virosomes, liposomes emulsions and mineral salts [90]. Only a few adjuvants have been approved for the implementation in human vaccines (Table 1). Only one of these adjuvants, CTB, has been approved for mucosal administration.

Table 1: Adjuvants licensed for use in human vaccines (adapted from [91, 92]).

Adjuvant	Class	Components	Diseases
Alum (1924)	Mineral salts	Aluminium phosphate or aluminum hydroxide	Diphtheria toxoid, tetanus
MF59 (Novartis; 1997)	Oil-in-water emulsion	Squalene, polysorbate (Tween 80; ICI Americas), sorbitantrioleate (Span 85; Croda International)	Fluad (seasonal influenza), Focetria (pandemic influenza), Aflunov (pre-pandemic influenza)

ASO_3 (GSK; 2009)	Oil-in-water emulsion	Squalene, Tween 80, α-tocopherol	Pandemrix (pandemic influenza), Prepandrix (pre-pandemic influenza)
Virosomes (Berna Biotech; 2000)	Liposomes	Lipids, hemagglutinin	Inflexal (seasonal influenza), Epaxal (hepatitis A)
ASO_4 (GSK; 2005)	Alum-absorbed TLR4 agonist	Aluminium hydroxide, MPL	Fendrix (Hepatitis B), Cervarix (human papilloma virus)
CTB	Bacterial toxin	Cholera toxin B subunit	Dukoral (Cholera)

2.3.4.1. Mucosal adjuvants

The need of mucosal vaccines fosters the search for adjuvants applicable for mucosal administration. Mucosal vaccines co-formulated with adjuvants represent a beneficial tool to overcome obstacles such as the large dosage due to the instability of antigens at mucosal surfaces, the poor immunogenicity and the insufficient induction of systemic and mucosal immune responses [93]. Adjuvants used in mucosal vaccines have a similar mode of action as compared to the parental vaccines. Commonly used mucosal adjuvants for pre-clinical studies comprise cholera toxin (CT) and its subunits and *Escherichia coli* heat labile enterotoxin (LT). However, safety concerns in terms of toxicity represent one of the major concerns for their application as adjuvant in human mucosal vaccines. In this line, Nasalflu (Berna Biotech AG, Switzerland) adjuvanted with the active LT was linked to several cases of Bell's palsy [94]. TLR agonists (TLR2, 3, 4, 5, 6, 7, 8 and 9) represent another widely studied group of potential mucosal adjuvants. TLR agonists mainly target APCs resulting in the activation of adaptive immune response, thereby inducing a strong cellular and humoral immune response. However, the use of a TLR4 agonist as a mucosal adjuvant has been reported to induce detrimental influenza-specific Th17 responses [95]. Furthermore, none of the TLR agonist promotes both mucosal and cellular responses. Some of them stimulate humoral responses (*e.g.* TLR2, TLR4), whereas others are more efficient in promoting cellular immunity (*e.g*. TLR9). Other potential mucosal adjuvants being used in pre-clinical studies are α-galactosylceramide (α-GalCer) and cyclic dinucleotides (CDNs) [96-98]. Thus, efforts are needed to identify mucosal vaccine formulations with a

negligible risk of side-effects but able to induce efficient immune responses tailored to the location and the threat of the invading pathogen.

Bacterial cyclic di-nucleotides - promising mucosal adjuvants

The family of cyclic di-nucleotides (CDNs), a group of natural compounds, consists of bis-(3', 5') –cyclic dimeric guanosine monophosphate (c-di-GMP), bis-(3', 5') –cyclic dimeric adenosine monophosphate (c-di-AMP) and (3', 5,)-cyclic adenosine monophosphate-guanosine monophosphate (cGAMP). These are well known secondary bacterial messenger, involved in biofilm formation, regulation of bacterial virulence and motility [99, 100]. In this line, c-di-GMP was demonstrated to decrease the pathogenicity of *Listeria monocytogenes*, *Mycobacterium tuberculosis* and *Vibrio cholera* [101-103]. c-di-AMP was shown to alter bacterial cell size and regulate cell envelope stress and biofilm formation favoring antibiotic resistance and bacterial virulence in *Staphylococcus aureus* and *Streptococcus suis* [104, 105]. On the other hand, the cGAMP produced by prokaryotes are 3′3′-cGAMP. A related compound to cGAMP known as 2′3′-cGAMP has been described in eukaryotes [106].

The c-di-GMP and c-di-AMP activate the crucial signaling molecule called STING (stimulator of interferon genes) that has been identified as an innate cytosolic DNA sensor and in turns leads to the activation of the TBK3-IRF3 signaling pathway resulting in the production of both type I IFNs and TNFα [107-110].

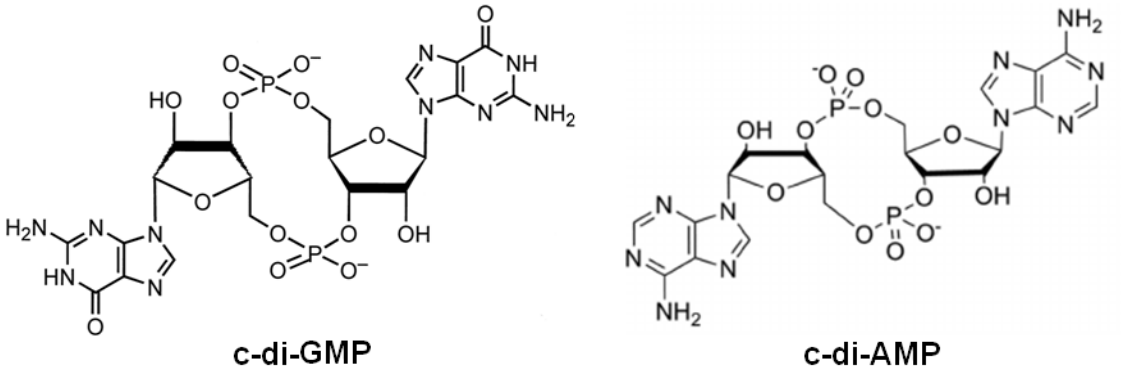

Figure 7: Chemical structures of bacterial cyclic di-nucleotides (adapted from [111]).

CDNs have recently demonstrated to exhibit strong immune modulatory properties [112]. In animal models, intranasally delivered c-di-GMP was shown to provide protection against *Klebsiella* or *Streptococcus pneumonia* challenge by stimulating the production of several pro-inflammatory cytokines and chemokines, as

well as by recruiting immune effector cells to the site of infection [113]. Interestingly, CDNs were shown to be active as adjuvants when administered via mucosal or parental routes, thereby inducing a strong humoral response at systemic (IgG) and mucosal (IgA) levels. In addition, CDNs were demonstrated to mediate cellular immunity by inducing antigen-specific multifunctional $CD4^+$ and cytotoxic T cells [97, 114, 115]. Studies comparing the adjuvant properties of c-di-AMP and c-di-GMP provided evidence that the immunostimmulatory properties of individual CDN molecules differ. The c-di-AMP exhibited improved capacity in stimulating the activation of human DCs *in vitro* as compared to c-di-GMP. Interestingly, *in vivo* co-administration of c-di-AMP with Ovalbumin (OVA) as model antigen resulted in significantly improved stimulation of immune responses at mucosal and systemic levels as compared to c-di-GMP [97]. Further, in comparison to c-di-GMP and cGAMP, c-di-AMP was shown to be a strong inducer of Th17 responses used as mucosal adjuvant [97, 116]. A proof-of-concept study showed that mice vaccinated intranasally with recombinant influenza nucleoprotein (rNP) co-administered with c-di-AMP generated significant antigen-specific cellular and humoral immunity in both mucosal and systemic compartments which conferred protection against a sublethal influenza challenge [117]. This renders c-di-AMP a promising candidate adjuvant for the development of mucosal vaccines.

2.4. IL-17 ‘a proinflammatory cytokine’

IL-17 secreting cells predominantly resides at the mucosal surfaces and are therefore one of the features induced by mucosal vaccines. The IL-17 cytokine family consists of IL-17A, IL-17B, IL-17C, IL-17D, IL-17E and IL-17F. The biological functions and regulation of IL-17A and IL-17F are well studied, whereas much less is known about the other members. IL-17 mediates its biological functions via surface receptors which are ubiquitously expressed among non-hematopoietic cells, such as fibroblasts and epithelial cells, and innate and adaptive immune cell populations. IL-17A and IL-17F cytokines are recognized by the heterodimeric form of the receptor complex IL-17RA and IL-17RC. Functionally, both IL-17A and IL-17F mediate proinflammatory responses [118, 119]. In brief, the activation of IL-17RA-C complex by ligation of IL-17 initiates innate defense and repair responses that include the induction of chemokines, cytokines and anti-bacterial peptides [120].

Innate IL-17 producing cells

Innate IL-17 producing cells are an integral part of IL-17-mediated immune responses during stress, injury or in the presence of invading pathogens. Large populations of innate cells such as γδ T cells, iNKT cells, lymphoid-tissue inducer (LTi)-like cells, neutrophils and paneth cells have been recognized as the early sources of IL-17 production [121]. Innate IL-17 producing cells predominantly reside at the mucosal surfaces such as lung, intestinal mucosa and skin, where they possess a pre-activated phenotype and recognize the antigen via an array of sensory receptors expressed on their surface. Innate IL-17-secreting cells acts directly on epithelial cells promoting secretion of antimicrobial peptides and defensins, which protect the host against infections. Innate IL-17-secreting cells also induce epithelial cells to secrete the granulocyte colony-stimulating factor (G-CSF) and CCL20. This mediates neutrophil recruitment to the site of infection, thereby triggering rapid non-specific immunity against infectious agents such as *Citrobacter rodentium* [122, 123], *Klebsiella pneumonia* [124-126], *S. aureus* and *Candida albicans* [127-129] (Figure 8).

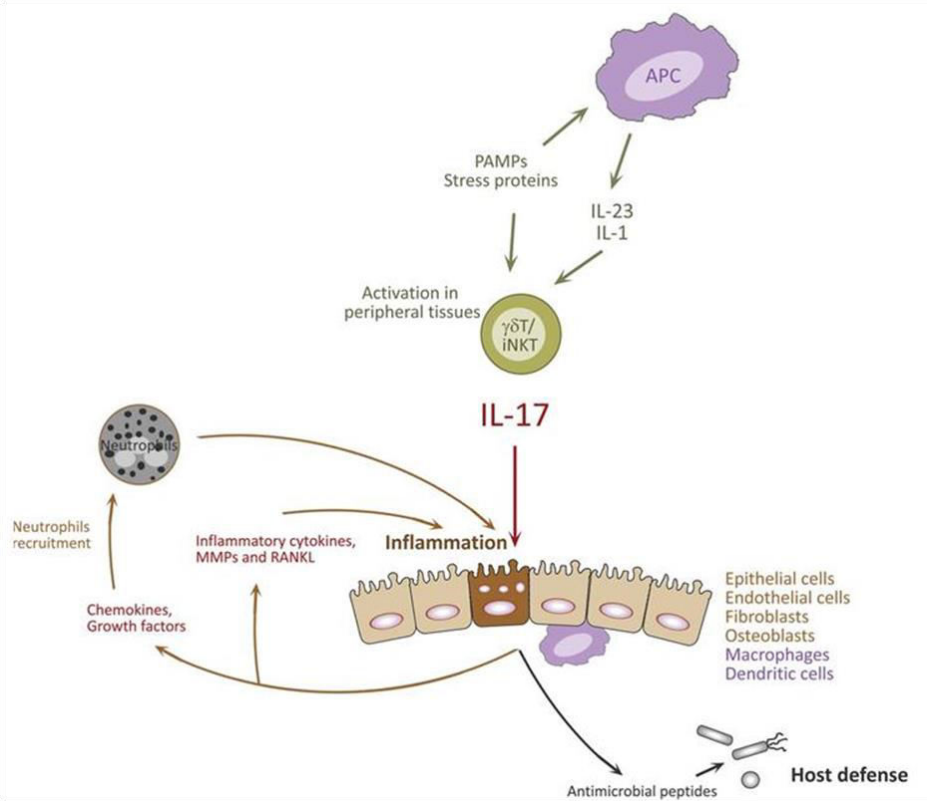

Figure 8: Functions of innate IL-17 secreting cells: Infections or other stress conditions promote APCs to produce proinflammatory cytokines. These cytokines are required for the activation of innate IL-17-secreting cells. Secreted IL-17 induces the secretion of inflammatory cytokines, chemokines and growth factors by various cell types of target tissues, thereby resulting in neutrophil recruitment. IL-17 also acts directly on epithelial cells to promote therelease of defensins, regenerating (REG) proteins and S100 proteins, which have antimicrobial activities and protect the host against infections (modified from [121]).

Adaptive IL-17 producing cells

A decade ago, the dogma of immune regulation by Th cells was amended. The new lineage named Th17 was characterized by their ability to secrete IL-17A, IL-17F and IL-22. Th17 cells are dependent on STAT3 signaling and can differentiate from other Th cells based on the expression of the lineage transcription factor RORγt [130]. Within the adaptive arm, much emphasis has been placed on Th17 cell as the source of IL-17. However, some cytotoxic T cells termed Tc17 as well as B cells have been identified to contribute to IL-17 secretion. IL-17 secreting B cells have been detected in response to *Trypanosoma cruzi* infection [131]. IL-17$^+$ Tc17 have been described in various conditions, such as infections, anti-tumor activities and autoimmune inflammation. Irrespective of their potential in providing immunity, Tc17 cells have received only marginal attention. Apart from their role in infections and autoimmunity, Th17 cells have

received considerable attention in the field of vaccine development due to the observed Th17 induction upon administration of vaccines via mucosal routes.

Differentiation of Th17 cells

Upon TCR activation, naïve CD4 T cells differentiate into different Th lineages based on the cytokine milieu in the surrounding environment. In mice, naïve CD4 T cells differentiate into Th17 cells in the presence of IL-6, IL-23, IL-1β and TGF-β. These cytokines establish the early commitment to the Th17 lineage by activating STAT3, which in turn induces the expression of IL-21 which is required for Th17 expansion. Autocrine signaling of IL-21 promotes STAT3-dependent expression of IL-23R, IL-17A and the transcription factor RORγt. Furthermore, IL-23 is required for the maintenance and stabilization of Th17 effector functions [132, 133] (Figure 9).

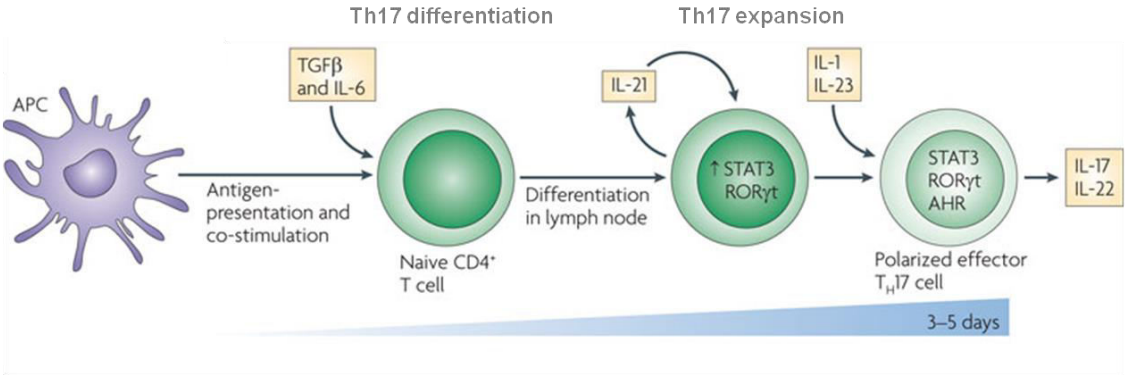

Figure 9: Differentiation of Th17 cells: IL-6 and TGF-β secreted by APCs initiate the differentiation of naive $CD4^+$ T cells to Th17 cells by activating STAT3. Autocrine signaling of IL-21 promotes expression of IL-23R, IL-17A and RORγt. IL-23 is responsible for Th17 maintenance and expansion (adapted from [134]).

Functions of IL-17 secreting cells – matter of concern

In addition to their crucial role in the fight against infectious pathogens, such as bacteria and fungi, $IL\text{-}17^+$ cells can also contribute to chronic inflammation by providing the proinflammatory cytokine milieu. In a collagen-induced arthritis model, γδ T cells were identified as the early source of IL-17 in response to IL-1β and IL-23 and the cause of disease progression [135]. Furthermore, production of IL-17 has been reported to inhibit Th1 differentiation thereby inhibiting the production of IFNγ and IL-2, which are required for the induction of CTLs and anti-viral activity [136]. Thus, the inhibition of Th1 cells by Th17 cells was shown to lead to viral persistence in a case of Theiler's murine encephalomyelitis virus (TMEV) infection [137]. In addition, Th17 cells have been

associated with many autoimmune diseases including multiple sclerosis (MS), rheumatoid arthritis (RA), inflammatory bowel disease and psoriasis. Using experimental mouse model for autoimmune encephalomyelitis (EAE) which resembles human MS, it was revealed the key role played by IL-17 and associated cytokines in driving central nervous system inflammation and lesion formation [138-140]. IL-17A was also detected in synovial fluid in an RA mouse model where it is associated with disease progression [141, 142]. Current clinical studies targeting IL-17 and IL-23 displayed promising results for the treatment of human autoimmune disorders such as psoriasis [143, 144], RA [145, 146] and MS [147, 148]. Therefore, gaining knowledge of functional and regulatory mechanisms of IL-17$^+$ cells might benefit the development of novel immune therapeutics against infectious agents and in addition reduce the inflammatory damage in non communicable diseases.

IL-17-inducing vaccines

Despite the bad reputation of IL-17, studies performed in experimental animal models have shown that vaccine-induced Th17 responses can mediate protective immunity against a wide range of pathogens, such as *Bordetella pertusis, M. tuberculosis, K. pneumonia and Pseudomonas aeruginosa* [149-153]. Vaccines consisting of highly conserved outer membrane proteins of *K. pneumoniae* were shown to induce a strong Th17 response and to confer protection against a range of different *K. pneumoniae* strains [149]. Further, a live-attenuated vaccine against *P. aeruginosa* PA14ΔaroA induces Th17 cell-dependent protective immunity against heterologous strains of *P. aeruginosa* [154]. In addition, vaccination with the mycobacterial peptide ESAT-6(1-20) conferred protection against subsequent challenge with *M. tuberculosis* by induction of IL-17$^+$ CD4 T cells which are required for the recruitment of IFNγ$^+$ T cells [153]. The mechanism of protection initiated by the vaccine-induced Th17-mediated defense against pathogens consists of the secretion of antimicrobial peptides by epithelial cells, neutrophil recruitment to the site of infection, initiation of humoral immunity and augmentation of other T cell effector populations. The role of IL-17 in activating B cells as well as in GC and inducible-BALT (*i*BALT) formation is very well documented [142, 155, 156]. In addition, Th17 cells have been reported to enhance pIgR expression on lung and intestinal epithelial cells, thereby regulating the influx of sIgA into the lumen [157, 158]. Irrespectively of these findings, to date there is no direct evidence linking IL-17 secretion and vaccine-induced immune responses.

The role of IL-17 in the combat against influenza infections is also still under debate, with reports supporting its contribution to both protective but also pathogenic roles. A study demonstrated that IL-10-deficient mice displayed a strong Th17 response resulting in increased survival upon challenge with lethal doses of influenza A/PR8 (H1N1) virus [159]. In contrast, other studies suggested that the use of Th17 cell-inducing adjuvants, such as CTB and TLR4 agonists, might result in increased morbidity and exacerbated lung injury upon subsequent influenza challenge [95, 160]. Therefore, an in-depth understanding of the mechanisms controlling pathogenic versus protective Th17 cell responses will facilitate the design of efficient mucosal vaccines. In addition, the identification of novel Th17 cell-modulating adjuvants displaying a good safety profile will also have a tremendous impact on the design of safe and effective vaccines.

3. Aim of the thesis

In the last years, the crucial role of IL-17 secreting cells in the fight against mucosa associated bacterial and fungal infections as well as their important impact in regulating immune responses have been emphasized. However, their influence in the fight against viral infections and their significance for mucosal vaccine design has not been completely elucidated. Mucosal infections like influenza represent a major health problem worldwide leading to 250,000 – 500,000 deaths annually. The existing vaccines often mediate only inadequate protection which strongly points to the need for the establishment of improved or new vaccination approaches. The implementation of adjuvants represents one key approach to enhance the immunogenicity and efficacy of mucosal vaccines. The c-di-AMP recently demonstrated to elicit potent mucosal immunity, and it has also been shown to induce strong Th17 responses following i.n. administration. However, the underlying mechanisms resulting in c-di-AMP mediated Th17 cell differentiation still remain elusive. Thus, the first specific objective of this thesis was to dissect the immunological factors contributing to c-di-AMP induced Th17 differentiation. To this end, an *in vitro* co-culture system consisting of $CD4^+$ T cells and BMDCs was established to elucidate factors contributing to c-di-AMP-mediated Th17 differentiation. Flow cytometry analysis and CBA (cytometric bead array) were applied to elucidate the immunological factors involved in c-di-AMP-induced Th17 differentiation.

Our current knowledge on the impact of Th17 cells in the stimulation of adaptive immunity, which encompasses (i) initiation of humoral immunity by regulating GC and *i*BALT formation and (ii) enhancement of other T helper cell responses, highlights the potential of Th17 cells as a target for in mucosal vaccination strategies. However, the proinflammatory role of IL-17, which is well documented in auto-immune diseases, should not be neglected. Therefore, the second objective of this thesis was to elucidate the impact of c-di-AMP activated IL-17 secreting cells in the generation of antigen-specific immune responses. To this end, wild type and IL-17a/f deficient mice were immunized with either the model antigen OVA or an inactivated influenza vaccine co-administered with the Th17-stimulating adjuvant c-di-AMP. An advanced multi-parametric flow cytometry approach was developed which enabled the multifunctional characterization of antigen-specific T and B cells. In addition, ELISA was performed to investigate humoral immunity by determining antigen-specific antibody titers (IgG and IgA). Further to investigate the underlying mechanisms responsible for c-di-AMP

induced Th17-dependent antigen-specific immunity, *in vitro* co-culture studies, immunohistochemistry and RT-PCR were performed to detect colocalization of T_{FH} cells and GC B cells in GCs and gene expression. The results derived from this thesis deliver crucial insight into the underlying mechanisms by which c-di-AMP-induced Th17 cell differentiation as well as their contribution to the generation of antigen-specific immunity. The obtained knowledge will pave the way towards the development of novel mucosal vaccine.

4. Materials and methods

4.1. Materials

4.1.1. Technical equipment

Table 2: Technical equipment

Equipment	Company
Centrifuge Biofugepico	Heraeus, Germany
Centrifuge Megafuge R40	
Centrifuge Multifuge 3S-r	
Cell counter, Z2 Coulter counter	Beckman Coulter, Germany
Cell culture plates	Greiner, Germany
Cell strainer 100 µm	BD Bioscience, USA
Cell tric 50 µm	PArtec GmbH, Germany
ChemiDocTM MP Imaging System	Bio-Rad, Germany
Coverplates	Thermo Scientific, Germany
CTL Immunospotanalyser	Cellular Technology, Ltd., Germany
ELISA Reader Synergy2	BioTek, Germany
ELISA Washer	BioTek, Germany
Falcon tubes	Greiner, Germany
Flow cytometry tubes 1.2 ml	MP Biomedicals, France
Flow cytometry tubes 5 ml	BD Bioscience, USA
Fortessa	BD Bioscience, USA
Flow cytometry AriaII	BD, USA
Handystep	Brand, Germany
High binding ELISA plates	Greiner, Germany
Heating magnetic stirrer	IKA Labortechnik, Germany
Incubator, Heracell 240i	Thermo Scientific, Germany

Mangomix	Bioline, Germany
pH-meter	Hannah Instruments, Germany
Pipettes (0.2–2µl, 2-20µl, 20-200µl, 100-1000µl)	Thermo Scientific, Germany
Pipettboy	Thermo Scientific, Germany
Plate washer ELx 405	BioTek, Germany
Precision 2000 automated microplates pipettes	BioTek, Germany
Serological pipets	Roth, Germany
Sterile hood Hera Safe	Thermo Scientific, Germany
Synergy 2 Multi-ModeMicroplate Reader	BioTek, Germany
Thermomixer compact	Eppendorf, Germany
Vortex Genie-2	Omnilab, Germany
Water bath	Köttermann, Germany

4.1.2. Chemical and reagent

Table 3: Chemicals and reagents

Chemicals	Company
2,2'-azino-bis (3-ethyibenzthiazoline-6 sulfonic acid) diammonium salt (ABTS)	Sigma-Aldrich, Germany
3-amino-9-ethyl-carbazole (AEC substrate)	BD Pharmingen, USA
Acetic acid (CH_3COOH)	Merk, Germany
Acetonitrile (CH_3CN)	Sigma-Aldrich, Germany
Ampuwa®	Serumwerk, Germany
Avidin-HRP (horseradish peroxidase) conjugated	BD Pharmingen
Ammonium chloride (NH_4Cl)	Merk, Germany
β-mercaptoethanol	Merk, Germany
Blocking solution for immunofluorescence staining	Zytomed systems, Germany
Bovine serum albumin (BSA)	Sigma-Chemie, Germany

Brefeldin A	Sigma-Chemie, Germany
Citrat acide-1-hydrate ($C_6H_8O_7*H_2O$)	Invitrogen, Germany
Citrate Buffer	Sigma-Aldrich, Germany
Collagenase D	Roche, Germany
Concanavalin A from*canavaliaensiformis*	Sigma-Aldrich, Germany
DEPC-treated water	ThermoFisher, Germany
Dimethyl sulfoxide (DMSO)	Sigma-Aldrich, Germany
Dulbecco's Modified Eagle's Medium (DMEM) (low and high glucose)	Gibco, UK
Dnase	Roche, Germany
dNTP mix	ThermoFisher, Germany
Ethylenediaminetetraactic acid (EDTA)	Fluka, Switzerland
Ethanol 100%	Fluka, Switzerland
Fetal calf serum, South America (FCS)	Greiner Bio-One, USA
Formaldehyde > 36.5%	Riesel-de-Haën, Germany
GeneRuler DNA ladder mix	Thermo Scientific, Germany
Gentamicine	Gibco, UK
L-Glutamine	Gibco, UK
Granulocyte-macrophage colony stimulating factor (GM-CSF)	eBioscience, USA
Hepes	Gibco, UK
Hydrogen peroxide (H_2O_2)	Sigma-Aldrich, Germany
^{3}H-thymidine	PerkinElmer, USA
Ionomycin	BD, USA
Isofluran® Curamed vet inhalation anesthetic	Essex Tierarznei, Germany
Isopropanol	Merk, Germany
Isoton II (acid-free balanced electrolyte solution)	Beckman Coulter, USA
Kappa master mix	Kapa Biosystems, Germany

MangoMix	Bioline, Germany
2-Mercaptoethanol (50mM)	Gibco, UK
Midori green advanced green DNA stain	Nippon Generics, Germany
Minimal essential medium (MEM)	Gibco, UK
OVA protein	EndoGrade, Hyglos, Germnay
Oligo (dT)18 primer	ROTH, Germany
Paraformaldehyde (PFA)	Merk, Germany
Penicillin/streptomycin (100 units/ml penicillin G sodium; 50µg/ml streptomycin sulfate in 85% saline)	Gibco, UK
Phorbol 12-myrisate 13-acetate (PMA)	Sigma-Aldrich, Germany
Peanut agglutinin (PNA)	Sigma-Aldrich, Germany
Potassium chloride (KCl)	Fluka, Switzerland
Potassium hydrogen carbonate ($KHCO_3$)	Merk, Germany
Potassium dihydrogen phosphate (KH_2PO_4)	Carl-Roth, Germany
Proteinase K	Bioline, Germnay
5x reaction mixture	ThermoFisher, Germany
RevertAid^{TM} H minus Reverse Transcriptase	ThermoFisher, Germany
RPMI 1640 medium (+L-glutamine)	Gibco, UK
Receptor destroying enzyme (RDE)	Sigma-Aldrich, Germany
Sodium acetate (CH_3CooNa)	Merk, Germany
Sodium carbonate (Na_2CO_3)	Carl-Roth, Germany
Sodium chloride (NaCl)	Carl-Roth, Germany
Sodium dihydrogen phosphate (NaH_2PO_4)	Merk, Germany
Sodium hydrogen carbonate ($NaHCO_3$)	Merk, Germany
Sodium hydroxide (NAOH)	Carl-Roth, Germany
Sulfuric acid	Sigma-Aldrich, Germany
Tris/HCl	Sigma-Aldrich, Germany

Trizol	Sigma-Aldrich, Germany
Trypan Blue	Sigma-Aldrich, Germany
Trypsin	Sigma-Aldrich, Germany
Tween 20	Carl-Roth, Germany

4.1.3. Antibodies for flow cytometry

Table 4: Antibodies used in flow cytometry analysis

Antigen	Flurochrome	Clone	Dilution	Company
CD3	V500	500A2	1:200	BD Horizon, USA
CD3	BV785	17A2	1:200	BioLegend, USA
CD4	PE-Cy7	RM4.5	1:1000	eBioscience, Germany
CD4	BV605	RM4.5	1:800	BioLegend, USA
CD4	Alexa700	RM4.5	1:500	BioLegend, USA
CD4	APC-A750	RM4.5	1:500	eBioscience, Germany
CD4	BV421	RM4.5	1:500	BioLegend, USA
CD8	PE-Cy7	53-6.7	1:800	eBioscience, Germany
CD8	BV650	53-6.7	1:300	BioLegend, USA
CD11b	PE-Cy7	M1/70	1:800	eBioscience, Germany
CD11b	BV605	M1/70	1:300	BioLegend, USA
Cd11b	PB	M1/70	1:800	BioLegend, USA
CD11c	FITC	N418	1:800	eBioscience, Germany
CD11c	APC	N418	1:300	eBioscience, Germany
CD11c	BV785	N418	1:200	BioLegend, USA
CD19	PB	6D5	1:800	BD Horizon, USA

CD19	BV785	6D5	1:800	BioLegend, USA
CD19	APC-Cy7	6D5	1:600	BD Horizon, USA
CD25	PE	PC61	1:300	BD Horizon, USA
CD27	PE-Cy7	LG.7F9	1:1200	eBioscience, Germany
CD44	BV785	1M7	1:150	BioLegend, USA
CD44	APC	1M7	1:400	eBioscience, Germany
CD45R	APC-Cy7	R.A3-6B2	1:200	BD Horizon, USA
CD62L	FITC	MEL-14	1:1000	BD Horizon, USA
CD62L	BV605	MEL-14	1:250	BioLegend, USA
CD69	BV605	H1.2F3	1:100	BioLegend, USA
CD86	PE	GL1	1:500	BD Horizon, USA
CD86	BV605	GL1	1:150	BioLegend, USA
CD138	BV421	281-1	1:400	BioLegend, USA
CD138	BV711	281-2	1:200	BioLegend, USA
CXCR5	PE-Cy7	2G8	1:500	BD Horizon, USA
F4/80	FITC	BM8	1:100	eBioscience, Germany
F4/80	PerCP-Cy5.5	BM8	1:200	BioLegend, USA
IgA	Bio	1-1-44-2	1:200	eBioscience, Germany
IgG1	PE	A85.1	1:200	BD Horizon, USA
ICOS	PE	E398.4A	1:400	BioLegend, USA
IFNγ	BV711	XMG1.2	1:300	BioLegend, USA
IFNγ	BV650	XMG1.2	1:200	BioLegend, USA
IL-2	APC-Cy7	JES6-5H4	1:200	BD Horizon, USA
IL-4	APC	11B11	1:200	eBioscience, Germany
IL-10	BV421	JES5-16E3	1:150	BioLegend, USA
IL-12/IL-23p40	Alexa647	C17.8	1:400	eBioscience, Germany
IL-17	V450	TC11-18H10	1:200	BD Horizon, USA

IL-17	FITC	eBio17B7	1:500	eBioscience, Germany
IL-17	BV605	TC11-18H10.1	1:300	BD Horizon, USA
IL-17RA	PE	PAJ-17R	1:100	eBioscience, Germany
IL-21	APC	Rat IgG_{2B}	1:20	R&D, USA
Ly6G	PE-Cy7	1A8	1:200	BioLegend, USA
MHCI	Alexa	AF6-S8.5	1:200	BioLegend, USA
MHCI	PB	H-2Kb	1:200	BioLegend, USA
MHCII	FITC	AF6-120.1	1:100	BD Horizon, USA
NK1.1	APC	PK136	1:400	eBioscience, Germany
NK1.1	Bv510	PK136	1:100	BioLegend, USA
NKp46	A660	29A1.4	1:200	eBioscience, Germany
Rorγt	PE	B2D	1:100	eBioscience, Germany
TNFα	PerCPeF710	MPG-XT22	1:200	eBioscience, Germany
γδTCR	PE	GL3	1:200	BioLegend, USA
Streptavidin	BV605	-	1:400	BioLegend, USA
Streptavidin	BV650	-	1:400	BioLegend, USA

4.1.4. Antibodies for Enzyme-linked immunospot Assay (ELISPOT)

Table 5: Antibodies used in ELISPOT

Antibody	Conjugated	Dilution	Company
Anti-mouse IFNγ	Purified	1:200	BD Pharmagen, USA
Anti-mouse IFNγ	Biotinylated	1:250	BD Pharmagen, USA
Anti-mouse IL-2	Purified	1:200	BD Pharmagen, USA
Anti-mouse IL-2	Biotinylated	1:250	BD Pharmagen, USA
Anti-mouse IL-4	Purified	1:200	BD Pharmagen, USA
Anti-mouse IL-4	Biotinylated	1:250	BD Pharmagen, USA

Anti-mouse IL-17A	Purified	1:250	eBioscience, USA
Anti-mouse IL-17A	Biotinylated	1:250	eBioscience, USA
Streptavidin	HRP	1:100	BD Pharmagen, USA

4.1.5. Antibodies for Enzyme-linked immunosorbent Assay (ELISA)

Table 6: Antibodies used in ELISA

Antibody	Conjugated	Dilution	Company
Goat, anti-mouse IgA	Purified	1:500	Sigma-Aldrich, Germany
Goat, anti-mouse IgA	Biotinylated	1:5000	Southern Biotech, USA
Goat, anti-mouse IgG	Biotinylated	1:5000	Sigma-Aldrich, Germany
Goat, anti-mouse IgG1	Biotinylated	1:5000	Southern Biotech, USA
Goat, anti-mouse IgG2c	Biotinylated	1:5000	Southern Biotech, USA
Goat, anti-mouse pIgR	Biotinylated	1:200	R&D, USA
α-goat IgG	HRP	1:5000	Jackson Immuno Research, Germany
Streptavidin	HRP	1:1000	BD Pharmagen, USA

4.1.6. Solutions and buffers

Table 7: Solutions and buffers

Solution/buffer	Composition
ABTS	0.3 g/L ABTS in 0.1 M citric acid
ABTS + H_2O_2	0.03% (v/v) H_2O_2 in ABTS solution
Acetate solution (0.1 M)	148 ml acetic acid, 0.2 mM + 352 ml of 0.2 mM sodium acetate; adjust volume to1L with H_2O,pH 5.0
ACK lysis buffer	0.1M mM EDTA, 1mM $KHCO_3$, 155 mM NH_4Cl, pH 7.3
Aminoethylcarbazole (AEC) stock solution	100mg AEC substrate in 10 ml DMF

AEC + H_2O_2	333.3 µl AEC stock solution in 10 ml 0.1 M acetate solution, 5µl H_2O_2 (30%)
3% Avicel	15 g Avicel + 500 ml dH_20
1% Avicel-DMEM (100 ml)	33,3 ml 3% Avicel + 66,7 ml DMEM
Blocking Buffer (ELISA)	PBS + 3% BSA
Blocking Buffer (FOCI assay)	0.5% Tween20 + 1% BSA in PBS
Carbonate buffer (0.1 M)	4.401 g $NaHCO_3$ + 1 L H_2O, pH 8.2
Calcium saline	1 g $CaCl_2$*$2H_20$ + 9 g NaCl + 1.2 g H_3BO_3 + 0.052 g $Na_2B_4O_7$*$10H_20$
Dilution buffer (ELISA)	PBS + 0.1% Tween 20 + 1% BSA
Dilution buffer (ELISPOT)	1x PBS containing 10% FCS
Fixative (FOCI assay)	4% formalin in PBS
Fixative (MN assay)	80% acetone + 20% PBS
Infection medium	DMEM + 0.1% BSA + 2.5 µg/ml N-Acetylated Trypsin (NAT)
Lung digestion medium	RPMI 1640 containing 5% FCS, 2.5% Hepes, 0.2 mg/ml collagenase D, 0.1 mg/ml Dnase
MACS buffer	0.5% BSA; 0.5% saponin/PBS (w/v)
Overlay	1% Avicel-DMEM + 10% BSA + 5mg/ml NAT
2% Paraformaldehyde (PFA)	2% PFA/PBS (w/v), pH 7.0 (fixation)
1 x PBS (phosphate-buffered saline)	8 g NaCl, 0.2 g KCl, 1.44 g Na_2HPO_4*$7H_2O$, 0.24 g KH_2PO_4 in 1 L H_2O, pH 7.2
Quencher	0.5% Triton x100 + 20mM Glycine in PBS
Trypan blue solution	0.1% Trypan blue in PBS (w/v)
Virus diluents	DMEM + 1% PenStrep + 0.1% BSA + 2.5 µg/ml NAT + 25nM Hepes
Wash buffer (ELISA)	PBS + 0.1% Tween 20

Wash buffer (ELISPOT)	PBS + 0.05% Tween 20

4.1.7. Antigen and adjuvants

Table 8: Antigen and adjuvant

Antigen / Adjuvant	Company
A-galactosylceramide polyethylene glycol (αGCMPEG)	HZI, Germany
Cyclic-di-adenosine-monophosphate (c-di-AMP)	BioLog, Germany
H5N1 (NIBRG-14; see 4.1.10)	NIBSC, UK
Lipopolysaccharide (LPS)	Sigma-Aldrich, Germany
Ovalbumin (OVA; Grade VII, LPS free)	Sigma-Aldrich, Germany

4.1.8. Cell line used in experiments

Table 9: Cell line used in the experiments

Cell Type	Description
MDCK	Madin-Darby Canine Kidney (MDCK) cells are adherent epithelial cells which are suitable transfection host and are used in influenza research, provided by Prof. Dr. Klaus Schughart (INFG, HZI, Germany)

4.1.9. Cell Culture Media

Table 10: Cell culture media

Media	Supplements
RPMI 1640 complete	10% v/v FCS heat inactivated (h.i.), 100 U/ml penicillin, 50 µg/ml streptomycin, 2mM L-glutamine

RPMI 1640 for BMDCs	10% v/v FCS heat inactivated (h.i.), 100 U/ml penicillin, 50 µg/ml streptomycin, 2mM L-glutamine, 2-mercaptoethanol 50 µM, 50 µg/ml gentamycin
DMEM	100 U/ml penicillin, 50 µg/ml streptomycin
MEM	10% v/v FCS h.i., 100 U/ml penicillin, 50 µg/ml streptomycin

4.1.10. Influenza virus

Table 11: Influenza virus strains used for challenge studies

Strain	Description
H5N1 (formaldehyde-inactivated, mouse-adapted)	The influenza reference virus NIBRG-14 is a reassortant prepared by reverse genetics from A/Vietnam/1194/2004 (H5N1) virus and A/PR/8/34(H1N1) virus (NIBSC, UK)

4.1.11. Mice

Table 12: Mice used in the experiments

Mouse	Description	Provider
Wild type (WT)	C57/BL6	Harlan, Germany
IL-17a/f$^{-/-}$	Animal lacking functional IL-17a/f, developed on C57/BL6 background [161]	Kindly provided by Prof. Dr. ImmoPrinz (MHH, Hannover, Germany)
SFB	NOD-Scid, mono-colonized mice, breed at hygienic conditions	Kindly provided by Prof. Dr. Andrea Bleich (MHH, Hannover, Germany)

4.1.12. Primers for genotyping IL-17a/f$^{-/-}$ mice

Table 13: Primers used in PCR for genotyping (Provided by Eurofins)

Primer	Sequence

KO IL17 fw	Atccaatccccatcacctt
KO IL17 rv	Gttgggacttgccattctga
WT IL17 fw	Ctttcagggtcgagaagatgctg
WT IL-17 rv	Aagcagtttgggacccctttaca

4.1.13. Primers for assessing gene expression

Table 14: Primers used in qPCR for gene expression (provided by Eurofins)

Primers	Sequence
pIgRfw	Gtgcccgaaactggatcacc
pIgRrv	Tggagacccctgaaaagacagt
Gapdhfw	Aggtcggtgtgaacggatttg
Gapdhrv	Tgtagaccatgtagttgaggtca

4.1.14. PCR cycle

Table 15: PCR cycle for the SybrGreen program

Steps	Temperature [°C]	Time [sec]	Cycles	Analysis
Pre-incubation	95	60	1	
Amplification	95	3	40	Quantification
	60	30		
Melting curve	95	continuous	1	Melting curve
Cooling	37	60	1	

4.1.15. Kits used for cytokine and antibody detection

Table 16: Kits used for cytokine and antibody detection

Kit	Manufacturer
Mouse Th1/Th2/Th17/Th22 13plex Kit FlowCytomix	eBioscience, USA
Mouse GM-CSF, IL-23, IL-1β, TGF-β1 FlowCytomixsimplex Kit	eBioscience, USA
LEGENDplex™Multi-Analyte Flow Assay Kit	BioLegend, USA
MILLIPLEX® MAP Kit	Merck KGaA, Germany
Live/Dead® Fixable dead cell stain Kit	Life technologies, Germany
Mouse IFNγ, IL-2, IL-4 or IL-17 ELISPOT pair kit	BD Bioscience, Germany

4.2. Methods

4.2.1. *IL-17a/f$^{-/-}$ genotyping by PCR*

To ensure the appropriate phenotype of the IL-17 a/f$^{-/-}$ mice, a polymerase chain reaction (PCR) based genotyping was performed. For this, tail derived DNA samples were analyzed by PCR. Briefly, the tails were lysed in lysis buffer containing proteinase K overnight at 56˚C under constant shaking at 800 rpm. Proteinase K is a serine protease that is used here to degrade native as well as denatured proteins. Proteinase K was deactivated by exposing the samples to 95˚C for 10 min after the lysis procedure. Then, the samples were cooled down and 3 µl of sample suspensions were used for a PCR reaction of a total volume of 20 µl. A single reaction contained 10 µl of DNA Mangomix, 5.5 µl H_2O, and 1 µl of each primer (Table 13) at a final concentration of 10 µM. The protocol of the PCR cycle is displayed in Figure 10.

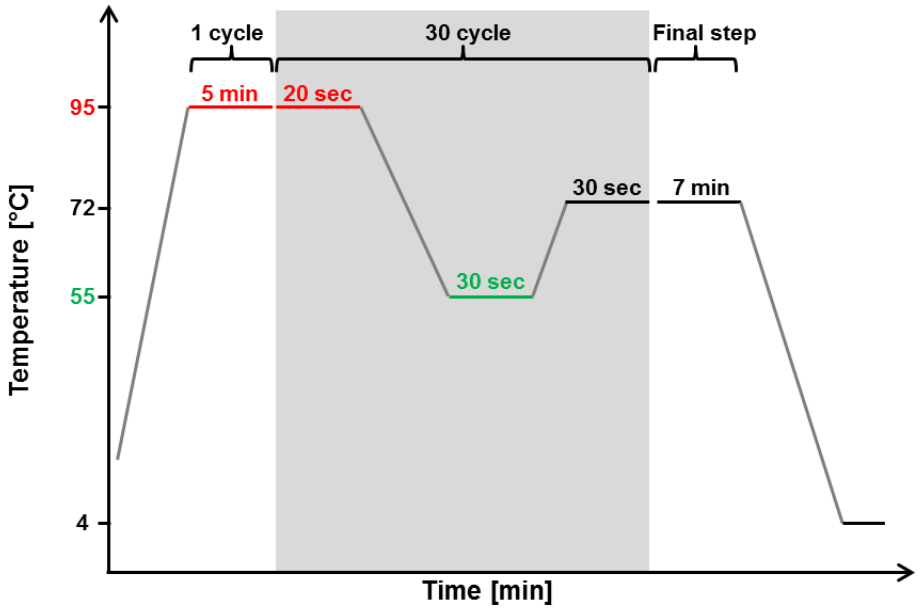

Figure 10: PCR temperature cycles for IL-17a/f genotyping: Lysed tail samples were mixed with the appropriate primers. PCR was performed using the displayed temperature cycle protocol.

The PCR products were analyzed by agarose gel electrophoresis. To this end 4% (w/v) agarose gels were prepared in TAE buffer containing Midori Green (25 µl/l), a nucleic acid dye, which upon exposure to ultraviolet (UV) light, emits green fluorescence when bound to DNA and therefore allows the visualization of DNA bands. PCR samples were loaded onto the gel and the Gene Ruler Ladder Mix was used as a DNA fragment size standard. The gel electrophoresis was performed for 1 h at 110 V. Following, the DNA

was visualized by exposing the gel to UV light at a wavelength of 530 nm using the GelDocXRS system.

4.2.2. c-di-AMP induced Th17 differentiation

4.2.2.1. Generation of BMDCs

To generate BMDCs, bone marrow derived cells were isolated from femur and tibia of 6-8 weeks old wild type (WT) and IL-17a/f$^{-/-}$ mice. For this, mice were euthanized using CO_2 and hind legs were dissected. The bones were cleaned of muscle tissue, incubated for 1-2 min in 70% (v/v) ethanol, rinsed in fresh RPMI medium and then, the ends of the bones were removed. The bone marrow cells were flushed by pressing fresh RPMI medium through the medullary cavity of femur and tibia. The cell suspension was transferred into 50 ml falcon tubes and centrifuged for 10 min at 1200 rpm at room temperature. The supernatant was discarded and the pellet was re-suspended in ACK lysis buffer (Table 7) for 1 min to remove the erythrocytes. Next, 10 ml RPMI medium was added to stop the reaction, followed by another centrifugation step for 10 min at 1200 rpm at room temperature. The supernatant was discarded and the cell pellet was re-suspended in 10 ml RPMI medium and pressed through a 100 µm filter mesh. The cell number was determined as described in section 4.2.7, adjusted to a final concentration of 1×10^6 cells/ml and distributed at a concentration of 5×10^6 cells in 5 ml per well in a 6 well plate. Cell differentiation towards DCs was directed by the presence of 5 ng/ml mouse GM-CSF in the growth RPMI medium. The cells were incubated at 37˚C in a humidified atmosphere containing 5% CO_2, with exchanging half of the volume per well with fresh medium every second day until day 7. At this time the cells were ready to be used for *in vitro* experiments.

4.2.2.2. *In vitro* assessment of Th17 differentiation

The effect of c-di-AMP induced Th17 differentiation was assessed *in vitro* by co-culturing c-di-AMP primed BMDCs together with sorted CD4$^+$ T cells. BMDCs were stimulated in GM-CSF free medium. Briefly, the culture medium was gently removed and replaced by fresh medium supplemented with 40 µg/ml OVA, 5 µg/ml c-di-AMP alone or in combination or with medium asa control. After the treatment BMDCs were incubated for 24 h at 37°C in a humidified atmosphere containing 5% CO_2, secreted

cytokines present in the supernatant as well as surface expression of activation markers and intracellular cytokines were analyzed.

Further, for the *in vitro* assessment of Th17 differentiation treated BMDCs were co-cultured together with sorted $CD4^+$ T cells. For this, CD4 T cells were sorted using FACS Aria II system (BD, Bioscience, USA) and activated for 2 days with plate bound αCD3 and αCD28. For sorting of naïve non-activated $CD4^+$ T cells, single cell suspensions from spleen were stained with the following antibodies: anti-CD4, anti-CD25, anti-CD62L and anti-CD44 and naïve $CD4^+$ T cells were sorted as $CD4^+CD25^-CD44^{low}CD62L^{hi}$ lymphocytes. After 2 days of activation, 5×10^5 $CD4^+$ T cells were co-cultured with 5×10^4 c-di-AMP primed BMDCs in a ratio 1:10 and incubated for 2 days. Following, intranuclear FACS staining as mentioned in 4.2.10 was performed, and IL-17 and RORγt expression were evaluated (Figure 11).

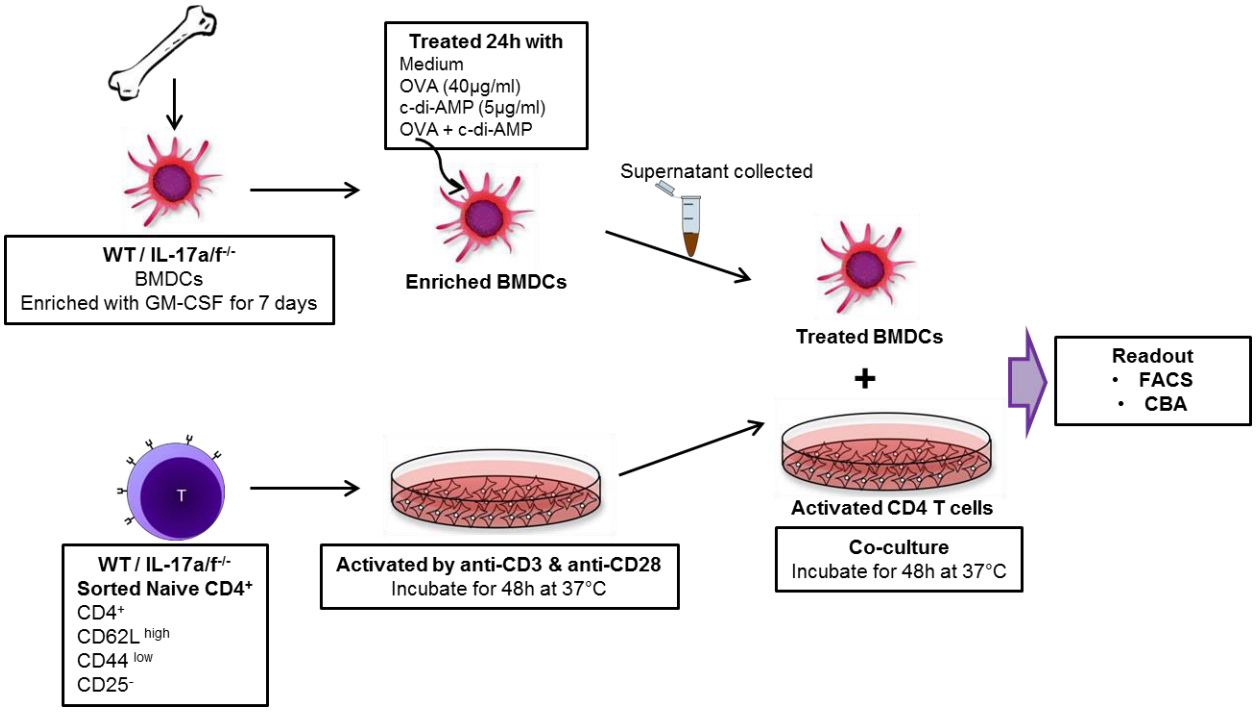

Figure 11: Scheme of *in vitro* experiments to evaluate the mechanism of c-di-AMP-induced Th17 differentiation: Murine bone marrow cells derived from WT and IL-17a/$f^{-/-}$ mice were cultured for 7 days in the presence of GM-CSF to enrich BMDCs. The enriched cells were then treated with OVA (40 µg/ml) alone or co-treated with c-di-AMP (5 µg/ml) for 24 h. Untreated cells were used as controls. Simultaneously CD4 T cells were sorted and activated for 2 days with plate bound αCD3 and αCD28. Subsequently, CD4 T cells were co-cultured with BMDCs and incubated for 2 days. Following, IL-17 secretion and RORγt expression were evaluated on $CD4^+$ T cells by FACS. In addition, surface expression of the activation markers MHC class I and II, CD86, IL-17RA and IL-12/IL-23p40, and the secretion of IL-6, TNFα, IL-1β, TGFβ, IL-17 and IL-23 by BMDCs were assessed.

4.2.3. c-di-AMP induced plasma B cell differentiation

4.2.3.1. *In vitro* activation of B cell upon treated with c-di-AMP

The effect of c-di-AMP on the activation of B cells was assessed *in vitro* by treating sorted B cells with or without c-di-AMP. B cells were sorted using FACS Aria II system (BD, Bioscience, USA). For sorting B cells, single cell suspension from spleens was stained with anti-CD19 and anti-B220 and B cells were sorted as $CD19^+B220^+$ lymphocytes. Following, B cells were treated with 40 µg/ml OVA, 5 µg/ml c-di-AMP alone or in combination or with the medium as acontrol for 1 h. After 1 h, B cells were washed to remove the medium containing c-di-AMP and were further supplemented with fresh medium and incubated for 24 h at 37°C in a humidified atmosphere containing 5% CO_2. Then, the surface expression of B cell activation markers was analyzed by using flow cytometry.

4.2.3.2. *In vitro* assessment of plasma B cell differentiation

The effect of c-di-AMP on plasma B cell differentiation was assessed *in vitro* by co-culturing sorted T_{FH} cells and GC B cells from WT and IL-17a/f$^{-/-}$ mice supplemented with c-di-AMP. T_{FH} cells and GC B cells were sorted using a FACS Aria II system (BD, Bioscience, USA). For sorting of GC B cells and T_{FH} cells, single cell suspension from spleen and cervical lymph nodes (cLNs) were stained with the following antibodies: anti-CD19, anti-PNA, anti-CD4 and anti-CXCR5. GC B cells were sorted as $CD19^+PNA^+$ lymphocytes and T_{FH} cells were sorted as $CD4^+CXCR5^+$ lymphocytes. The cells were plated into a 96 well V-bottom plates at a ratio of 1:1 (5×10^4 cells/well each) and incubated for 6 days at 37˚C. Anti-CD3 and anti-CD28 were added to each well to induce T_{FH} cell activation. To address the role of IL-17 in plasma B cell differentiation exogenous IL-17A was added into one set of T_{FH}:GC B cells sorted from IL-17a/f$^{-/-}$ mice supplemented with c-di-AMP. Every second day the plate was centrifuged at 300 rpm for 1 min and 100 µl of supernatant was collected and stored at -20˚C for further analysis of secretory components. The cells were supplemented with 100 µl of fresh complete RPMI medium. After incubation, FACS staining for surface markers as mentioned in 4.2.10 was performed and the plasma B cell differentiation was evaluated based on CD138 expression.

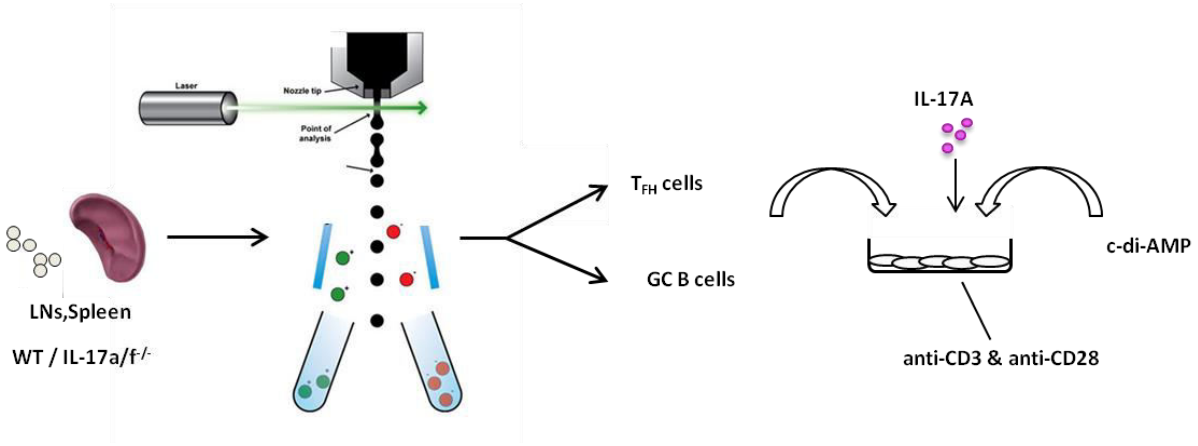

Figure 12: Scheme of *in vitro* experiments to evaluate the mechanism of c-di-AMP induced plasma B cell differentiation: Sorted T_{FH} cells and GC B cell from wild type (C57BL/6) and IL-17a/f$^{-/-}$ mice were co-cultured for 6 days in the presence of c-di-AMP (5 µg/ml). Then, plasma B cell differentiation was evaluated by FACS.

4.2.4. Mouse immunization experiments

The influence of c-di-AMP-stimulated Th17-mediated immune responses on adaptive immunity was assessed in immunization experiments. WT and IL-17a/f$^{-/-}$ mice were vaccinated with 10 µg of OVA antigen or 0.5 µg of NIBRG-14 antigen alone or co-administered with 5 µg c-di-AMP per dose/mouse. The control groups received PBS alone. The mixture of antigen and adjuvant were formulated in PBS 30 min before the i.n. administration of 10 µl per nostril. For this, animals were anesthetized with isofluorane and 20 µl of the vaccine formulation were administered per mouse. Five to six animals per group of 8-14 weeks old mice were immunized on day 0, 14 and 28 as shown in Figure 13. Animals were sacrificed 14 days after the 2nd boost and samples were collected, as mentioned in 4.2.5.

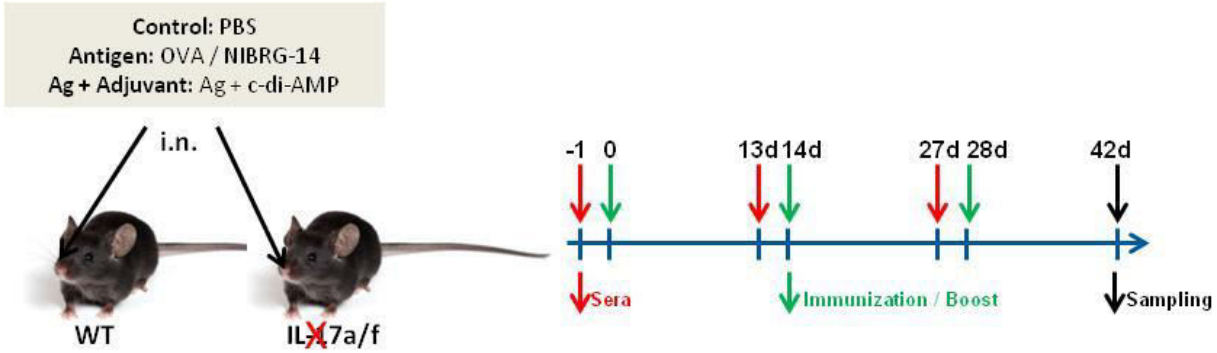

Figure 13: A schematic overview of mouse immunization experiments. The picture of the mouse is adopted from [162].

4.2.5. Sample collection

To collect the different organs for further *in vitro* studies or *ex vivo* analysis, animals were anesthetized with isoflurane. To detect serum derived antibodies or cytokines, blood samples were collected from the retro-orbital complex, centrifuged for 5 min at 8000 × g, and sera were stored at -20˚C for further analysis of IgG titers. The mice were euthanized by exposure to CO_2 and spleen, cLNs, lung as well as nasal and lung lavage samples were collected. Briefly, the abdominal area of the mice was sprayed with ethanol and the spleens, cLNs and lung were removed, placed in complete RPMI medium and processed separately, as described in 4.2.6. The samples for analysis of IgA in the nasal cavity and lung were collected in a 1.5 ml tubes which were prefilled with 10 µl of 40 mM PMSF. Then, the samples were centrifuged at 8000 × g for 10 min and the supernatants were stored at -20˚C.

4.2.6. Preparation of single cell suspension

4.2.6.1. Spleen

To perform ELISPOT and FACS staining single cell suspensions of spleens were obtained by mincing the organs through a 100 µm cell mesh using the flat end of a 2 ml syringe plunger. Cell suspensions were transferred to a 15 ml Falcon tube and centrifuged at 240 × g for 10 min at 4˚C. The supernatant was discarded and erythrocytes were lysed by re-suspending the pellets in ACK lysis buffer (Table 7, 1 ml/spleen). After incubation for 1 min, the lysis was stopped by filling the tubes with complete RPMI medium. The cell suspensions were centrifuged at 240 × g for 10 min at 4˚C, the supernatant was discarded and the pellets were re-suspended in complete RPMI (2 ml/spleen). Subsequently, the cells were filtered through a 100 µm mesh to remove fat and debris, washed twice with RPMI medium and the cell number was determined. The splenocytes were stored on ice until further use.

4.2.6.2. Cervical Lymph Nodes

To determine the functionality of immune cells in terms of cytokine secretion by FACS single cell suspensions of cLNs were obtained by mincing the organs through a 100 µm cell mesh using the flat end of a 2 ml syringe plunger. Cell suspensions were transferred to a 15 ml tube and centrifuged at 240 × g for 10 min at 4˚C. The supernatant was discarded and the pellets were re-suspended in complete RPMI

(2 ml/cLNs). Subsequently, the cells were filtered through a 100 µm mesh to remove fat and debris, washed twice with RPMI medium and the cell number was determined. The cells were stored on ice until further use.

4.2.6.3. Lung

To determine the functionality of immune cells in terms of cytokine secretion by FACS single cell suspension of lungs were obtained. For this, the thoracic diaphragm was deflated and the ribcage was cut from both sides in order to expose the lungs. Lungs were perfused through the heart with 2 ml PBS/mouse and meshed through a 100 µm mesh in digestion medium (Table 7, 5 ml/lung) by using the flat end of a 2 ml syringe plunger. The suspensions were transferred to a 15 ml tube and subsequently digested for 20 min at 37˚C in a water bath. The digestion was stopped by filling up the tube with complete RPMI medium (10 ml/lung). The cell suspension was centrifuged at 240 × g for 10 min at RT and supernatant was discarded. To separate the lymphocytes, a density gradient centrifugation was performed. For this, the pellet re-suspended in 4 ml 30% Easycol Separating Solution (r = 1.124 g/ml, Biochrom AG, diluted in complete RPMI medium) was carefully pipetted onto 4 ml of 70% Easycol Separating Solution. The density gradient was centrifuged at 1020 × g for 20 min at RT without abrake. The lymphocytes were collected at the interface between the two density solutions and transferred to a new 15 ml tube. The cells were re-suspended in 10 ml RPMI and centrifuged at 240 × g for 10 min at 4˚C. This step was repeated to ensure complete removal of remaining Easycol Separating Solution. To lyse the erythrocytes, the cell pellet was re-suspended in ACK lysis buffer (Table 7, 500 µl/lung) and the reaction was stopped after 1 min by filling up the tubes with complete RPMI medium. The cells were centrifuged at 240 × g for 10 min at 4˚C, washed twice with RPMI medium and the cell number was determined. The cells were stored on ice until further use.

4.2.7. Cell counting

The cell cytometer was used to determine the number of cells in suspensions. The cells were diluted in Isotone II at a ratio 1:1000 and measured using the multi-size analyzer and Multi32 Coulter Z2®Acc Comp® software. Cells with a diameter between 5-16 µm were counted. A size below 5 µm was considered as debris and excluded.

4.2.8. Detection of cytokine production in spleen cells from immunized mice by ELISPOT

ELISPOT was performed to assess the number of IFNγ, IL-2, IL-4 and IL-17 by splenocytes following vaccination according to the ELISPOT kit manufacturer's instructions. Briefly, the 96 well HTS filter plates were coated overnight at 4˚C with 100 µl of anti-mouse IFNγ, IL-2, IL-4 or IL-17 capture antibodies diluted in PBS (Table 5). The following day, the plates were washed with complete RPMI medium two times and blocked for 2 h at RT. For cell activation, 100 µl of spleen cells were distributed on plates at a concentration of 5×10^5 cells/well and re-stimulated with OVA (5 µg/ml) or NIBRG-14 (0.2 µg/ml). Unstimulated cells served as background control. Then, the splenocytes were incubated for either 24 h (IFNγ) or 48 h (IL-2, IL-4, IL-17) at 37˚C in a humidified atmosphere containing 5% CO_2. For the detection, cell suspensions were aspirated and the wells were washed with deionized water and with wash buffer (PBS containing 0.05% Tween-20) followed by 2 h incubation with the corresponding detection antibody diluted in PBS (Table 5). After washing with wash buffer and 1 h incubation with avidin-horseradish peroxidase (HRP) diluted in PBS (Table 5), the plates were finally washed with wash buffer and PBS. Spot development was monitored 5-60 min after the addition of the substrate solution (AEC + H_2O_2, Table 7). The reaction was stopped by washing the plates with deionized water. The plates were scanned using a CTL ELISPOT reader and the spots were quantified using the ImmunoSpot image analyzer software v3.2. Spot number values of the cells without re-stimulation were subtracted from the spot number values of the antigen-re-stimulated cells. Then, the average spot number value of triplicates was calculated for each group.

4.2.9. Re-stimulation of cells for multifunctional T and B cell analysis

To analyse the functionality of lymphocytes in terms of cytokine secretion, cells were re-stimulated overnight with the antigen. For this, cells seeded at a concentration of 1×10^7 cells/ml into 12 well plates were incubated in complete medium with or without OVA (40 µg/ml) or NIBRG-14 (1 µg/ml) for 16 h at 37˚C in a humidified atmosphere containing 5% CO_2. For additional 6 h, brefeldin A and monensin were added into the cell suspension to block the cytokine transport from the endoplsmic reticulum to the golgi apparatus. Afterward, cells were collected into 2ml FACS tubes and washed with PBS by centrifuging them at 240 × g for 10 min at 4˚C. The pellets were then re-

suspended in PBS and the phenotypic and functional analysis of the cells was performed using FACS analysis, as described in 4.2.10.

4.2.10. Preparation of samples for flow cytometry analysis

Surface staining

Single cell suspensions were transferred to a V-bottom plate and centrifuged at 320 × g for 5 min at 4˚C. Then, cells were re-suspended in 100 µl PBS containing FcR-block (diluted 1:2000) and incubated for 20 min at 4˚C. Cells were washed with 100 µl PBS/well and the plate was centrifuged at 320 × g for 5 min at 4˚C. The supernatants were discarded and the wash step was repeated. Antibodies for the surface staining were diluted in a volume of 50 µl per sample and added to the cells. After 20 min of incubation at 4˚C, cells were washed twice with PBS and in case no intracellular staining was carried out, cells were re-suspended in 100 µl 2% PFA, transferred to FACS tubes containing 100 µl PBS and stored until acquisition.

Intracellular staining

To determine the cytokines secreted by immune cells intracellular staining was performed. Cells were re-suspended in 100 µl of cytofix/cytoperm buffer/well (BD Bioscience, USA) to fix the cells. Following 20 min incubation at 4˚C, cells were washed with 100 µl/well of 1x Perm wash buffer and centrifuged at 320 × g for 5 min at 4˚C. The supernatant was discarded and the washing step was repeated. The cells were re-suspended in 50 µl/well of 1x Perm wash buffer that contained the appropriate diluted antibodies (Table 4). After 20 min incubation at 4˚C, cells were washed with 100 µl of 1x Perm wash buffer and centrifuged at 320 × g for 5 min at 4˚C. The supernatant was discarded and the cells were washed once again. Then, cells were re-suspended in 200 µl PBS, transferred to FACS tubes and stored at 4˚C until acquisition.

Intranuclear staining

To determine the transcription factor expression by immune cells, intranuclear staining was performed. Cells were re-suspended in 100 µl/well of 1x Fixation/Permeabilization buffer (eBioscience, USA) to fix the cells. Following 1 h incubation at 4˚C, cells were washed with 100 µl of 1x Permeabilization buffer and centrifuged at 320 × g for 5 min at 4˚C. The supernatant was discarded and the cells were washed once again. Next, the cells were re-suspended in 50 µl/well of Permeabilization buffer that contained the

appropriate diluted antibodies (Table 4). After 20 min incubation at RT, cells were washed with 100 µl of 1x Permeabilization buffer and centrifuged at 320 × g for 5 min at 4˚C. The supernatant was removed and the wash step was repeated. Afterward, cells were re-suspended in 200 µl PBS, transferred to FACS tubes and stored at 4˚C until the analysis. Immune cells, *i.e.* T cells, were gated as displayed in the gating strategy (Figure 14).

Single stainings and compensation beads were prepared for each used fluorochrome for later compensation purposes to prevent false positive signals. The FACS measurement was performed by Fortessa (BD Bioscience, USA) and FlowJo was used for the analysis (Treestar Inc.).

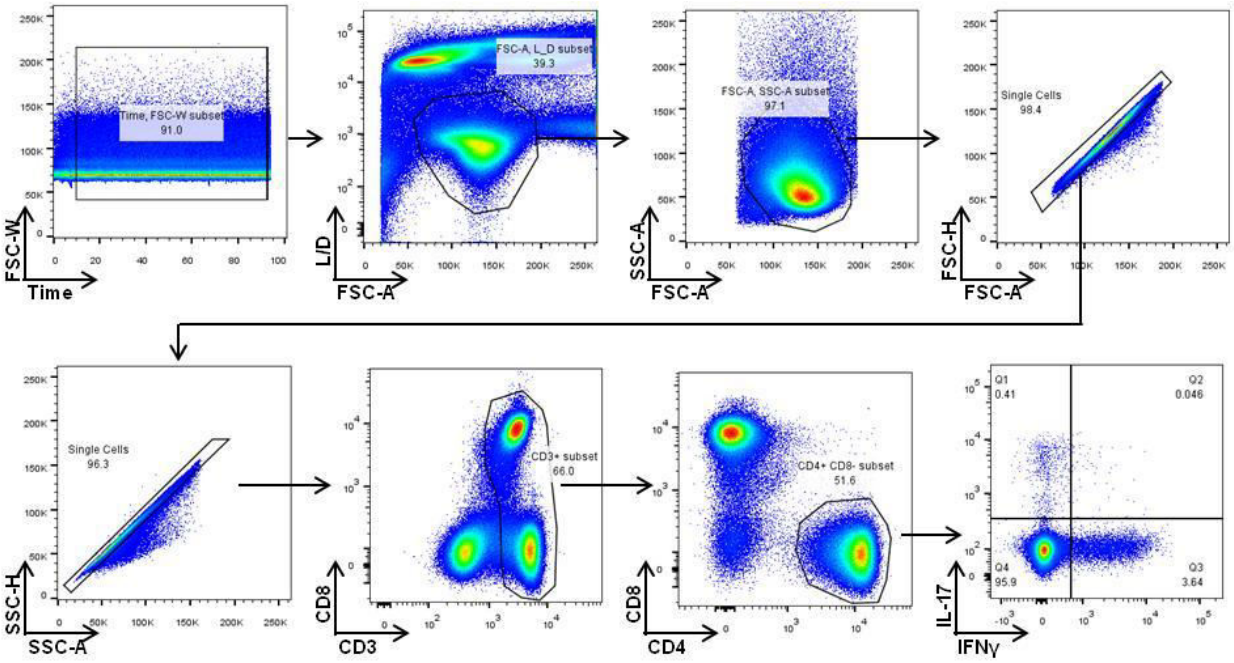

Figure 14: Gating strategy: Measurement distribution was excluded by gating SSC-W vs Time. Then, T cells were identified as the living single lymphocyte population that expresses CD3. Cells within this CD3 gate were further characterized into CD4 and CD8 phenotype. Further, from the CD4 gate the functionality of the cells was characterized based on the cytokine secretion.

4.2.11. Cell proliferation for cytokine assay

Splenic cells obtained from immunized mice were re-stimulated with the respective antigen to induce cytokine secretion. For this, 100 µl of spleen cells were distributed on 96-well plates at a concentration of 5×10^5 cells/well and further re-stimulated with OVA (40 µg/ml) or NIBRG-14 (2 µg/ml) at 37˚C in a humidified atmosphere containing 5% CO_2. Unstimulated cells served as the background control. After 72 h of incubation,

the plates were centrifuged at 300 rpm for 1 min and 100 µl of the supernatant was collected and stored at -20˚C for further analysis of secreted cytokines, described in 4.2.12.

4.2.12. Cytometric bead array (CBA)

The 13-plex FlowcytomixKit (CBA, AffymetrialeBioscience) combined with the analytes from the simplex Kits were used to assess changes in cytokine levels induced by re-stimulation of splenic cells derived from immunized animals. The lyophilized standards were centrifuged for a few seconds and reconstituted in sterile H_2O, according to the volume stated on each standard vial, swirled thoroughly and kept at RT for 20 min. Then, the standards were diluted 1:20 and filled up to 200 µl volume with assay buffer. A serial 1:3 dilution of the standard mix was performed. The vial containing the bead mix for each of the analytes was vortexed for 5 seconds and 1/20 of the final volume of each bead set was pipetted into a microcentrifuge tube. The tube was filled up to the final needed volume with 1x assay buffer. Then, the bead mix was vortexed and centrifuged for 5 min at 3000 × g. The supernatant was discarded and the pellet was re-suspended in the equal volume of 1x assay buffer that was removed. To prepare the biotin-conjugate solution 1/20 of the total needed volume (50 µl/test) of each biotin conjugate was pipetted to a new vial and filled up to the needed volume with 1x assay buffer. The prepared standard dilutions and the supernatant were plated into individual wells at a volume of 25 µl/well. In each well, including blanks that contained 1x assay buffer instead of the sample, 25 µl of the bead mix and 50 µl of the biotin conjugate were added. The plate was further incubated for 2 h at RT, protected from light. Next, the wells were washed with 100 µl 1x assay buffer and centrifuged for 5 min at 200 × g. The supernatants were discarded and the wash step was repeated. Then, 50 µl of a diluted streptavidin-PE solution was added and incubated for 1 h at RT, protected from light. The plate was washed twice as described above and the samples were transferred into FACS tubes in 300 µl 1x assay buffer. The setup beads were used to configure the flow cytometer. Samples were measured using the FACS Fortessa (BD Bioscience, USA) and analyzed with the FlowCytomix™ Pro 3.0 Software (Affymetrix/eBioscience).

4.2.13. In vivo Cytotoxic T Lymphocyte (CTL) assay

To assess the functionality of antigen-specific Th1 response, CTL assays were performed. For this, splenocytes from naïve mice were collected and single cell

suspensions were prepared in complete RPMI medium. The cells were then washed 3x with RPMI medium without FCS. Then, the cell concentration was adjusted to 20×10^6 cells/ml and the cells were divided into two aliquots of equal cell count. One aliquot of cells was labelled with 0.1 µM CFSE and the other with 1 µM CFSE and incubated for 7 min in the dark at 37˚ C. The reaction was stopped by filling up the falcon tubes with FBS and incubated for 10 min at 37˚ C. Then, the cells were centrifuged for 10 min at 240 × g and each pellet was resuspended with 20 ml of complete RPMI medium. The aliquot of 1 µm CFSE-labelled cells was pulsed with 15 µg/ml SINFEKL (OVA-peptide) for 1 h at 37°C whereas the second aliquot of cells was not pulsed. Next, cells were washed 2x with complete RPMI medium, the cell concentration was adjusted to 1×10^8 cells/ml in PBS and the two aliquots were pooled with the same amount of cells at 1:1 ratio. Subsequently, immunized mice were injected i.v. with 200 µl of CFSE-labeled donor cells and after 48 h of adoptive transfer spleen and lungs were collected and single cell suspensions were performed. The lysis capacity of CTLs in the spleens and lungs was assessed by FACS as a correlate of reduced $CFSE^+$ cell frequencies, according to the formula mentioned below.

$$\%\ \text{of lysis} = 100 - \left(\frac{(\%\ \text{of peptide pulsed cells})/(\%\ \text{of unpulsed cells})\ \text{immunized}}{(\%\ \text{of peptide pulsed cells})/(\%\ \text{of unpulsed cells})\ \text{control}}\right) \text{x}\ 100$$

4.2.14. ELISA measurement of antigen-specific IgG, IgG1 and IgG2c titers

To assess antigen-specific serum IgG, IgG1 and IgG2c titers ELISA was performed. For this, high-affinity binding 96 well plates were coated with 100 µl/well of OVA or NIBRG-14 at a concentration of 2 µg/ml diluted in coating buffer and incubated overnight at 4˚C. Then, plates were washed six times with wash buffer (PBS + 0.1% Tween-20) and blocked with 200 µl/well of blocking buffer (PBS + 3% BSA) and incubated for 1 h at 37˚C. The serum samples were diluted 1:1000 for OVA and 1:10,000 for NIBRG-14 in blocking buffer and 200 µl/well were added to the first column. Serial 1:2 dilutions (column 1 to11) were performed using the ELISA robot (Precision 2000, BioTek). Wells only incubated with blocking buffer served as blank control. The plates were incubated for 2 h at 37˚C, and then washed six times with wash buffer. Following addition of 100 µl/well of detection antibodies (Table 6) diluted in dilution buffer (PBS + 0.1% Tween-20 + 1%BSA), plates were incubated for 1 h at 37˚C followed by six times of wash procedure, described above. Then, 100 µl/well of streptavidin-HRP diluted at 1:1000 in dilution buffer were added and the plates were incubated for 30 min at

37˚C. Subsequently, the plates were washed again six times and incubated in the dark for 15 min at RT with 100 µl/well of ABTS substrate solution. The absorbance of light at 405 nm wavelength was measured using a synergy 2 Multi-Mode Microplate Reader. Titers were determined by subtracting the mean of the black samples as background. The results are expressed as endpoint titers, which are determined as the dilution that yielded the first OD405 value above the double value of the blank mean.

4.2.15. ELISA measurement of total IgA and antigen-specific IgA

To investigate humoral mucosal immune responses, antigen-specific IgA titers were measured by ELISA. High-affinity binding 96-well plates were coated overnight at 4˚C with 100 µl/well of either OVA or NIBRG-14 (2 µg/ml) or with anti-mouse IgA (2 µg/ml) dissolved in coating buffer. The lavage samples were diluted in blocking buffer 1:50 for the determination of total IgA and 1:10 for assessment of OVA-specific IgA. For determining NIBRG-14-specific IgA titers the starting dilution was 1:1000 for total IgA and 1:500 for NIBRG-14-specific IgA. The blocking buffer was used as blank control. The detection steps were performed as described in 4.2.13 for the measurement of IgG titers, but using a biotinylated goat- anti-mouse IgA antibody diluted 1:5000 in dilution buffer. Titers were determined by subtracting the mean of the blank samples as background. The concentrations shown in the result represent the end point of normalized concentration calculated as the amount of antigen-specific IgA concentration in 1 µg of total IgA concentration.

4.2.16. Microbial 16S analyses

To assess the microbial composition in the feces 16 S analyses were performed. Fecal pellets were collected and frozen immediately at -20°C until processing. DNA isolation was done using a phenol-chloroform based protocol. The methods used for 16S rRNA sequencing analyses are based on the Human Microbiome Project HMP. In brief, we employed Illumina Mi-seq 250 bp paired-end sequencing of the hypervariable V4 region. The obtained reads were assembled; quality controlled and clustered using the QIIME v1.8.0 (Quantitative Insights into Microbial Ecology) analysis pipeline. In short, quality filtering was set up to -q 30, minimum read length 200 bp and a minimum number of sequences per sample = 1000. The operational taxonomic unit (OTU) clusters and representative sequences were determined using open-reference OTU picking using UCLUST at 97% identity, followed by taxonomy assignment using the

RDP Classifier with a bootstrap confidence cutoff of 80%. The OTU absolute abundance table and mapping file are used for statistical analyses and data visualization in the R statistical programming environment, package PHYLOSEQ.

4.2.17. Immunofluorescence staining

Immunofluorescence staining to determine GC formation by evaluating localization of GC B cells and T_{FH} cells in draining LNs was performed at mousepathology platform at HZI, Braunschweig. For this, mice were immunized (day 0 and 6) with NIBRG-14 co-administered with c-di-AMP via i.n. route and the animals were sacrificed at day 12 and samples (cLNs and spleen) were collected. Samples were fixed in 4% neutrally buffered formaldehyde for 24 h and embedded in paraffin. Consecutive sections of 3 µm thickness were cut with a Microm HM 340E Microtom. Paraffin-embedded sections were subsequently deparaffinized and rehydrated. Heat-induced epitope retrieval was used. Tissue sections were cooked in citrate buffer using a pressure cooker. All further steps were performed in coverplates. Tissue sections were blocked with blocking solution for 5 min at RT. Working concentrations of primary antibodies were determined by performing titration of the stock solution and testing on a known positive specimen. The primary antibodies anti-CXCR5 and anti-PNA were incubated overnight at 4°C, with a working concentration of 1 to 50. For CXCR5 staining, tissue sections were incubated with primary antibody anti-CXCR5 and the secondary antibody Alexa Fluor 594-conjugated AffiniPure Goat anti-rabbit IgG for 30 minutes at RT. Background staining was performed with DAPI. Slides were covered with Vectashield Mounting Medium Hard Set (H -1400). Immunofluorescence stainings were evaluated two times randomized and blinded to the experimental groups at a Zeiss fluorescence microscope

4.2.18. Gene expression assessment by RT PCR

4.2.18.1. RNA extraction by TRIZOL

RNA from lung tissue was extracted to generate cDNA for the assessment of pIgR expression. For this, mice were immunized (day 0 and 14) with NIBRG-14 co-administered with c-di-AMP via i.n. route and the animals were sacrificed at day 15, 20 and 25 post immunization, and lung and lung lavage was collected. Lung tissues with a length of 2 cm long were collected and transferred into a microfuge tube containing 1mm beads and 1 ml of TRIZOL. The tissue was homogenized by placing the tubes in the beadbeater for 1 min and then rested on ice for 1 min. The step was repeated 3-4

times until the tissue was homogenized. Into each tube, 200 µl of chloroform was added, vortexed vigorously for 15 sec and incubated at RT for 3 min. The samples were centrifuged at 12,000 × g for 15 min at 4°C and the upper aqueous phase was collected without disturbing the interface. Then, 500 µl of isopropyl was added and the samples were incubated at -20°C overnight. Next day samples were centrifuged at 12,000 × g for 30 min at 4°C and the supernatant was discarded. The pellet was washed by re-suspending it in 1 ml of 75% EtOH. Samples were vortexed and centrifuged at 7,500 × g for 5 min at 4°C and the supernatant was discarded. The pellet was air-dried and dissolved in 100 µl of ddH_2O and stored at -80°C until further use.

4.2.18.2. cDNA generation and gene expression assessment by qPCR

To assess the mechanism for IgA response, pIgR expression was determined by synthesizing cDNA from RNA extracted from lung tissue. In a nuclease free tube 2 µg of RNA, 5 µl Oligo (dT) 18 primer and up to10 µl Diethyl pyrocarbonate (DEPC)-treated water were added and briefly centrifuged. The mixture was incubated at 65°C for 5 min, cooled on ice and briefly centrifuged. Then, 1x master mix was prepared containing 4 µl reaction buffer, 2 µl dNTP mix, 1 µl RevertAid^{TM} H minus Reverse Transcriptase and 3 µl DEPC-treated water. Next, 10 µl of master mix was added to the tubes containing the RNA mix. The tubes were briefly centrifuged and the samples were further incubated at 42°C for 60 min and then the reaction was terminated by heating at 85°C for 5 min. At the end, 180 µl of water was added to 20 µl of cDNA.

To perform qPCR 1x master mix consisting of 5 µl kappa master mix plus 0.5 µl primers (Table 14) was added into qPCR plates containing 4.5 µl cDNA. The plate was spun down and covered with the qPCR lid. The plate was loaded into the Real-Time cycler and SybrGreen detection program was run. The PCR cycle for SybrGreen protocol is mentioned in Table 15. Quantitative gene expression for pIgR was normalized to a house-keeping gene (GAPDH) expression.

4.2.19. Propagation and titration of influenza virus

4.2.19.1. Virus propagation in embryonated hen's eggs

Stocks of H5N1 virus were prepared by propagating virus in specific pathogen-free (SPF) eggs.The SFB eggs were placed in a humidified incubator at 37°C with 70% humidity with regular rotation for 10 days. Virus dilutions (10^{-3} and 10^{-4}) were prepared

in 1x PBS and placed on ice. The blunt end of all eggs was disinfected using iodine and with a sterile needle, a small hole was pierced in the shell over the air sac of each egg. Then, 200 µl of diluted virus solution was injected into the allantoic cavity and the eggs were sealed using glue. Further, the eggs were incubated for 48 h at 37°C and 50-70% humidity without rotation. Afterward, the eggs were placed overnight at 4°C to ensure that the embryo was dead. The virus was harvested by opening the blunt side of the eggs with a knife. Carefully the outer membrane was removed and the embryo was pressed with a spoon sideways and the allantoic fluid was collected with a pipette and placed into a 15 ml falcon tube on ice. The presence of the virus was determined by performing hemagglutination (HA) assay.

4.2.20. Hemagglutination assay

The HA assay was performed to determine the presence of the virus. From the undiluted virus obtained from each egg 100 µl were added to the first column of a 96 well V-bottom plate. In the remaining columns 50 µl of PBS was added and a serial 1:2 dilutions (column 1 to 11) was performed. Furthermore, 50 µl of 1% chicken red blood cells (RBCs) was added to each well and the plate was incubated at RT for 30 min. Wells containing RBCs in suspension were evaluated as positive yields, whereas in wells where the RBCs had settled down were evaluated as a negative yield. Falcons containing positive yield of the virus were pooled, aliquoted in 500 µl eppis and stored at -80°C for further use.

4.2.21. Microneutralization (MN) assay

MDCK cells were adjusted to 1.5×10^5 cells/ml in MEM medium. 200 µl of cells were added to each well in a 96 flat-bottom plate and were incubated for 4 h at 37°C, 5% CO_2. In another V-bottom plate, 50 µl of virus diluent was added to each well and additionally 40 µl of virus diluent was added into row A. 10 µl of RDE-treated serum samples were added into the row A and a serial 1:2 dilution (row B to H) was performed. Further 50 µl of virus containing 100 $TCID_{50}$ diluted in virus diluent was added into each well. Cells only incubated with medium or virus served as cell controls (CC) or virus controls (VC) respectively. The virus-serum mixtures were gently agitated and incubated for 1 h at 37°C, 5% CO_2. Virus-serum mixtures were then added to PBS-washed MDCK cell monolayers and 100 µl of virus diluent was added and the plates were incubated for overnight. Next day the medium was removed and cells were washed with 200 µl of PBS. 100 µl of cold fixative was added to each well and

incubated at RT for 10 min. Fixative was removed and the plates were washed three times with wash buffer. The plates were incubated for 2 h at 37˚C, and then washed three times with wash buffer. Following addition of 100 µl/well of primary antibody (anti-influenza A NP) diluted 1:1000 in blocking buffer (PBS + 0.1% Tween-20 + 1%BSA) plates were incubated for 1 h at RT followed by three times of wash procedure. Then, 100 µl/well of secondary antibody (Anti-Goat-HRP) diluted at 1:1000 in blocking buffer were added and the plates were incubated for 1 h at RT. Subsequently, the plates were washed for five times with wash buffer and 100 µl/well of freshly prepared substrate (o-phenylenediaminedihydrochloride) was added and incubated at RT for 10-15 min at RT and the reaction was stopped using stop solution (1 N H_2SO_4). The absorbance of light at 490 nm wavelength was measured using a synergy 2 Multi-Mode Microplate Reader. The virus neutralizing antibody end point titer was determined using the following equation.

$$\mathrm{X} = (\text{Average OD of CC wells}) + \left(\frac{(\text{Average OD of VC wells})/(\text{Average OD of CC wells})}{2}\right)$$

4.2.22. Challenge of immunized mice

Mice immunized with inactivated H5N1 as described in 3.2.6 were challenged with 2.5×10^4 foci forming units of the H5N1 virus diluted in 20 µl of PBS by i.n. route on day 42 post immunization. For the next following 7 days the animals were monitored with respect to their weight development and health conditions. Mice that had lost 20% of their starting bodyweight or showed abnormal clinical features with respect to physiological conditions were sacrificed and considered as killed by the infection.

4.2.23. Statistical analysis

Data were analyzed using the GraphPad Prism 6 software (GraphPad Software, USA). Statistical differences were assessed using student's *t* test for the comparison of independent groups. Two-way ANOVA statistical tests were performed for the comparison of multiple groups. Values of $p \leq 0.05$ were considered as statistically significant and in the figures * indicates $p \leq 0.05$, ** indicates $p \leq 0.01$, *** indicates $p \leq 0.001$, **** indicates $p \leq 0.0001$ and n.s. indicates not significant.

5. Results

5.1. Distribution of immune cells in WT and IL-17a/f deficient mice

The immune cell composition in WT and IL-17a/f$^{-/-}$ mice was analyzed in order to exclude possible discrepancies due to differences in the genetic background. This assessment represents a prerequisite for the subsequent immunization studies to evaluate the impact of c-di-AMP-induced IL-17 response in the generation of antigen-specific immune responses. For this, cells from spleensand lungs of naïve WT and IL-17a/f$^{-/-}$ mice were isolated and stained for the expression of surface markers that define specific immune cell populations: neutrophils (CD11c^{-} CD11b^{+} Ly6G^{+}), γδ T cells (CD3^{+}γδTCR^{+}), Th cells (CD3^{+} CD4^{+}), DCs (CD11c^{+}), NKT cells (CD3^{+} NK1.1^{+}) and CTLs (CD3^{+} CD8^{+}). The evaluation of the frequencies of γδ T cells, Th cells, DCs, NKT cells and CTL cells showed no significant differences between WT and IL-17a/f$^{-/-}$ mice (Figure 15).However, the frequency of neutrophils was significantly reduced in both spleen and lung of IL-17a/f$^{-/-}$ mice as compared to WT mice.

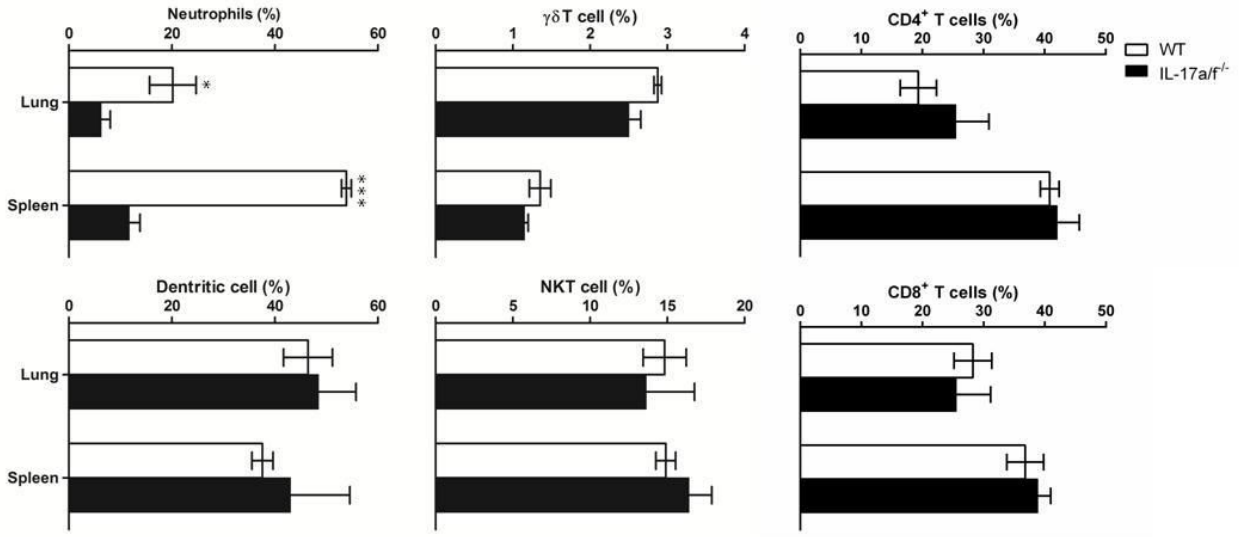

Figure 15: Distribution of immune cell populations in WT and IL-17a/f$^{-/-}$ mice: Splenocytes and lung lymphocytes were isolated from WT and IL-17a/f$^{-/-}$ mice, stained for specific surface markers of neutrophils (CD11c^{-} CD11b^{+} Ly6G^{+}), γδ T cells (CD3^{+} γδ TCR^{+}), Th cells (CD3^{+} CD4^{+}), DCs (CD11c^{+}), NKT cells (CD3^{+} NK1.1^{+}) and CTLs (CD3^{+} CD8^{+}), and further analyzed by flow cytometry. Frequencies of the cell populations were compared in naïve WT and IL-17a/f$^{-/-}$ mice. Columns represent the mean ± SEM (n=3), one out of two independent representative experiments is shown. Asterisks denotes significant values comparing WT and IL-17a/f$^{-/-}$ mice as calculated by unpaired t-test; *** $p < 0.0001$; * $p < 0.05$.

5.2. Comparison of two different adjuvants for their potential to induce IL-17 secreting cells

To assess whether *in vivo* administration of the adjuvants c-di-AMP and αGalCerMPEG can stimulate innate IL-17 secreting cells, a kinetic experiment was performed. For this, WT derived lung lymphocytes and splenocytes isolated 12 h or 72 h after i.n. administration of 5 µg of either αGalCerMPEG or c-di-AMP were analyzed for innate IL-17 secretion. The following innate immune cells known to secrete IL-17 after stimulation were investigated: γδ T cells, NKT cells, NK cells and $CD3^{-}CD4^{+}$LTi cells. Administration of αGalCerMPEG resulted in significantly increased MFI of lung IL-17^{+}γδ T cells and NKT cells at both investigated time points (Figure 16A and B left). Splenocytes displayed elevated MFI of IL-17^{+}γδ T cells and NKT cells 72 h, but not 12 h after αGalCerMPEG treatment (Figure 16A and B right). A αGalCerMPEG-induced secretion of IL-17 by NK cells and $CD3^{-}CD4^{+}$LTi cells was not detected (Figure 16C and D). In contrast, the adjuvant c-di-AMP did not induce any stimulation of innate IL-17 secretion cells at the different analyzed time points. These data demonstrate that αGalCerMPEG but not c-di-AMP induces innate IL-17 secretion.

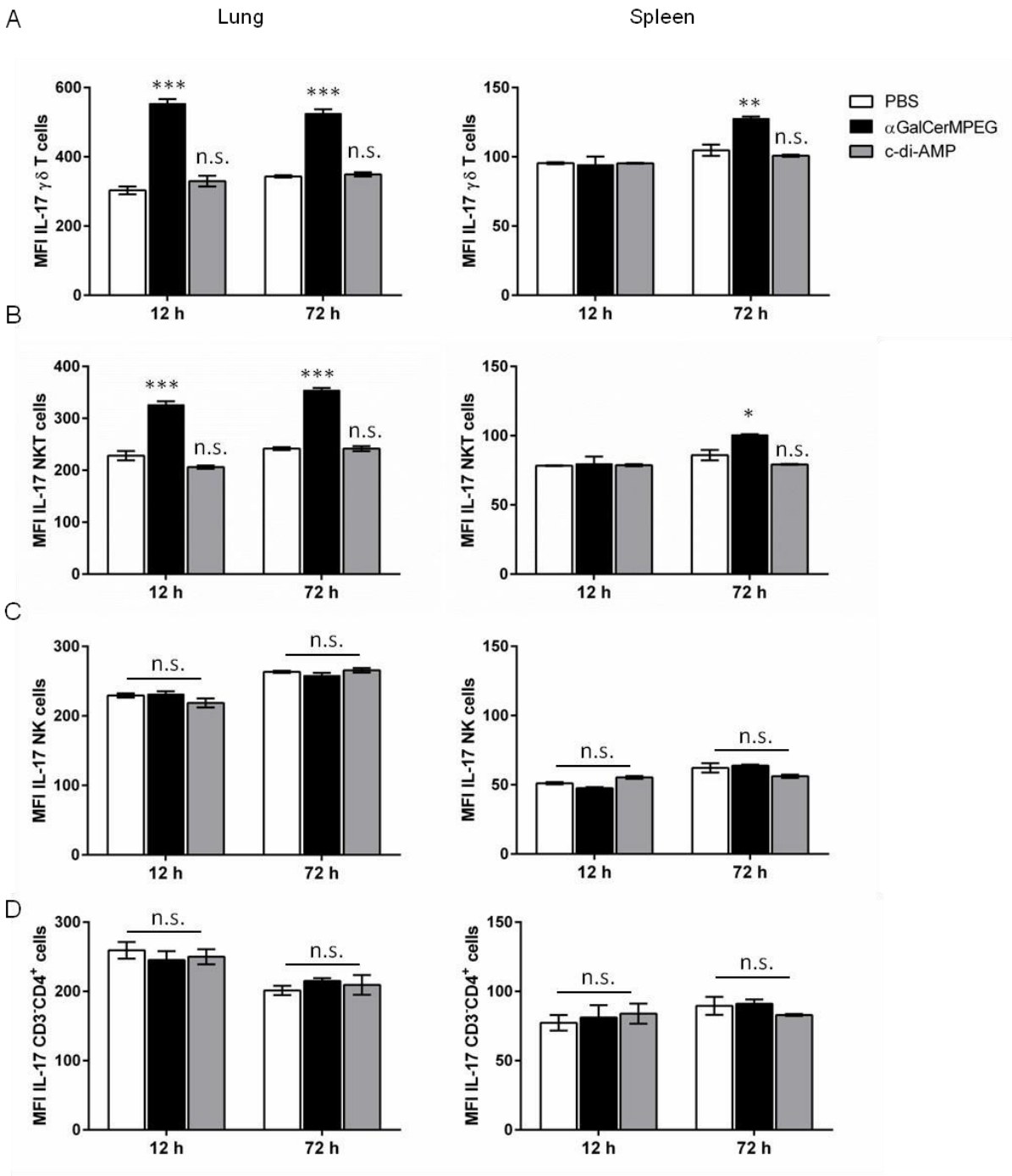

Figure 16: IL-17 secretion by γδ T cells and NKT cells upon adjuvant treatment: Naïve WT mice were i.n. administered with a single dose of αGalCerMPEG (5 µg) or c-di-AMP (5 µg). After 12 and 72h splenocytes and lung lymphocytes were isolated and subjected to flow cytometry analysis. MFI of IL-17 secreted by A) γδ T cells ($CD3^+\gamma\delta TCR^+$), B) NKT cells ($CD3^+NK1.1^+$), C) NK cells ($CD3^-NK1.1^+$) and D) $CD3^-CD4^+$cells are shown. Columns represent the mean ± SEM of one experiment (n=3). Asterisks denote significant values as calculated by Two-way ANOVA as compared to untreated controls; *** $p < 0.001$; ** $p < 0.01$; * $p < 0.05$; n.s. = not significant.

These findings show that although αGalCerMPEG blocks adaptive IL-17 responses as recently demonstrated in our group [163], it can induce the activation of certain innate IL-17 secreting immune cells. In contrast, c-di-AMP appears not to be able to stimulate innate IL-17 responses, whereas it has been shown by ELISPOT analysis to activate antigen-specific splenic IL-17 secretion [97]. To address which adaptive immune cells secrete IL-17 and whether also lung-derived immune cells can become activated by c-di-AMP, immunization studies in WT and IL-17a/f$^{-/-}$ mice using OVA as model antigen were performed. The antigen-specific immune responses were analyzed by FACS. WT mice immunized i.n. with OVA co-administered with c-di-AMP revealed significantly enhanced frequencies of splenic and lung IL-17-secreting CD4$^+$ T cells as compared to PBS and OVA alone (Figure 15A and B). This illustrates that c-di-AMP used as a mucosal adjuvant induces a strong Th17 response locally and systemically. As expected, immunization of IL-17a/f$^{-/-}$ mice with OVA co-administered with c-di-AMP did not induce any IL-17 secretion, thereby confirming the genetic background of the IL-17 deficient mouse strain.

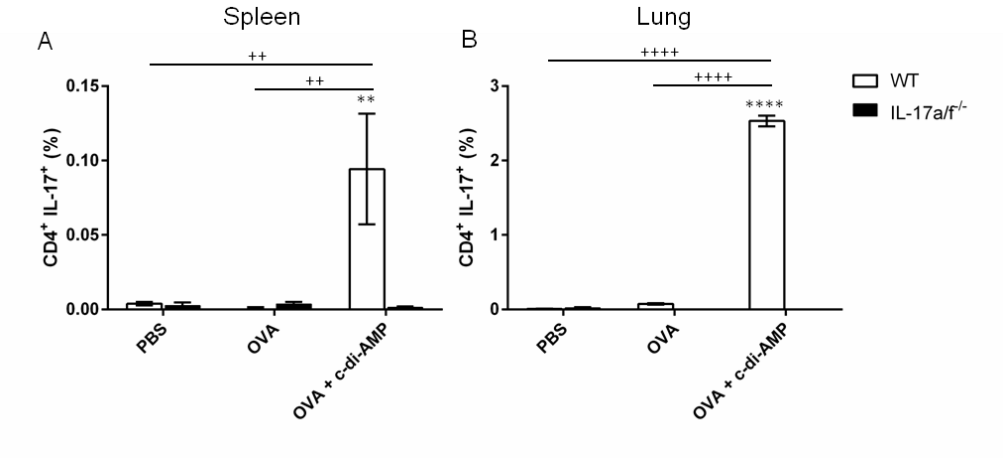

Figure 17: c-di-AMP-induced IL-17 secretion by CD4$^+$ T cells: WT and IL-17a/f$^{-/-}$ mice were i.n. immunized with PBS, OVA alone (10 µg/dose) or OVA co-administered with c-di-AMP (5 µg/dose) on days 0, 14 and 28. Splenocytes and lung lymphocytes of immunized mice were re-stimulated with OVA (40 µg/ml) overnight. The cells were incubated with brefeldin A (5 µg/ml) and monensin (6 µg/ml) for additional 4 h and then they were analyzed for IL-17-producing CD4$^+$ T cells (CD3$^+$ CD4$^+$) by flow cytometry. Frequencies of CD3$^+$CD4$^+$IL-17$^+$ cells in A) spleen and B) lung are shown. Results are expressed as subtracted background of unstimulated samples from stimulated samples. Columns represent the mean ± SEM of one experiment (n=5). Shown is one representative out of three independent experiments. Asterisks denote significant values as calculated by Two-way ANOVA comparing WT and IL-17a/f$^{-/-}$ mice;**** $p < 0.0001$; ** $p < 0.01$. Plus denote significant values as calculated by Two-way ANOVA comparing WT mice immunized with PBS, OVA alone or with OVA co-administered with c-di-AMP; ++++ $p < 0.0001$; ++ $p < 0.01$.

5.3. Mechanism of c-di-AMP-induced Th17 differentiation

As described above, c-di-AMP preferentially induces strong Th17 responses rather than innate IL-17 secreting cells following i.n. administration. However, the mechanisms contributing to the observed c-di-AMP-induced Th17 differentiation are still elusive. To address this point, an *in vitro* co-culture system consisting of $CD4^+$ T cells and BMDCs was established. Recent findings in our lab showed that c-di-AMP has the capacity to activate BMDCs as assessed by the up-regulation of co-stimulatory molecules and MHC class I and II expression [96, 115]. This model was used to investigate whether BMDCs derived from WT and IL-17a/f$^{-/-}$ mice differ in their capacity to differentiate $CD4^+$ T cells into Th17 cells upon c-di-AMP stimulation.

5.3.1. BMDCs derived from IL-17a/f$^{-/-}$ mice display reduced maturation upon treatment with c-di-AMP

To compare the maturation of BMDCs derived from WT and IL-17a/f$^{-/-}$ mice, BMDCs were treated with OVA or c-di-AMP alone or in combination and analyzed for their expression of CD86, MHC class I and MHC class II by FACS. Treatment with OVA alone did not result in BMDCs maturation as compared to untreated (medium) samples independently of the used mouse strain. However, stimulation with c-di-AMP alone or co-cultured with antigen induced a significant maturation of BMDCs in both WT and IL-17a/f$^{-/-}$ mice, as demonstrated by the enhanced surface expression of CD86, MHC class I and MHC class II (Figure 18A, B and C). The c-di-AMP induced expression of the maturation markers CD86 and MHC class I was more intense in BMDCs derived from WT as compared to IL-17a/f$^{-/-}$ mice (Figure 18A and B). No significant differences were observed in MHC class II expression comparing WT and IL-17a/f$^{-/-}$ mice upon treatment with OVA + c-di-AMP (Figure 18C). Interestingly, c-di-AMP-stimulated BMDCs displayed also an enhanced expression of IL-17RA in WT mice (Figure 18D). These findings show that BMDCs derived from IL-17a/f$^{-/-}$ mice display a reduced maturation after c-di-AMP treatment as compared to cells from WT mice.

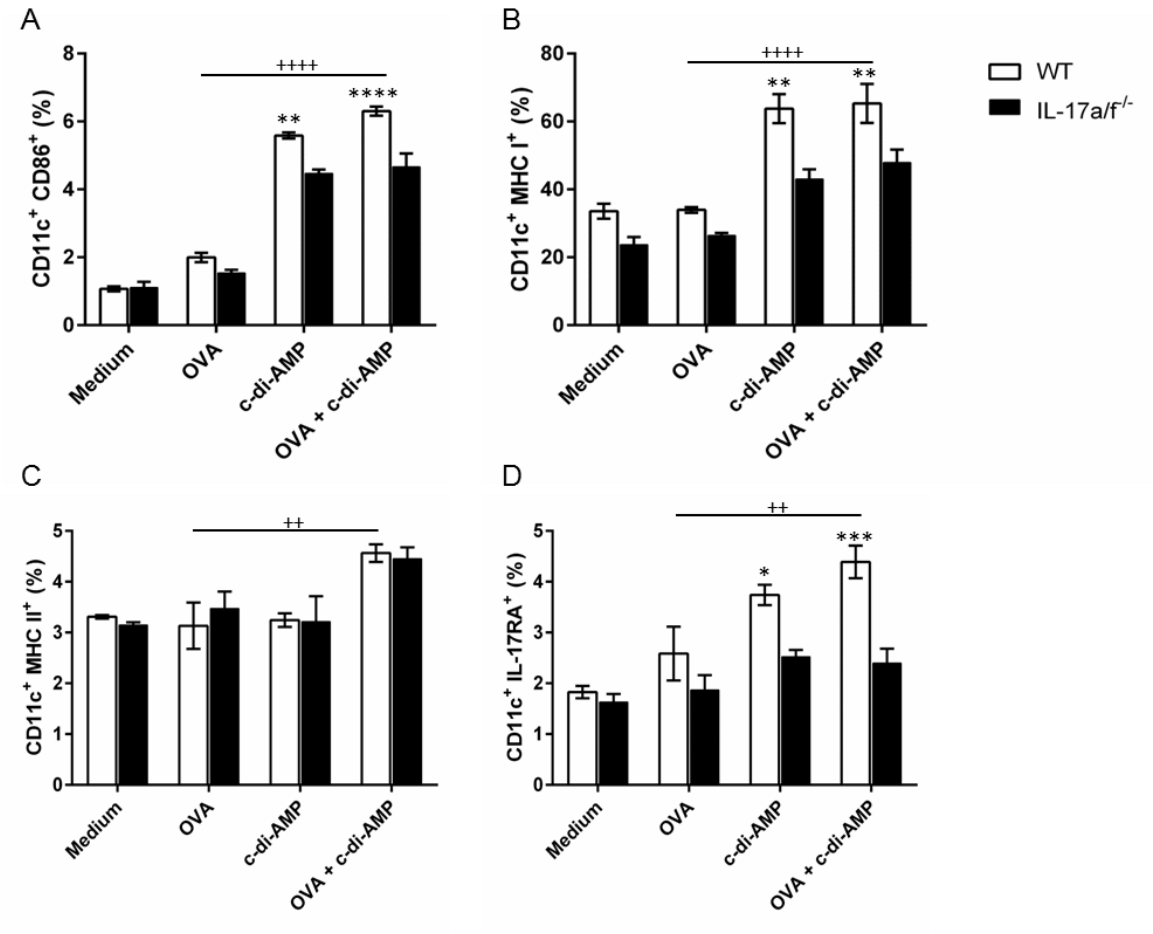

Figure 18: Expression of maturation markers and IL-17RA by BMDCs upon *in vitro* stimulation: GM-CSF-enriched BMDCs derived from WT and IL-17a/f$^{-/-}$ mice were left untreated or treated with OVA (40 µg/ml) or c-di-AMP (5 µg/ml) alone or in combination for 24 h. BMDCs (CD11c^{+}) were then stained for maturation markers A) CD86, B) MHC I C) MHC II and D) IL-17RA and analyzed by flow cytometry. Columns represent the mean ± SEM of one experiment (n=3). Shown is one representative out of three independent experiments. Asterisks denote significant values as calculated by Two-way ANOVA when comparing WT and IL-17a/f$^{-/-}$ BMDCs; **** $p < 0.0001$; *** $p < 0.001$; ** $p < 0.01$; * $p < 0.05$. Plus denote significant values as calculated by Two-way ANOVA when comparing BMDCs derived from WT mice treated with OVA alone and in combination with c-di-AMP; ++++ $p < 0.0001$; ++ $p < 0.01$.

5.3.2. BMDCs derived from IL-17a/f$^{-/-}$ mice are defective in driving Th17 differentiation upon c-di-AMP stimulation

The observed impaired maturation of BMDCs derived from IL-17a/f$^{-/-}$ mice suggested that deficient IL-17 production by DCs might affect Th17 differentiation. To address this issue the potential of c-di-AMP-stimulated BMDCs derived from WT or IL-17a/f$^{-/-}$ mice to mediate the differentiation of WT CD4^{+} T cells into Th17 cells was evaluated.To this end, CD4^{+} T cells derived from WT mice were activated by plate bound antibodies

(αCD3 and αCD28). BMDCs derived from either WT or IL-17a/f$^{-/-}$ mice were stimulated for 48 h with either OVA or c-di-AMP alone or OVA+c-di-AMP in combination, and then co-cultured with WT CD4^{+} T cells under different culture conditions (i.e. in presence of fresh medium or the supernatant fluids from the re-stimulated BMDCs). WT CD4^{+} T cells co-cultured with medium or supernatant derived from BMDCs supplemented with OVA alone, c-di-AMP alone or in-combination did not result in c-di-AMP induced Th17 generation. However, WT CD4^{+} T cells co-cultured with WT BMDCs-derived supernatant supplemented with OVA and c-di-AMP induced the differentiation of WT CD4^{+} T cells into Th17 cells as assessed by IL-17 secretion and RORγt expression. In contrast, WT CD4^{+} T cells co-cultured with BMDCs-derived supernatant from IL-17a/f$^{-/-}$ mice exhibited impaired effects on promoting Th17 differentiation (Figure 19A and B). These data suggest that an intacted IL-17 axis is required in BMDCs for achieving optimal maturation and subsequent stimulation of Th17 differentiation.

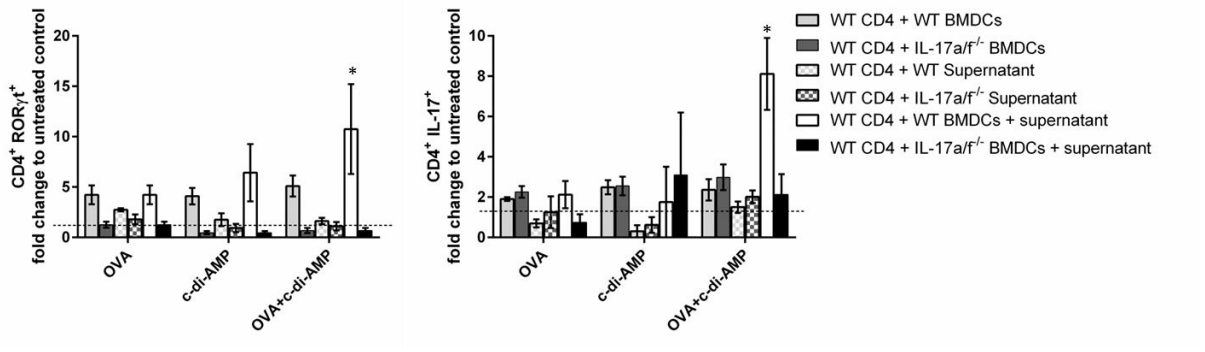

Figure 19: Th17 differentiation upon *in vitro* c-di-AMP stimulation: GM-CSF-enriched BMDCs derived from WT and IL-17a/f$^{-/-}$ mice were stimulated with either OVA alone (40 µg/ml), or c-di-AMP alone (5 µg/ml) or OVA in combination with c-di-AMP, and co-cultured with WT CD4^{+} T cells for 48 h. The cells were incubated with brefeldin A (5 µg/ml) and monensin (6 µg/ml) for additional 4 h, then stained for markers for Th17 differentiation (RORγt and IL-17) and further analyzed by flow cytometry. Columns represent the mean ± SEM of one experiment (n=3). Shown is one representative out of two independent experiments.Asterisks denote significant values as calculated by Two-way ANOVA when comparing WT and IL-17a/f$^{-/-}$ CD4^{+} T cells; * $p < 0.05$.

5.3.3. Identification of secreted mediators contributing to c-di-AMP-induced Th17 differentiation

BMDCs derived from IL-17a/f$^{-/-}$ mice showed impaired capacity to induce Th17 differentiation of CD4^{+} T cells. This suggests differences in the secreted cytokine profiles of WT and IL-17a/f$^{-/-}$ derived BMDCs stimulated with c-di-AMP. It has previously been reported that IL-1β, TGF-β, IL-6 and IL-23 secreted by DCs are involved in the development and maintenance of Th17 cells [164]. Thus, studies were performed to

address whether a changed cytokine secretion profile of BMDCs derived from IL-17a/f$^{-/-}$ mice is responsible for the impaired Th17 differentiation. To this end, the concentration of cytokines known to be required for Th17 differentiation was evaluated in the supernatant fluids of WT or IL-17a/f$^{-/-}$ derived BMDCs treated with OVA or c-di-AMP alone or in combination. The secretion of IL-23 was not detectable under any condition. The level of IL-1β and TGFβ production by WT and IL-17a/f$^{-/-}$ mice was not impacted by treatment with OVA alone, c-di-AMP alone or c-di-AMP co-administered with OVA as compared to untreated controls (Figure 20). However, IL-1β levels were in general higher in IL-17a/f$^{-/-}$ mice as compared to WT mice, regardless of the treatment. On the other hand, BMDCs derived from WT or IL-17a/f$^{-/-}$ mice stimulated with OVA +c-di-AMP or c-di-AMP alone exhibited enhanced IL-6 secretion as compared to untreated controls and OVA alone (Figure 20). No significant difference in the concentration of IL-6 was observed when comparing BMDCs derived from WT and IL-17a/f$^{-/-}$ mice (Figure 20).

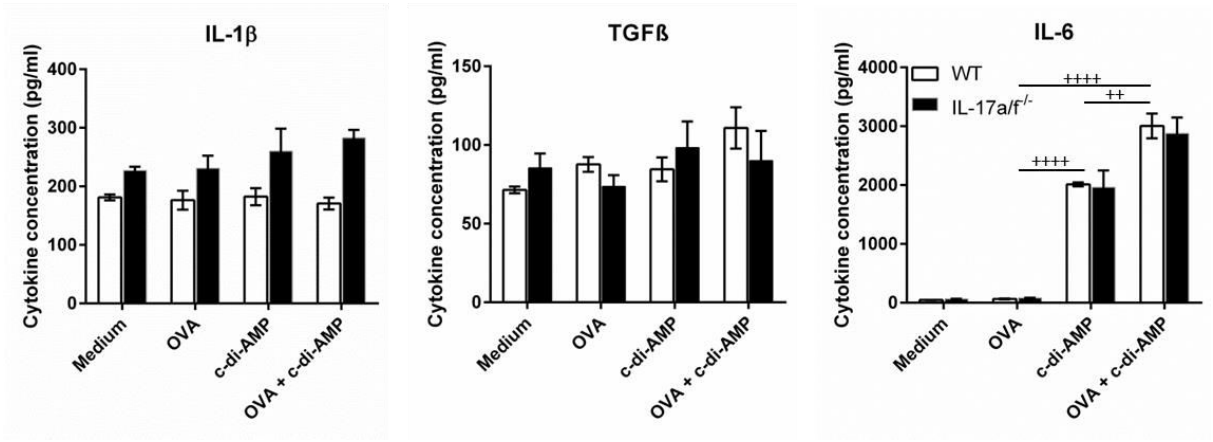

Figure 20: Cytokine secretion upon *in vitro* stimulation of BMDCs: GM-CSF-enriched BMDCs derived from WT and IL-17a/f$^{-/-}$ mice were stimulated *in vitro* with OVA alone (40 µg/ml), c-di-AMP alone (5 µg/ml) or OVA + c-di-AMP for 24 h. Subsequently, the supernatant was collected and analyzed for the concentration of IL-1β, TGFβ and IL-6 by cytometric bead array. Columns represent the mean ± SEM of one independent experiment (n=3). Plus denote significant values as calculated by Two-way ANOVA when comparing BMDCs derived from WT mice treated with OVA alone and with OVA in combination with c-di-AMP; ++++ $p < 0.0001$.

Since IL-23 was not detected in the supernatant of treated BMDCs, the frequency of cells expressing IL-12/IL-23p40 was evaluated by FACS. IL-12/IL-23p40 antibody reacts with the p40 subunit of IL-12 (p35p40) and IL-23 (p19p40) and is widely used to determine the frequency of cells expressing IL-12/IL-23 intracellularly by FACS. To this end, BMDCs treated for 24 h with OVA or c-di-AMP alone or in combination were incubated with brefeldin A and monensin for additional 4 h and subsequently analyzed. The frequency of IL-12/IL-23p40^{+} CD11c^{+} BMDCs derived from WT and IL-17a/f$^{-/-}$ mice

following stimulation with OVA and c-di-AMP was 20 and 10-fold higher as compared to the control and OVA-stimulated samples, respectively (Figure 21A and B). However, $CD11c^{+}$ BMDCs derived from IL-17a/$f^{-/-}$ mice displayed reduced frequencies of IL-12/IL-23p40 expression on cells as compared to BMDCs derived from WT mice (Figure 21B). The MFI of IL-12/IL-23p40^{+} cells confirms that BMDCs derived from WT mice upon treatment with OVA and c-di-AMP have a higher capacity to induce IL-12/IL-23p40 expression as compared to BMDCs derived from IL-17a/$f^{-/-}$ mice (Figure 21C). These findings suggest that the observed defective Th17 differentiation of WT $CD4^{+}$ T cells co-incubated with IL-17a/$f^{-/-}$ derived BMDCs is in part due to an impaired IL-23 expression, thereby suggesting IL-23 as a crucial factor for c-di-AMP induced Th17 differentiation.

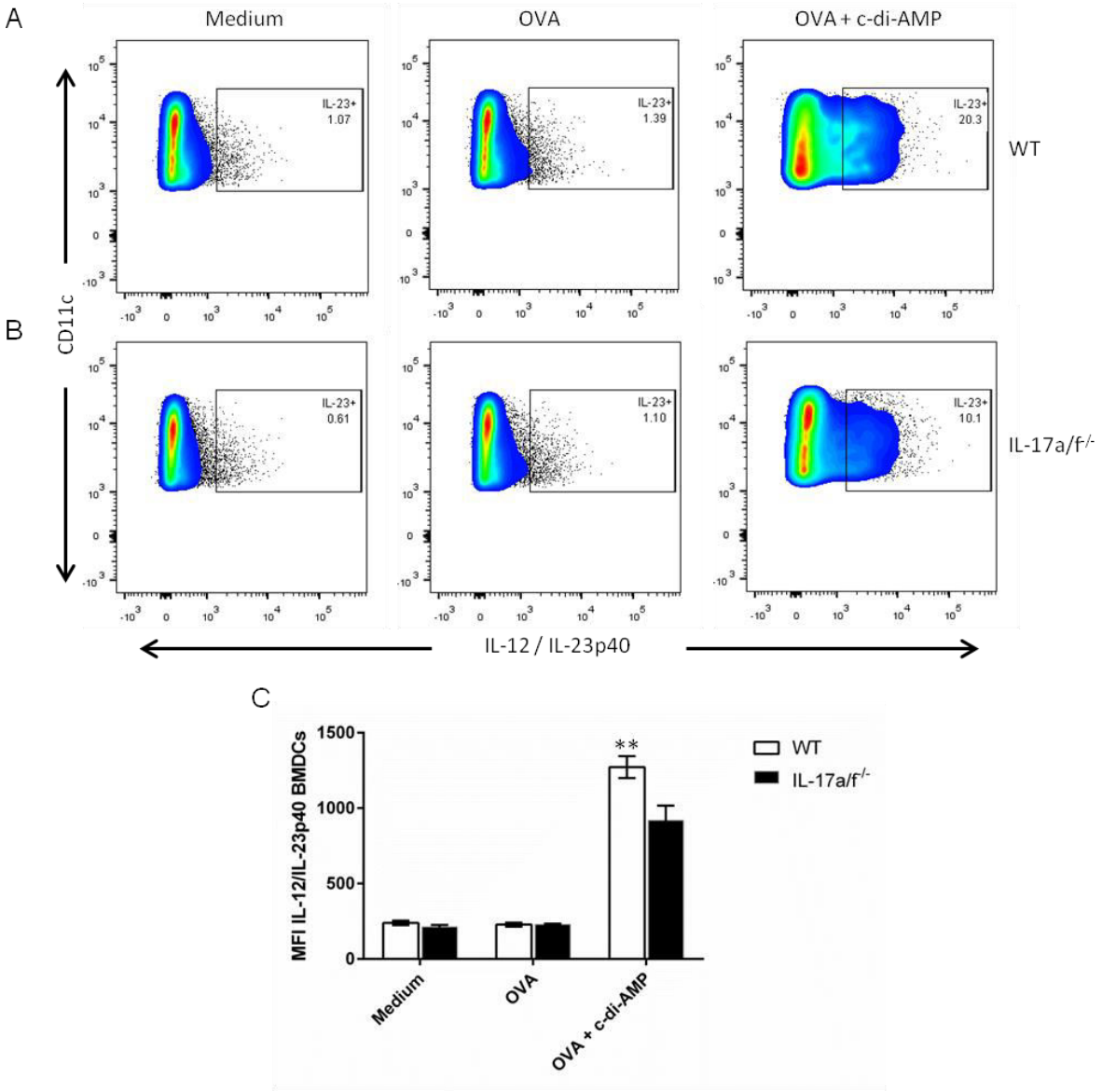

Figure 21: IL-12/IL-23p40 expression on BMDCs upon *in vitro* stimulation: GM-CSF-enriched BMDCs derived from WT and IL-17a/f$^{-/-}$ mice were left untreated (medium) or stimulated with either OVA alone (40 µg/ml) or OVA co-administered with c-di-AMP (5 µg/ml) for 24 h. Then, cells were incubated with brefeldin A (5 µg/ml) and monensin (6 µg/ml) for additional 4 h, further stained for the DC marker CD11c and intracellular IL-12/IL-23p40, and subsequently analyzed by flow cytometry. Frequencies of CD11c^{+}IL-12/IL-23p40^{+} cells derived from A) WT and B) IL-17/f$^{-/-}$ mice are shown. Results are depicted as percentage of IL-12/IL-23p40 producing cells within the CD11c^{+} cell subpopulation. C) MFI of IL-12/IL-23p40 expressed by BMDCs derived from WT and IL-17a/f$^{-/-}$ mice analyzed 24 h post treatment. Columns represent the mean ± SEM of one experiment (n=3). One representative out of two independent experiments is shown. Asterisks denote significant values as calculated by Two-way ANOVA when comparing WT and IL-17a/f$^{-/-}$ BMDCs; ** $p < 0.01$.

5.3.4. IL-6 is required for c-di-AMP-induced Th17 differentiation

The differentiation of naïve T cells into Th17 cells and the subsequent stabilization of this commitment were shown to be dependent on IL-6 and IL-23 respectively [165-167]. In addition, the stimulation of naïve T cells with IL-23 was described to result in the generation and expansion of pathogenic Th17 cells [168]. The strong increase in IL-6 levels and IL-23 expression on BMDCs 24 h after c-di-AMP stimulation hints towards a potential role for both cytokines with respect to the observed Th17 differentiation (Figure 19, Figure 20 and Figure 21). Therefore, to confirm the role of IL-6 and IL-23 for c-di-AMP-induced Th17 differentiation, the *in vitro* were repeated in the presence of αIL-6 and αIL-23 blocking antibodies and Th17 differentiation was analyzed by flow cytometry. As observed earlier, co-culture of WT $CD4^+$ T cells and BMDCs in the presence of c-di-AMP alone or in combination with OVA induced significant Th17 differentiation as compared to cultures supplemented with OVA alone. BMDCs derived from IL-17a/$f^{-/-}$ mice exhibited an impaired effect on Th17 differentiation under all tested conditions (Figure 20). The supplementation of αIL-6 blocking antibodies resulted in a significant reduction of Th17 ($CD4^+IL\text{-}17^+$) cells, whereas the addition of αIL-23 blocking antibodies had no impact on c-di-AMP-induced Th17 differentiation (Figure 22). These obtained results indicate that c-di-AMP-stimulated enhanced IL-6 secretion in WT and IL-17a/$f^{-/-}$ mice is required for the c-di-AMP-induced Th17 differentiation, as confirmed by an impaired c-di-AMP-induced Th17 differentiation upon blocking of IL-6 signaling.

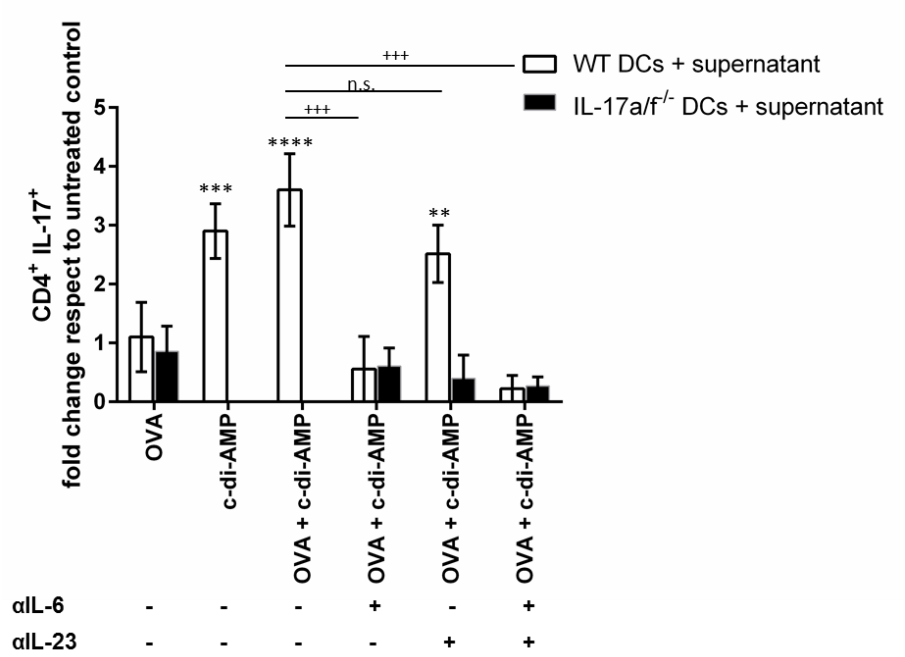

Figure 22: Impact of IL-6 and IL-23 blocking on c-di-AMP-induced Th17 differentiation: GM-CSF-enriched BMDCs derived from WT and IL-17a/f$^{-/-}$ mice were stimulated with OVA alone (40 µg/ml), c-di-AMP alone (5 µg/ml) or OVA + c-di-AMP and co-cultured with WT CD4^{+} T cells in the presence of αIL-6 or αIL-23 alone or in combination for 48 h. The cells were incubated with brefeldin A (5 µg/ml) and monensin (6 µg/ml) for additional 4 h and subsequently stained for the secretion of IL-17 by CD3^{+}CD4^{+} cells as a correlate of Th17 differentiation and analyzed by flow cytometry. Results are expressed as fold change respect to untreated controls. Columns represent the mean ± SEM of one experiment (n=3). Shown is one representative out of two independent experiments. Asterisks denote significant values as calculated by Two-way ANOVA comparing WT and IL-17a/f$^{-/-}$ CD4^{+} T cells; **** $p < 0.0001$; *** $p < 0.001$; ** $p < 0.01$. Plus denote significant values between different treatment groups of OVA co-administered with c-di-AMP as calculated by Two-way ANOVA; +++ $p < 0.001$; n.s. = not significant.

5.4. Impact of c-di-AMP-induced IL-17 secretion on the elicitation of antigen-specific adaptive immune response

The role of IL-17 in augmenting antigen-specific T helper cells, cytotoxic $CD8^+$ T cells and humoral responses still remains elusive. Therefore, immunization experiments were performed to evaluate the immune stimulatory potency of c-di-AMP-induced IL-17 secretion in the elicitation of antigen-specific immune responses. To this end, WT and IL-17a/f$^{-/-}$ mice were immunized by i.n. route with PBS, OVA alone (10 µg) or OVA co-administered with c-di-AMP (5 µg) on day 0, 14 and 28 (Figure 23). On day 42 serum, nasal and lung lavage samples were collected from the animals and analyzed for determining humoral (IgG and IgA production) immune responses. Single cell suspensions were also prepared from cLN, lung and spleen that were used to analyze cellular immune parameters (analysis of T and B cell functionality and cytokine production).

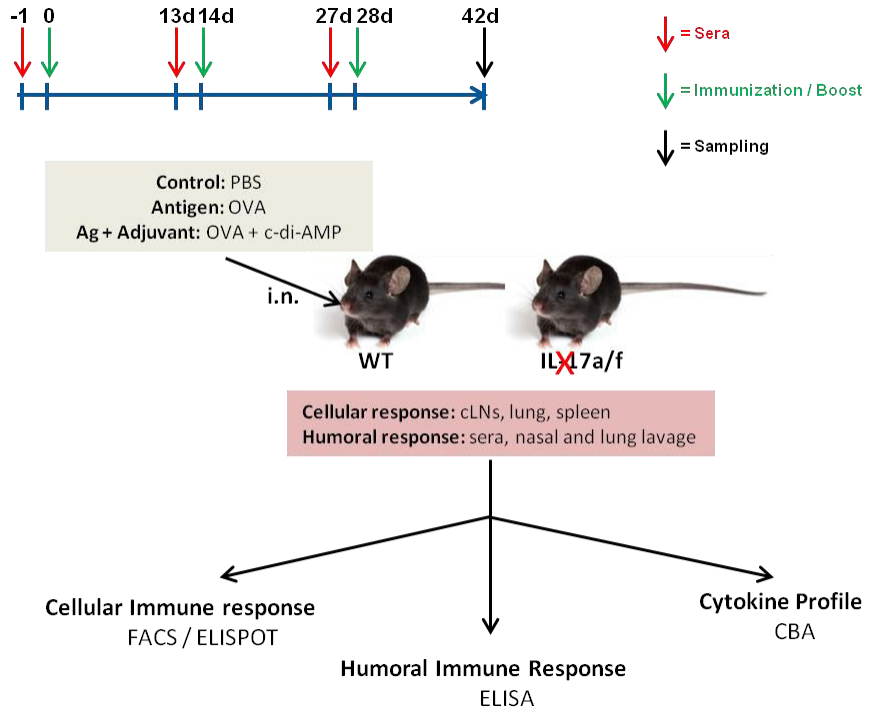

Figure 23: Experimental design for the evaluation of antigen-specific immune responses: WT and IL-17a/f$^{-/-}$ mice were i.n. immunized with PBS, OVA alone (10 µg/dose) or OVA co-administered with c-di-AMP (5 µg/dose) on day 0 and received booster doses at day 14 and 28. The sampling was performed on day 42 after the initial immunization. Nasal and lung lavages were collected to evaluate the mucosal humoral response (IgA production). Serum samples were collected in order to analyze the systemic humoral response (IgG production). Spleen and lung cells were re-stimulated with the antigen and antigen-specific activation was evaluated by FACS and ELISPOT. The cytokine profile in the supernatant of *ex vivo* re-stimulated splenocytes was evaluated by CBA.

5.4.1. c-di-AMP-induced IL-17 secretion enhances OVA-specific Th2 and humoral responses

To explore the potency of c-di-AMP-induced IL-17 secretion to enhance antigen-specific Th2 responses, the secretion of IL-4 by splenocytes was assessed by ELISPOT following re-stimulation with OVA. The number of IL-4-producing cells was significantly enhanced in samples derived from WT animals immunized with OVA co-administered with c-di-AMP as compared to samples derived from WT and IL-17a/f$^{-/-}$ animals immunized with PBS or OVA alone (Figure 24A). Furthermore, a significant reduction in the number of IL-4-producing cells was observed in IL-17a/f$^{-/-}$ mice immunized with OVA co-administered with c-di-AMP as compared to WT mice. To elucidate which specific cell population is responsible for the detected IL-4 secretion, splenic and lung single cell suspensions derived from individual animals were re-stimulated with OVA (40 µg/ml) and subjected to FACS analysis. In accordance with the data derived from the ELISPOT analysis, the absolute number of splenic IL-4 secreting CD4^{+} T cells was significantly reduced in IL-17a/f$^{-/-}$ animals immunized with OVA co-administered with c-di-AMP as compared to the WT counterparts (Figure 24B). IL-4 secreting cells were not detected in the lungs of WT or IL-17a/f$^{-/-}$ mice (data not shown). These data demonstrate that c-di-AMP-induced IL-17 secretion drives the stimulation of Th2 responses.

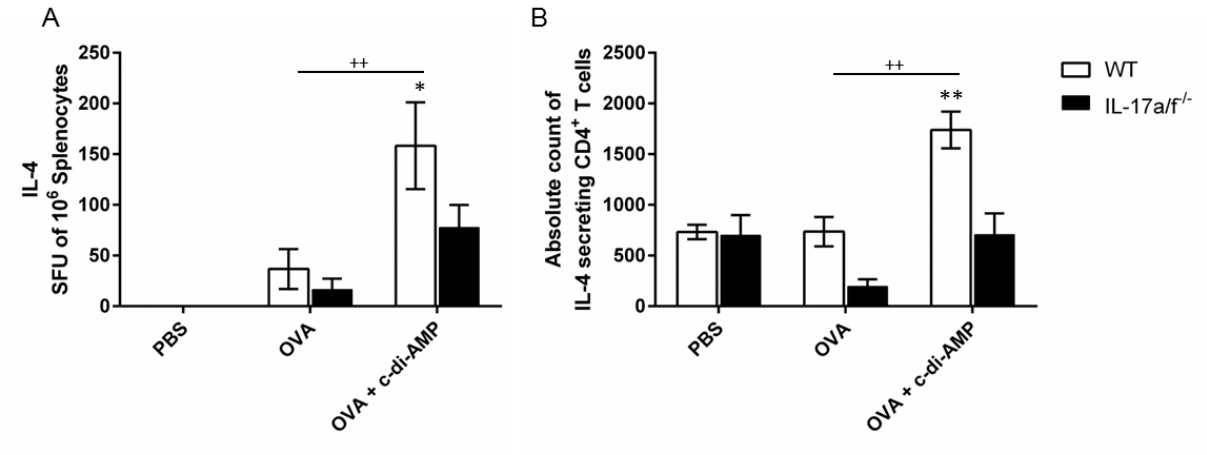

Figure 24: Impact of c-di-AMP-induced IL-17 secretion on antigen-specific Th2 responses: WT and IL-17a/f$^{-/-}$ mice were i.n. immunized with PBS, OVA alone (10 µg/dose) or OVA co-administered with c-di-AMP (5 µg/dose). Splenocytes were re-stimulated with OVA (40 µg/ml) overnight. The cells were incubated with brefeldin A (5 µg/ml) and monensin (6 µg/ml) for additional 4 h and were analyzed by ELISPOT and flow cytometry. A) IL-4-secreting cells identified by ELISPOT assay and B) absolute number of IL-4 secreting CD4^{+} T cells identified by flow cytometry. Results are expressed as subtracted background of unstimulated samples from stimulated samples. Columns represent the mean ± SEM of one experiment (n=5). Shown is one representative out of three independent experiments. Asterisks denote significant values as calculated by Two-way ANOVA when comparing WT and IL-17a/f$^{-/-}$ mice;** $p < 0.01$; * $p < 0.05$. Plus denote significant value as calculated by Two-way ANOVA when comparing WT mice immunized with OVA alone or OVA co-administered with c-di-AMP; ++ $p < 0.01$.

To understand the impact of c-di-AMP-induced IL-17 secretion on the OVA-specific Th1 response, splenocytes werere-stimulated with OVA (40 µg/ml) and the number of IFNγ producing splenic cells was evaluated by ELISPOT. In both WT and IL-17a/f$^{-/-}$ mice, the number of IFNγ-secreting splenic cells was significantly enhanced in the groups immunized with OVA co-administered with c-di-AMP as compared to OVA and PBS alone. Interestingly, IL-17a/f$^{-/-}$ mice immunized with OVA co-administered with c-di-AMP displayed a higher number of CD4^{+}IFNγ-secreting cells as compared to WT mice (Figure 25A). These findings were confirmed by FACS analysis of OVA re-stimulated (40 µg/ml) splenic and lung single cell suspensions that showed elevated frequencies of CD4^{+}IFNγ-secreting cells in both organs derived from IL-17a/f$^{-/-}$ mice immunized with OVA co-administered with c-di-AMP as compared to WT mice (Figure 25B and C). These data indicate that immunization with c-di-AMP induces Th1 responses that are stronger in the absence of IL-17 signaling.

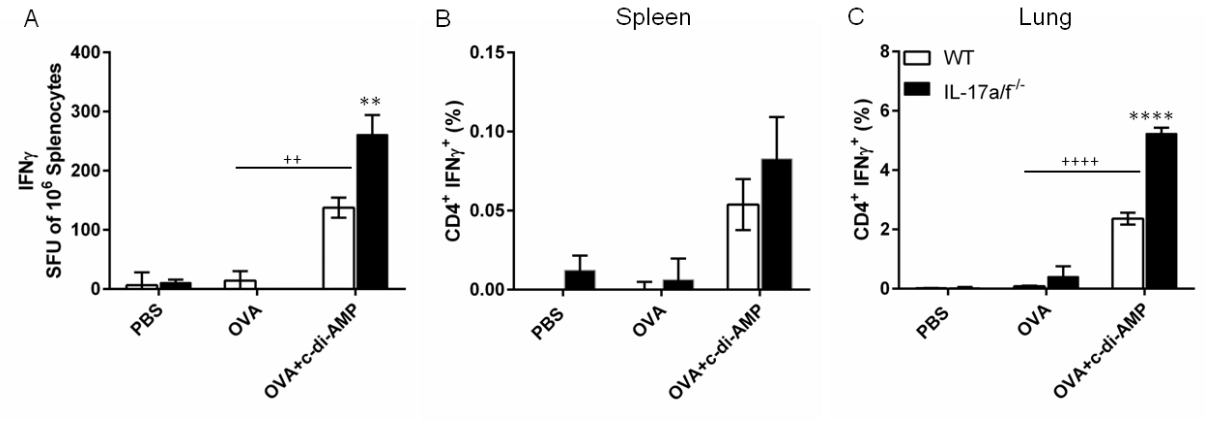

Figure 25: Impact of c-di-AMP-induced IL-17 on antigen-specific Th1 responses: WT and IL-17a/f$^{-/-}$ mice were i.n. immunized with PBS or OVA alone (10 µg/dose) or OVA co-administered with c-di-AMP (5 µg/dose). Splenic and lung lymphocytes were re-stimulated with OVA (40 µg/ml) overnight. The cells were incubated with brefeldin A (5 µg/ml) and monensin (6 µg/ml) for additional 4 h and then analyzed for A) IFNγ secreting cells by ELISPOT (splenocytes), and frequencies of B) splenic and C) lung-derived CD4$^+$ T cells by FACS. Results are expressed as subtracted background of unstimulated samples from stimulated samples. Columns represent the mean ± SEM of one experiment (n=5). Shown is one representative out of two independent experiments. Asterisks denote significant values as calculated by Two-way ANOVA when comparing WT and IL-17a/f$^{-/-}$ mice; **** $p < 0.0001$; ** $p < 0.01$. Plus denote significant valuesas calculated by Two-way ANOVA when comparing WT mice immunized with OVA alone and with OVA co-administered with c-di-AMP; ++++ $p < 0.0001$; ++ $p < 0.01$.

In addition to the Th responses, CTLs represent an important effector mechanism within the cellular immune system. Therefore, to address the impact of c-di-AMP-induced IL-17 secretion on CTLs, the frequency of lung-derived CD8$^+$ IFNγ-secreting was determined by FACS. Consistent with the findings presented for the Th1 response, an enhanced IFNγ secretion by CD8$^+$ cells was detected in samples derived from WT and IL-17a/f$^{-/-}$ mice immunized with OVA co-administered with c-di-AMP as compared to the PBS and OVA immunized groups. Interestingly, an enhanced number of lung-derived IFNγ-secreting CD8$^+$ cells was observed in IL-17a/f$^{-/-}$ mice immunized with OVA co-administered with c-di-AMP as compared to corresponding WT group (Figure 26A). Furthermore, the functionality of OVA-specific CTLs was evaluated by performing an *in vivo* CTL assay. For this, immunized mice were injected i.v. with CFSE-labeled donor cells pulsed with OVA antigen and the lysis capacity of CTLs in the lungs was assessed by FACS. The cytotoxic capacity was significantly enhanced in WT and IL-17a/f$^{-/-}$ animals immunized with OVA co-administered with c-di-AMP as compared to the PBS or OVA alone groups. IL-17a/f$^{-/-}$ mice displayed an enhanced lysis capacity as compared to WT mice (Figure 26B). These data demonstrate that c-di-AMP-induced CTL responses are further increased in the absence of IL-17 signaling.

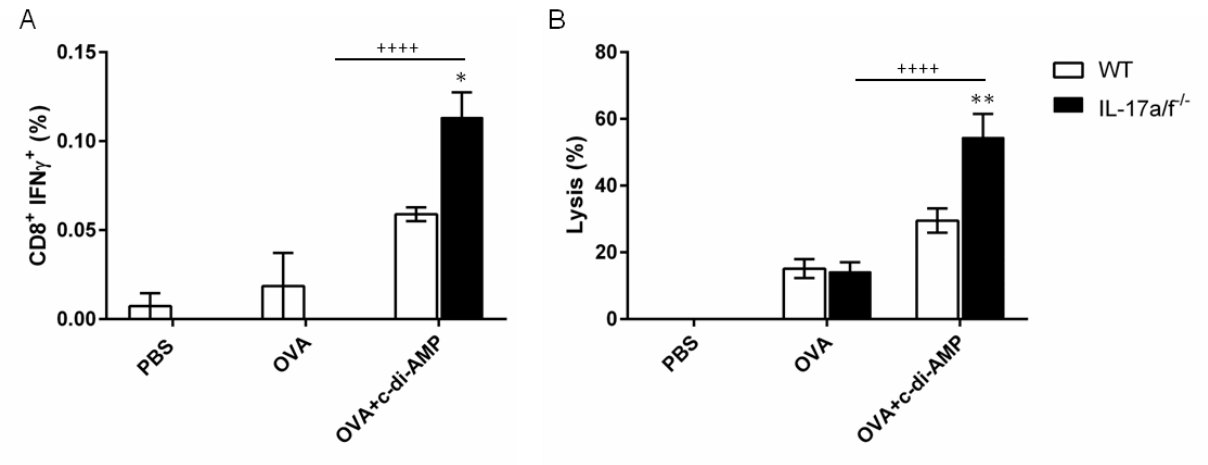

Figure 26: Impact of c-di-AMP-induced IL-17 secretion on the activation of cytotoxic T lymphocytes: WT and IL-17a/f$^{-/-}$ mice were i.n. immunized with PBS or OVA alone (10 µg/dose) or OVA co-administered with c-di-AMP (5 µg/dose). Lung lymphocytes were re-stimulated with OVA (40 µg/ml) overnight. The cells were incubated with brefeldin A (5 µg/ml) and monensin (6 µg/ml) for additional 4 h and then analyzed for A) the frequency of IFNγ producing CD8^{+} T cells by FACS, and B) cytolytic activity of lung cells from WT and IL-17a/f$^{-/-}$ mice upon immunization. Results are expressed as subtracted background of unstimulated samples from stimulated samples. Columns represent the mean ± SEM of one independent experiment (n=5). Asterisks denote significant values as calculated by Two-way ANOVA when comparing WT and IL-17a/f$^{-/-}$ mice; ** $p < 0.01$ * $p < 0.05$. Plus denote significant values as calculated by Two-way ANOVA when comparing WT mice immunized with OVA alone and with OVA co-administered with c-di-AMP; ++++ $p < 0.0001$.

Besides the cellular immune response, the humoral immune response plays an important role in providing protection against pathogens. Therefore, to understand the role of c-di-AMP-induced IL-17 for the generation of systemic humoral immunity, IgG titers in sera derived from immunized mice were analyzed by ELISA. Immunization of WT and IL-17a/f$^{-/-}$ mice with OVA co-administered with c-di-AMP stimulated enhanced IgG titers as compared to PBS and OVA alone (Figure 27A). Furthermore, a significantly lower level of IgG was detected in IL-17a/f$^{-/-}$ mice as compared to corresponding WT group (Figure 27A). The analysis of the IgG subclasses IgG1 and IgG2c in sera derived from mice immunized with OVA co-administered with c-di-AMP revealed significantly lower levels of IgG1 in IL-17a/f$^{-/-}$ mice as compared to WT mice. In contrast, no significant differences were observed regarding IgG2c titers (Figure 27B). These findings suggest that c-di-AMP-induced IL-17 secretion supports systemic humoral responses induced by Th2 cells as shown by high IgG1 titers. These results are in agreement with the observed T helper responses (see above).

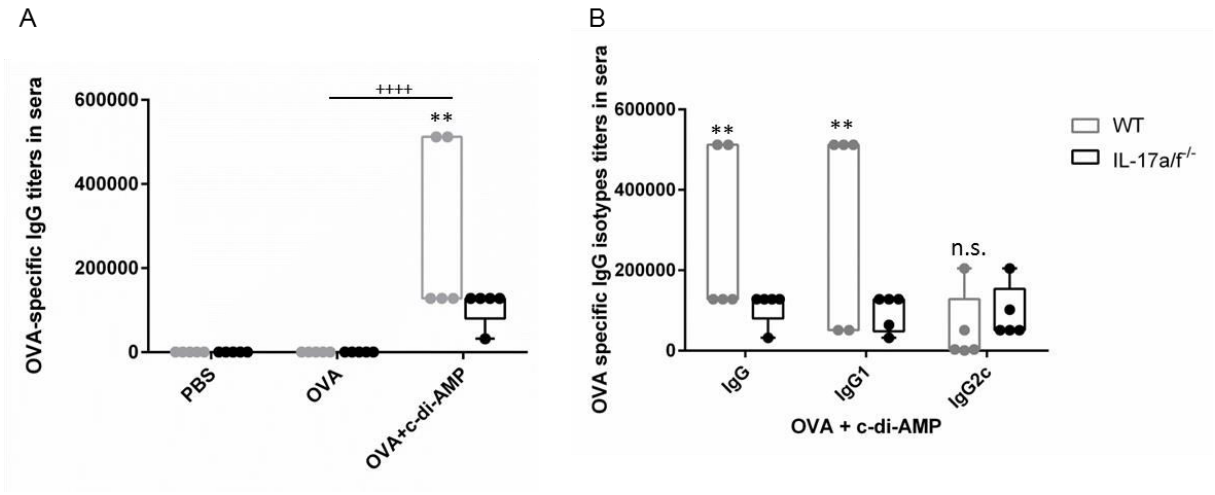

Figure 27: Impact of c-di-AMP-induced IL-17 secretion on antigen-specific IgG production: WT and IL-17a/f$^{-/-}$ mice were i.n. immunized with PBS, OVA alone (10 µg/dose) or OVA co-administered with c-di-AMP (5 µg/dose). Sera of individual animals were analyzed for the level of antigen-specific IgG and IgG isotype titers by ELISA. OVA-specific titres of A) IgG and B) IgG, IgG1 and IgG2c were determined. Boxes represent the interquartile range, horizontal lines show the mean value and whiskers show the overall range of the data. Columns represent the mean ± SEM of one experiment (n=5). Shown is one representative out of three independent experiments. Asterisks denote significant values as calculated by Two-way ANOVA when comparing WT and IL-17a/f$^{-/-}$ mice; ** $p < 0.01$; n.s. = not significant. Plus denote significant value as calculated by Two-way ANOVA when comparing WT mice immunized with OVA alone and with OVA co-administered with c-di-AMP; ++++ $p < 0.0001$.

To further understand the impact of c-di-AMP-induced IL-17 secretion on mucosal immunity, IgA concentrations were analyzed in nasal washes as well as lung lavage samples by ELISA. In both, WT and IL-17a/f$^{-/-}$ mice, the IgA concentrations were significantly enhanced in mice immunized with OVA co-administered with c-di-AMP as compared to PBS and OVA alone (Figure 28). Significantly lower levels of OVA-specific IgA were detected in nasal and lung lavage samples derived from IL-17a/f$^{-/-}$ mice as compared to WT mice (Figure 28A and B). This indicates that c-di-AMP-induced IL-17 secretion positively impacts the local mucosal humoral response.

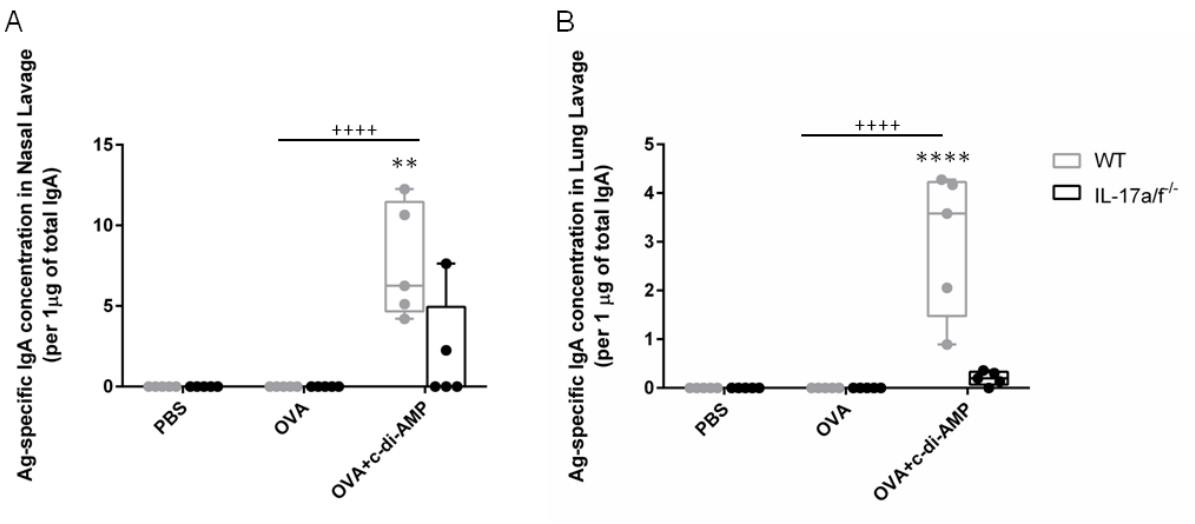

Figure 28: **Contribution of c-di-AMP-induced IL-17 secretion to the production of antigen-specific IgA response:** WT and IL-17a/f$^{-/-}$mice were i.n. immunized with PBS, OVA alone (10 µg/dose) or OVA co-administered with c-di-AMP (5 µg/dose). Nasal and lung lavage samples of individual animals were analyzed for the level of antigen-specific IgA in 1 µg of total IgA by ELISA. IgA concentrations detected in A) nasal and B) lung lavage samples. Boxes represent the interquartile range, horizontal lines show the mean value and whiskers show the overall range of the data. Columns represent the mean ± SEM of one experiment (n=5). Shown is one representative out of three independent experiments. Asterisks denote significant values as calculated by Two-way ANOVA when comparing WT and IL-17a/f$^{-/-}$ mice; **** $p < 0.0001$; ** $p < 0.01$. Plus denote significant value as calculated by Two-way ANOVA when comparing WT mice immunized with OVA alone and with OVA co-administered with c-di-AMP; ++++ $p < 0.0001$.

5.4.1.1. The contribution of c-di-AMP-induced IL-5 secretion to the induction of humoral immune responses

Activated immune cells secrete a variety of cytokines, thereby shaping and activating other immune cells. Thus, the c-di-AMP-induced cytokine environment was investigated to gain insights into the factors contributing to the induced humoral immune response. To this end, splenic cells obtained from immunized mice were stimulated *ex vivo* with OVA protein for 72 h and secreted cytokines (IFNγ, IL-2, IL-4, IL-5, IL-6, IL-13, IL-17 and IL-22) into supernatant fluids were analyzed by performing a CBA. *S*plenic cells obtained from WT and IL-17a/f$^{-/-}$ mice immunized with OVA co-administered with c-di-AMP showed enhanced levels of IFNγ, IL-2, IL-4, IL-5, IL-6, IL-13, IL-17 and IL-22 as compared to samples derived from mice immunized with PBS or OVA alone. The comparison of cell obtained from WT and IL-17a/f$^{-/-}$ mice immunized with OVA co-administered with c-di-AMP confirmed enhanced levels of IFNγ-secretion in IL-17a/f$^{-/-}$ as compared to WT mice. Besides lower levels of secreted IL-17- and IL-22, significantly reduced levels of IL-5 were observed in IL-17a/f$^{-/-}$ mice immunized as compared to WT

mice (Figure 29). Th2 cell-derived IL-5 is known to play a crucial role in initiating humoral immune responses [169]. This indicates IL-5 as one of the potential factors contributing to c-di-AMP-induced and IL-17-depentent humoral immune response.

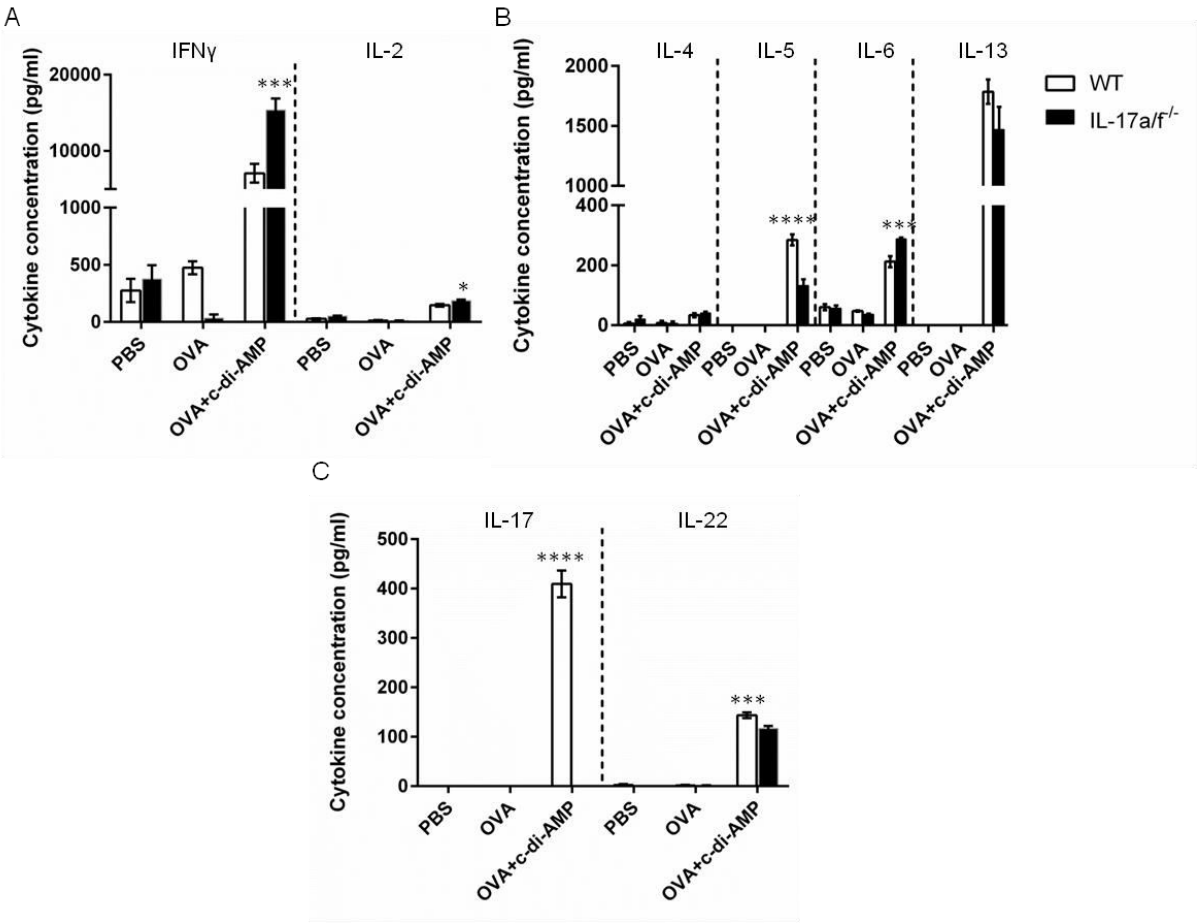

Figure 29: Immunization-induced serum cytokines: Splenic cells derived from WT and IL-17a/f$^{-/-}$ mice immunized with PBS, OVA alone or OVA-co-administered with c-di-AMP were re-stimulated *ex vivo* with OVA protein (20 µg/ml) for 72 h, the supernatant was collected and subsequently analyzed to determine the cytokine profiles by CBA. Concentrations of A) Th1 (IFNγ, IL-2), B) Th2 (IL-4, IL-5, IL-6, IL-13) and C) Th17 (IL-17, IL-22) cytokines were determined. Columns represent the mean ± SEM of one experiment (n=3).Shown is one representative out of two independent experiments. Asterisks denote significant values as calculated by Two-way ANOVA when comparing WT and IL-17a/f$^{-/-}$ supernantant; **** $p < 0.0001$; *** $p < 0.001$; ** $p < 0.01$.

5.4.1.2. T_{FH} cells contributes to the c-di-AMP-induced antibody response by supporting plasma B cell differentiation

In addition to cytokines such as IL-5, T_{FH} cells play a crucial role in inducing humoral immune responses, since they are critical for GC reactions [170]. The generation of antigen-specific antibody responses requires interactions between B cells and $CD4^+$ T helper cells. In this context, T_{FH} cells are fundamentally required for the generation of T cell dependent B cell responses by providing cognate help to B cells [171]. Thus, T_{FH} cells might play a key role in the c-di-AMP-induced enhanced antibody response by supporting the differentiation of B cells into antibody secreting cells. T_{FH} cells are characterized by the expression of CD4, the chemokine receptor 5 (CXCR5) and the inducible costimulatory molecule receptor (ICOS). GC B cells, characterized by the expression of CD19 and PNA are mainly found in GCs and are known to interact with T_{FH} cells to differentiate into plasma B cells ($CD19^-$ $CD138^+$). Thus, to explore the role of T_{FH} cells for the enhanced humoral response observed upon administration of c-di-AMP, the frequency of T_{FH} cells, GC B cells and plasma B cells in cLNs of immunized animals were determined. Elevated frequencies of T_{FH} cells were observed in cLNs derived from IL-17a/f$^{-/-}$ mice as compared to WT mice immunized with PBS, OVA alone or co-administered with c-di-AMP (Figure 30A). However, while the frequency of T_{FH} cells in IL-17a/f$^{-/-}$ mice was not impacted by the immunization. Immunization of WT mice with OVA resulted in significantly increased frequencies of T_{FH} cells as compared to control WT mice immunized with PBS. The co-administration of c-di-AMP led to an additional significant increase of this cell type in WT mice (Figure 30A). Significantly increased frequencies of GC B cells and plasma B cells were also observed in WT and IL-17a/f$^{-/-}$ mice immunized with OVA co-administered with c-di-AMP as compared to mice immunized with PBS or OVA alone (Figure 30B and C). Furthermore, significantly reduced frequencies of GC B cells and plasma B cells were observed in IL-17a/f$^{-/-}$ mice immunized with OVA co-administered with c-di-AMP as compared to what observed in WT mice. These data demonstrate that c-di-AMP-induced IL-17 secretion contributes to the generation of GC B cells and plasma B cells and thus seems to contribute to the stimulation of antigen-specific humoral immune responses.

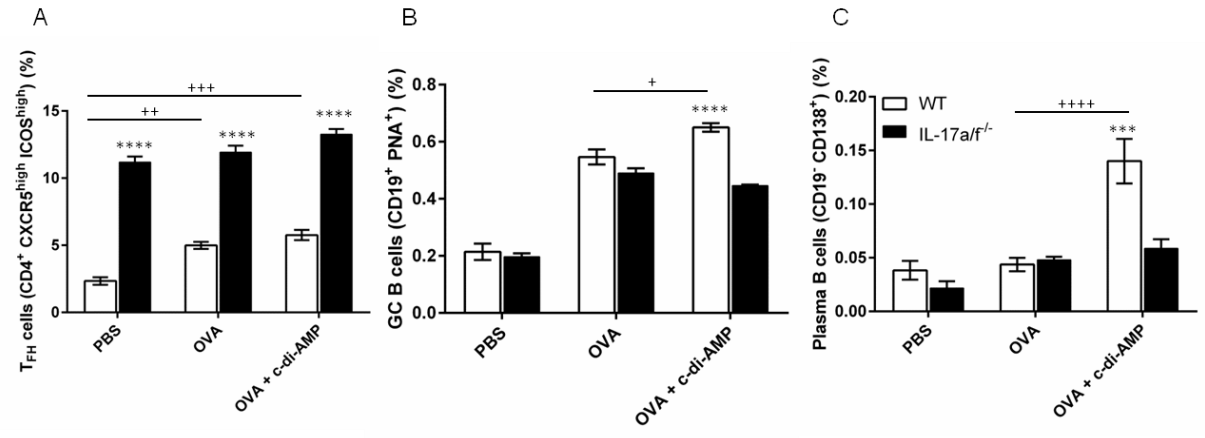

Figure 30: Frequencies of T_{FH} cells, GC B cells and plasma B cells upon immunization of WT and IL-17a/f$^{-/-}$ mice: WT and IL-17a/f$^{-/-}$ mice were i.n. immunized with PBS, OVA alone (10 µg/dose) or OVA co-administered with c-di-AMP (5 µg/dose). Cells from cLNs were isolated, stained *ex vivo* with antibodies specific for markers of T_{FH} cells ($CD4^+$ $CXCR5^+$), GC B cells ($CD19^+$ PNA^+) and plasma B cells ($CD19^-$ $CD138^+$) and analyzed by flow cytometry. Frequency of A) T_{FH} cells, B) GC B cells and C) plasma B cells were determined. Columns represent the mean ± SEM of one experiment (n=5, pooled samples with three replicates). Shown is one representative out of three independent experiments. Asterisks denote significant values as calculated by Two-way ANOVA when comparing WT and IL-17a/f$^{-/-}$ mice; **** $p < 0.0001$; *** $p < 0.001$. Plus denote significant value as calculated by Two-way ANOVA when comparing WT mice immunized with PBS, OVA alone and with OVA co-administered with c-di-AMP; ++++ $p < 0.0001$; ++ $p < 0.01$; + $p < 0.05$.

In previous studies c-di-AMP was shown to activate APCs, such as DCs and macrophages [97, 151]. In addition to the secretion of antibodies, B cells might also function as APCs, thereby mediating T_{FH} cell direct activation and supporting plasma B cell generation. However, the role of c-di-AMP in the direct activation of B cells has not been assessed yet. Therefore, to address the role of c-di-AMP in the activation of B cells, sorted B cells ($CD19^+B220^+$) derived from WT mice were incubated for 24 h in presence of OVA alone, c-di-AMP alone or OVA + c-di-AMP. MALP, a known B cell stimulus was used as a positive control [172]. Stimulated B cells were stained for the expression of the activation marker CD69 and the maturation markers CD86 and MHC class II. A significant up-regulation of CD69, CD86 and MHC class II surface expression was observed upon treatment with c-di-AMP alone or co-administered with OVA when compared to B cells treated with PBS or OVA alone (Figure 31A-C). In this context, treatment with c-di-AMP alone or in combination with OVA resulted in an expression level of CD86 and MHC class II comparable to the expression induced by MALP. This suggests that c-di-AMP directly activates B cells and hence can mediate T_{FH} cell activation, thereby supporting plasma B cell generation.

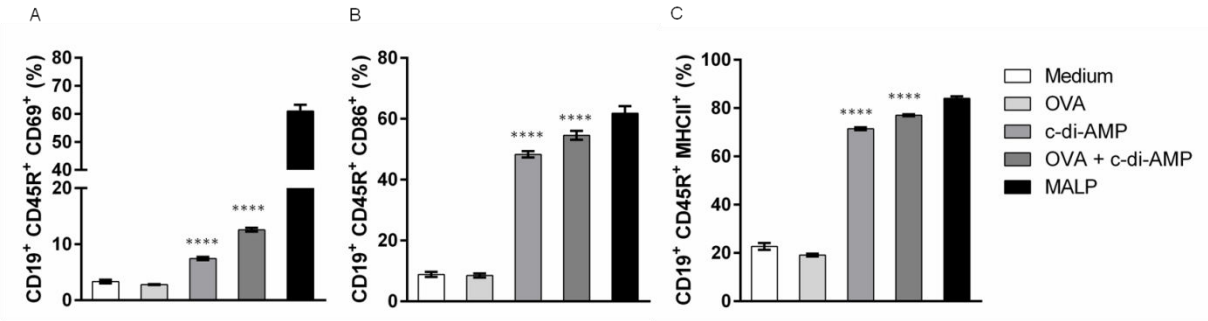

Figure 31: B cell activation upon *in vitro* stimulation: Sorted B cells ($CD19^+B220^+$) derived from WT mice were left untreated or stimulated with OVA alone (40 µg/ml), c-di-AMP alone (5 µg/ml) or OVA + c-di-AMP for 24 h. Cells were subsequently stained for activation (CD69) and maturation markers (CD86 and MHC II) and further analyzed by flow cytometry. Frequencies of A) CD69, B) CD86 and C) MHC II expressing B cells were determined. Columns represent the mean ± SEM of one experiment (n=3). Shown is one representative out of two independent experiments. Asterisks denote significant values as calculated by Two-way ANOVA when comparing different treatment conditions;**** $p < 0.0001$.

Furthermore, *in vitro* co-culture studies were performed to address whether T_{FH} cells can directly induce plasma B cell differentiation upon c-di-AMP stimulation. To this end, T_{FH} cells ($CD4^+CXCR5^+$) and GC B cells ($CD19^+PNA^+$) sorted from cLNs and spleen obtained from WT and IL-17a/f$^{-/-}$ mice were co-cultured for 6 days either in the presence of OVA alone, c-di-AMP alone, or OVA + c-di-AMP; control cells were left untreated. In addition, the role of IL-17 in c-di-AMP-induced plasma B cell differentiation was addressed by supplementing IL-17a/f$^{-/-}$ cultures with recombinant IL-17A (rIL-17A). Plasma B cell differentiation can be detected by the downregulation of CD19 and the upregulation of CD138 by B cells under stimulating conditions. Immunization of WT mice with OVA co-administered with c-di-AMP resulted in increased IgG1 titers, thus IgG1 plasma B cells was also analyzed. Cell cultures containing only GC B cells with different treatment conditions showed no $IgG1^+$ plasma B cell differentiation (Figure 32A). Interestingly, a significant increase in the frequency of $IgG1^+$ plasma B cells ($CD19^-CD138^+$) was observed in WT co-cultures of T_{FH} cells and GC B cells supplemented with OVA in combination with c-di-AMP as compared to untreated control cells, and cells treated with OVA or c-di-AMP alone. Furthermore, no plasma B cell differentiation was observed in IL-17a/f$^{-/-}$ culture conditions when compared to its WT counterpart (Figure 32B). However, the supplementation of rIL-17A to the IL-17a/f$^{-/-}$ conditions restored the differentiation of plasma B cells, thereby demonstrating the direct role of IL-17 for the observed c-di-AMP-induced plasma B cell differentiation. These data illustrate that c-di-AMP directly activates B cells and hence might mediate T_{FH} cell activation, thereby indirectly supporting plasma B cell generation. The increased frequency of T_{FH} cell observed in IL-17a/f$^{-/-}$ mice does not seem to play a role in plasma

B cell differentiation. These data highlight the importance of the IL-17-dependent c-di-AMP-mediated induction of IL-5 secretion as well as T_{FH} cells for the observed stimulation of an OVA-specific humoral immune response.

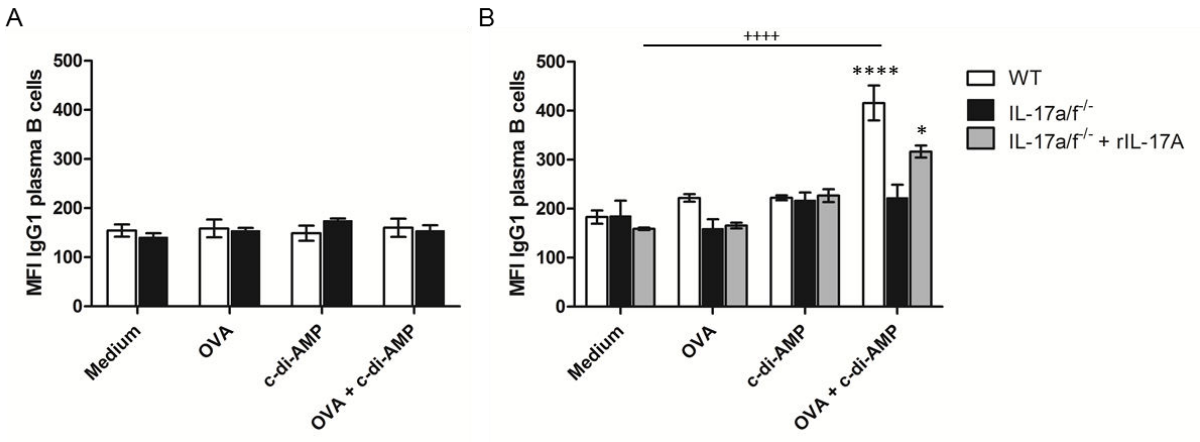

Figure 32: Restoration of plasma B cells differentiation by supplementation of IL-17a/f$^{-/-}$ cultures with rIL-17A: GC B cells (CD19^{+}PNA^{+})and T_{FH} cells (CD4^{+}CXCR5^{+}) were sorted from cLNs and spleens obtained from WT and IL-17a/f$^{-/-}$ mice and were left untreated or treated with OVA alone (40 µg/ml), c-di-AMP alone (5 µg/ml) or OVA + c-di-AMP for 6 days. rIL-17A was added to IL-17a/f$^{-/-}$ culture conditions as indicated. After 6 days, the cells were incubated with brefeldin A (5 µg/ml) and monensin (6 µg/ml) for additional 4 h, stained with antibodies specific markers of plasma B cell differentiation (CD138 and IgG1) and further analyzed by FACS. MFI of IgG1 plasma B cells in co-cultures with A) GC B cells alone and B) GC B cells together with T_{FH} cells. Columns represent the mean ± SEM of one experiment (n=3). Shown is one representative out of two independent experiments. Asterisks denote significant values as calculated by Two-way ANOVA when comparing WT and IL-17a/f$^{-/-}$ GC B cells;**** $p < 0.0001$; * $p < 0.05$. Plus denote significant value as calculated by Two-way ANOVA when comparing WT mice immunized with OVA alone and OVA co-administered with c-di-AMP; ++++ $p < 0.0001$.

5.4.2. Influence of the microflora on c-di-AMP-induced IL-17-mediated antigen-specific immune responses

Recent studies have illustrated novel complex mechanisms by which the microbiota impacts immune cell development and differentiation, which ultimately might influence the outcome of vaccine efficacy [173]. Prior immunization experiments were performed under non-co-housed conditions. However, the microflora has been shown to positively influence Th17 development in the small intestine. Thus, in order to assess the contribution of microbiota on immunization-induced immune responses, WT mice (bought by Harlan) and IL-17a/f$^{-/-}$ mice (bred at the HZI animal facility) were co-housed for 4 weeks prior to immunization to obtain analogous flora in both mouse strains.

To analyze the impact of the microflora on c-di-AMP-induced antigen-specific humoral immune responses, IgG titers in sera and IgA concentrations in the nasal and lung lavage samples of immunized mice were analyzed, comparing co-housed and non-co-housed conditions. Immunization of WT and IL-17a/f$^{-/-}$ mice with OVA co-administered with c-di-AMP stimulated significantly enhanced IgG titers and IgA concentrations in co-housed and non-co-housed conditions as compared to mice immunized receiving PBS or OVA alone. The comparison of non-co-housed WT and IL-17a/f$^{-/-}$ mice showed significantly enhanced IgG titers and IgA concentrations in WT mice (Figure 33A, B and C). Interestingly, upon co-housing increased IgG and IgG2c titers were detected in IL-17a/f$^{-/-}$ mice as compared to the co-housed WT group and non-cohoused IL-17a/f$^{-/-}$ groups (Figure 33A and B). No significant differences in IgG titers and its isotypes were observed in WT mice upon co-housing as compared to non-co-housed WT mice. No significant differences in IgG1 titers were detected in IL-17a/f$^{-/-}$ mice upon co-housing compared to non-co-housed IL-17a/f$^{-/-}$ mice (Figure 33B). Concerning IgA production, a trend towards reduced concentrations was observed in co-housed WT mice as compared to non-co-housed WT mice. No differences were observed in the IgA concentration in IL-17a/f$^{-/-}$ mice upon co-housing as compared to non-co-housed IL-17a/f$^{-/-}$ mice (Figure 33C). Interestingly, upon co-housing reduced IgA concentrations were detected in IL-17a/f$^{-/-}$ mice as compared to the corresponding co-housed WT group (Figure 33C). These results indicate that the microbiome significantly influences the quality of c-di-AMP-induced systemic humoral responses, promoting a shift with increase in IgG2c (IgG2c/1 ratios 0.33 and 0.90 in WT and 0.21 and 2.87 in IL-17a/f$^{-/-}$ mice, non-co-housed and co-housed respectively). No significant influence of the microbiome was observed with respect to c-di-AMP-induced mucosal IgA responses.

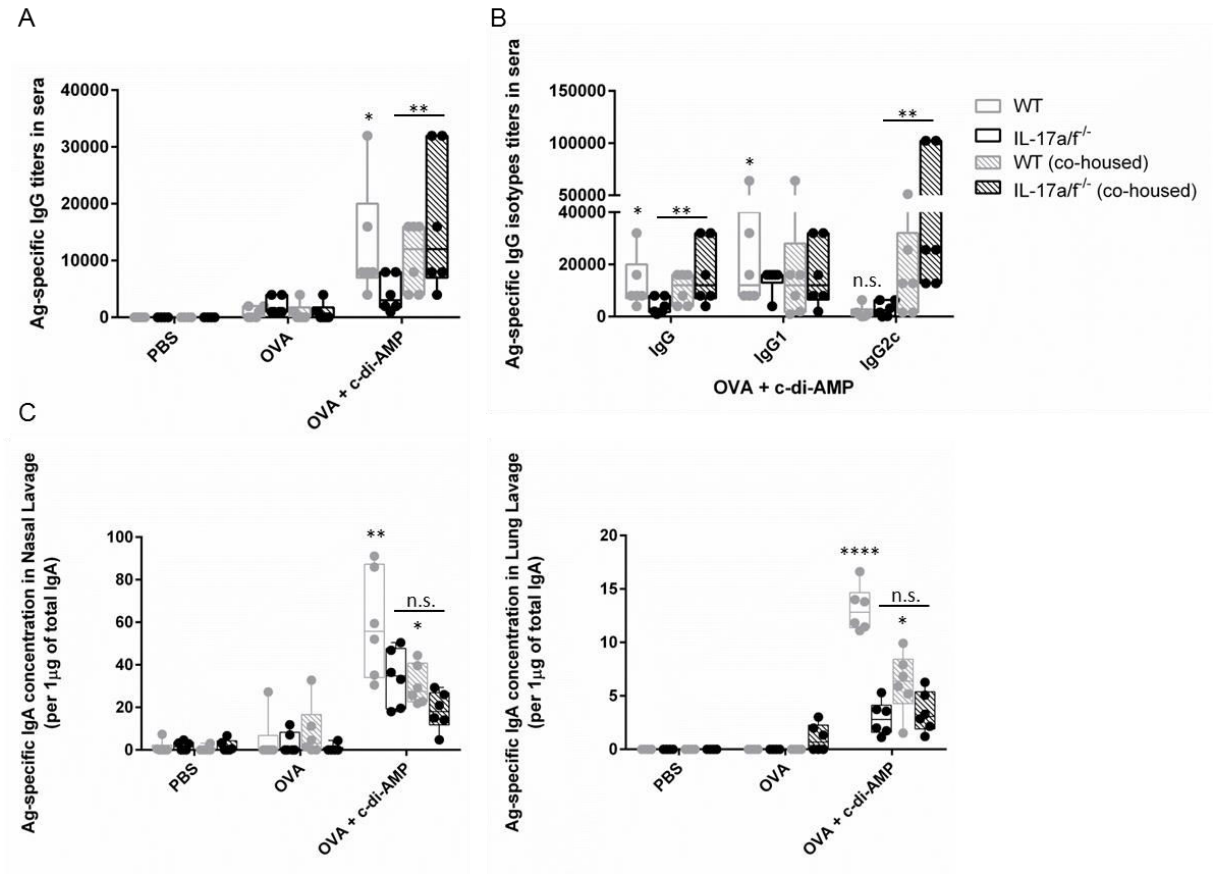

Figure 33: Impact of microbiota on c-di-AMP-induced antigen-specific humoral responses: WT and IL-17a/f$^{-/-}$ mice were co-housed for 4 weeks prior to immunization with PBS, OVA alone (10 µg/dose) or OVA co-administered with c-di-AMP (5 µg/dose) and compared to non-cohoused immunized mice. Serum samples of single animals were analyzed for the presence of antigen-specific IgG and its isotypes, and nasal and lung lavage samples were analyzed for the concentration of IgA by ELISA. Serum titers of antigen-specific A) IgG and B) IgG, IgG1 and IgG2c were determined. C) IgA concentrations in nasal and lung lavage samples were determined. Boxes represent the interquartile range, horizontal lines show the mean value and whiskers show the overall range of the data. Columns represent the mean ± SEM of one experiment (n=6). Shown is one representative out of two independent experiments. Asterisks denote significant values as calculated by Two-way ANOVA when comparing WT and IL-17a/f$^{-/-}$ mice; **** $p < 0.0001$; ** $p < 0.01$; * $p < 0.05$; n.s. = not significant.

To further analyze the impact of the microflora on c-di-AMP-induced antigen-specific cellular immune responses, splenocytes from individual animals were re-stimulated with OVA and the frequencies of IFNγ-, IL-4- and IL-17-secreting CD4$^+$ T cells were assessed comparing WT and IL-17a/f$^{-/-}$ mice held under co-housed and non-co-housed conditions. Immunization of WT and IL-17a/f$^{-/-}$ mice with OVA co-administered with c-di-AMP stimulated significantly enhanced frequencies of IFNγ- and IL-4-secreting CD4$^+$ T cells under co-housed and non-co-housed conditions as compared to PBS and OVA alone (Figure 34A, B and C). Furthermore, a trend of increased frequencies of IFNγ-

secreting CD4$^+$ T cells was observed in IL-17a/f$^{-/-}$ mice immunized with OVA co-administered with c-di-AMP as compared to correspondingly treated WT mice (Figure 34A). No significant differences in the frequency of IFNγ-secreting CD4$^+$ T cells were observed when comparing co-housed and non-cohoused conditions. On the other hand, a significantly reduced frequency of IL-4-secreting CD4$^+$ T cells was observed in samples derived from IL-17a/f$^{-/-}$ mice immunized with OVA co-administered with c-di-AMP as compared to its corresponding WT group (Figure 34B). The comparison of WT mice under co-housed and non-co-housed conditions showed significantly reduced IL-4 secretion by CD4$^+$ T cells under co-housed conditions. Similarly, a reduced frequency of IL-17-secreting CD4$^+$ T cells was observed in co-housed WT mice as compared to non-co-housed ones (Figure 34C). These data demonstrate that the microbiota significantly influence c-di-AMP-induced Th2 and Th17 cellular immune responses.

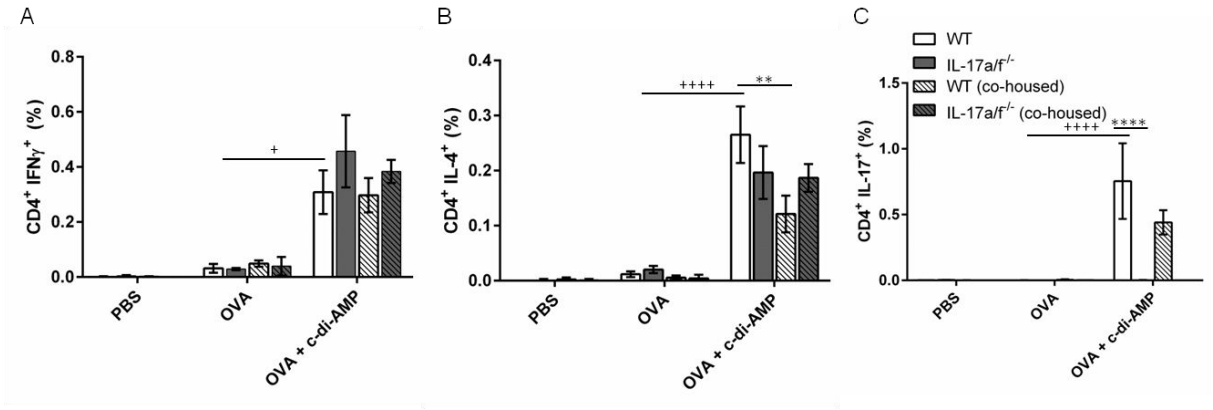

Figure 34: Impact of microbiota on c-di-AMP-induced antigen-specific Th2 responses: WT and IL-17a/f$^{-/-}$ mice were i.n. immunized with PBS, OVA alone (10 µg/dose) or OVA co-administered with c-di-AMP (5 µg/dose). Splenocytes were re-stimulated with OVA (40 µg/ml) overnight. The cells were incubated with brefeldin A (5 µg/ml) and monensin (6 µg/ml) for additional 4 h and were analyzed by flow cytometry. Frequencies of CD4$^+$ T cells secreting A) IFNγ, B) IL-4 and C) IL-17 were analyzed. Results are expressed as subtracted background of unstimulated samples from stimulated samples. Columns represent the mean ± SEM of one experiment (n=5). Asterisks denote significant values as calculated by Two-way ANOVA comparing WT and IL-17a/f$^{-/-}$ mice; **** $p < 0.0001$; ** $p < 0.01$. Plus denote significant values as calculated by Two-way ANOVA when comparing WT mice immunized with OVA alone and with OVA co-administered with c-di-AMP; ++++ $p < 0.0001$; ++ $p < 0.01$; + $p.< 0.05$.

In order to analyze the impact of the microflora on c-di-AMP-induced antigen-specific cellular mucosal immune responses, lung cells were re-stimulated with OVA and the frequencies of IFNγ- and IL-17-secreting CD4$^+$ T cells were assessed comparing WT and IL-17a/f$^{-/-}$ mice held under co-housed and non-co-housed conditions. Immunization of co-housed and non-co-housed WT and IL-17a/f$^{-/-}$ mice with OVA co-administered with c-di-AMP stimulated significantly enhanced frequencies of IFNγ-secreting CD4$^+$ T

cells as compared to animals receiving PBS or OVA alone (Figure 35A). IL-17a/f$^{-/-}$ mice immunized with OVA co-administered with c-di-AMP displayed a significantly increased frequency of IFNγ-secreting CD4^{+} T cells as compared to the correspondingly treated WT mice within the co-housed as well as non-co-housed groups (Figure 35A). Furthermore, a significant reduction in the frequency of IFNγ-secreting CD4^{+} T cells was observed comparing co-housed WT mice immunized with OVA co-administered with c-di-AMP to WT non-cohoused mice. A significant increase in the frequency of IFNγ-secreting CD4^{+} T cells was also observed comparing co-housed IL-17a/f$^{-/-}$ mice to non-co-housed IL-17a/f$^{-/-}$ mice immunized with OVA and c-di-AMP. With regard to IL-17-secreting CD4^{+} T cells, increased frequencies were detected in WT mice immunized with OVA-co-administered with c-di-AMP as compared to WT mice immunized with OVA or PBS. The comparison of WT mice held under co-housed and non-co-housed conditions showed significantly reduced frequencies of IL-17-secretion CD4^{+} T cells under co-housed conditions (Figure 35B). As expected, no IL-17 secretion was observed in IL-17a/f$^{-/-}$ mice. These results indicate that the microflora also impacts Th1 as well as Th17 responses at mucosal level.

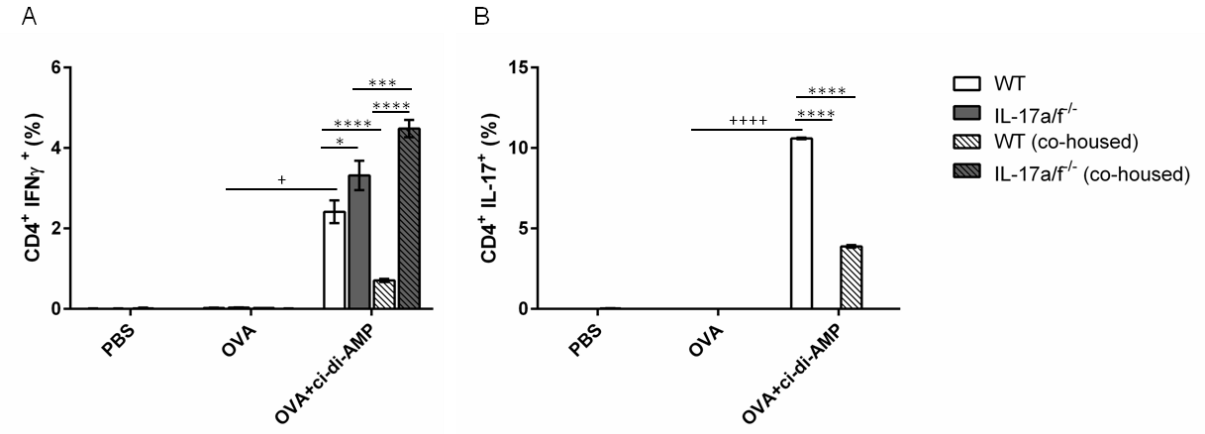

Figure 35: Impact of microbiota on c-di-AMP-induced antigen-specific Th1 and Th17 responses: WT and IL-17a/f$^{-/-}$ mice were i.n. immunized with PBS, OVA alone (10 µg/dose) or OVA co-administered with c-di-AMP (5 µg/dose). Lung cells were re-stimulated with OVA (40 µg/ml) overnight. The cells were incubated with brefeldin A (5 µg/ml) and monensin (6 µg/ml) for additional 4 h and were analyzed by flow cytometry. Frequencies of CD4^{+} T cells secreting A) IFNγ and B) IL-17 were determined. Results are expressed as subtracted background of unstimulated samples from stimulated samples. Columns represent the mean ± SEM of one experiment (n=5). Asterisks denote significant values as calculated by Two-way ANOVA when comparing WT and IL-17a/f$^{-/-}$ mice; **** $p < 0.0001$; *** $p < 0.001$;* $p < 0.05$. Plus denote significant values as calculated by Two-way ANOVA when comparing WT mice immunized with OVA alone and with OVA co-administered with c-di-AMP; ++++ $p < 0.0001$; + $p < 0.05$.

To further elucidate the impact of the microflora on IgG responses upon co-housing and immunization, the microbiota composition from the different mice strains were compared. For this, a 16s rRNA analysis of feces samples was performed. The overall microbial community was compared by applying R statistical programming and analyzed using PHYLOSEQ. Feces samples derived from non-co-housed untreated WT and IL-17a/f$^{-/-}$ mice showed a huge variability in the composition of the microbiota. Additionally, the microbial composition obtained from the same genotype clustered uniformly as observed in the non-metric multidimensional scaling (NMDS) plots (Figure36A). Furthermore, a lower relative abundance of segmented filamentous bacterium (*Clostridiacaea* SFB) microbial community was observed in IL-17a/f$^{-/-}$ mice when compared to untreated WT mice (Figure 36B).

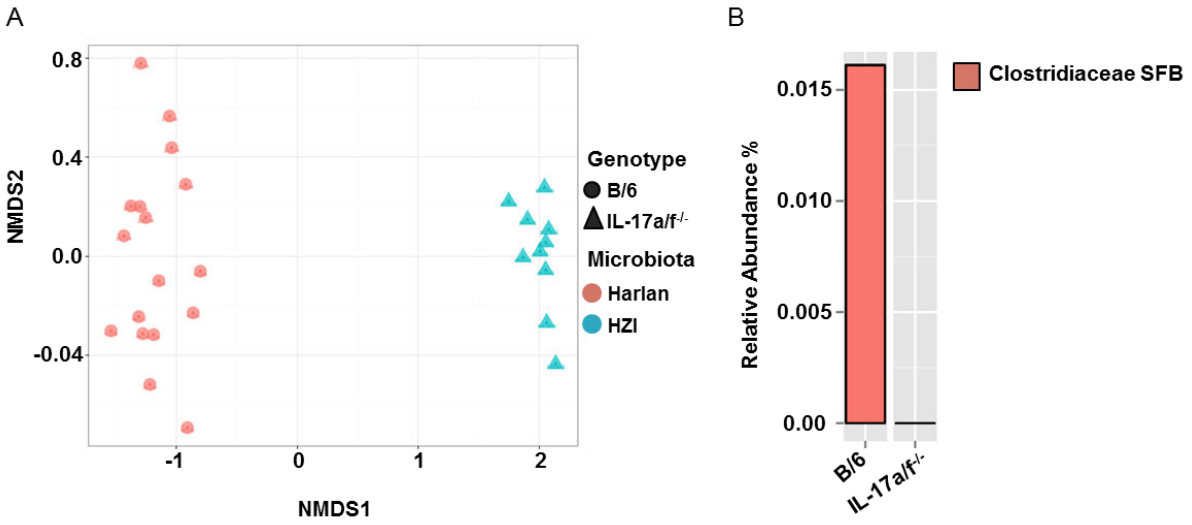

Figure 36: Microbial composition in WT and IL-17a/f$^{-/-}$ mice: Composition of the microbiota in feces samples derived from WT and IL-17a/f$^{-/-}$ mice were assessed using genomic bacterial 16s rRNA sequence. The plots represent A) NMDS and B) relative abundance of SFB bacterial community comparing WT and IL-17a/f$^{-/-}$ mice.

This finding is in accordance with recent reports stating that mice obtained from different commercial vendors have marked differences in the number of Th17 cells which correlates with the presence of members of the Cytopaga-Flavobacter-Bacteroides phylum namely SFB [174, 175]. Thus, to address whether the low abundance of SFB found in IL-17a/f$^{-/-}$ mice impacts the c-di-AMP-induced Th17-mediated antigen-specific humoral response, IL-17a/f$^{-/-}$ mice were colonized with feces obtained from mice mono-colonized with SFB. WT controls were left untreated. 4 weeks after fecal transplant WT and IL-17a/f$^{-/-}$ mice were i.n. immunized with OVA alone or co-administered with c-di-AMP, according to the prime boost protocol described above (5.4). Subsequently,

serum IgG titers and concentrations of IgA in nasal and lung lavage samples were analyzed by ELISA. As observed earlier, immunization of WT and IL-17a/f$^{-/-}$ mice with OVA co-administered with c-di-AMP stimulated significantly enhanced IgG titers and IgA concentrations as compared to PBS and OVA alone (Figure 37A, B and C). Interestingly, IL-17a/f$^{-/-}$ mice showed lower IgG and IgG1 titers as compared to WT mice immunized with OVA and c-di-AMP independently of the fecal transplant (Figure 37A and B). Similarly IL-17a/f$^{-/-}$ mice displayed significantly reduced IgA concentrations in nasal and lung lavage samples as compared to WT mice immunized with OVA and c-di-AMP independently of the fecal transplant (Figure 37C). However, in the lung lavage samples IgA concentrations were slighlty increased in SFB colonized IL-17a/f$^{-/-}$ mice when compared to non-colonized IL-17a/f$^{-/-}$ mice.This finding suggests that SFB alone is not sufficient to influence c-di-AMP-induced Th17-mediated antigen-specific humoral response.

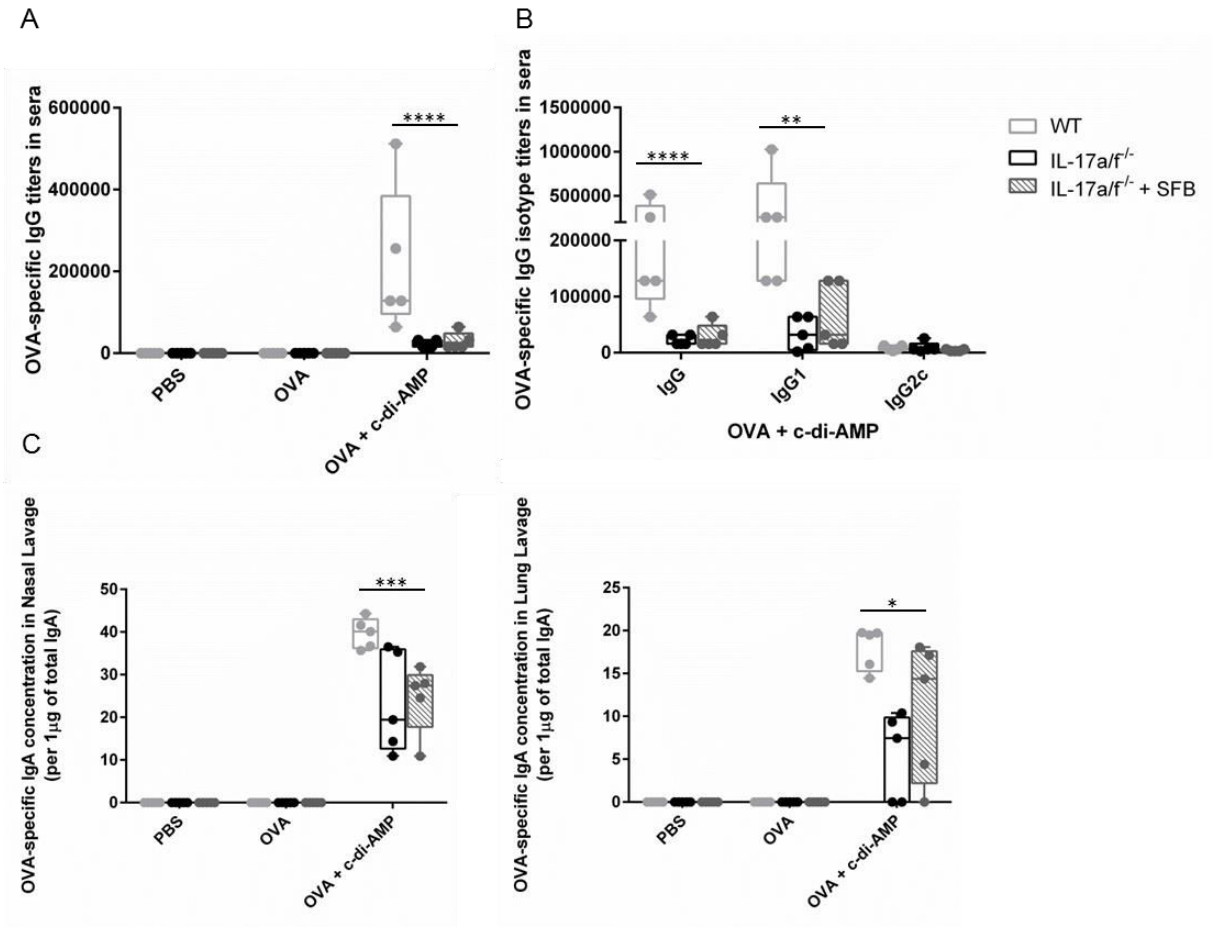

Figure 37: **Impact of SFB on the outcome of c-di-AMP-induced antigen-specific humoral response:** Oral fecal transplant using feces from SFB mice into IL-17a/f$^{-/-}$ mice was performed 4 weeks prior to immunization with PBS, OVA alone (10 µg/dose) or OVA co-administered with c-di-AMP (5 µg/dose). Transplanted IL-17a/f$^{-/-}$ mice were compared to non-cohoused WT and IL-17a/f$^{-/-}$ mice. Sera and nasal and lung lavage samples of single animals were analyzed for IgG titers and IgA concentrations by ELISA. OVA-specific serum titers of A) IgG and B) IgG, IgG1 and IgG2c were determined. C) Concentration of OVA-specific IgA in nasal and lung lavage samples. Boxes represent the interquartile range, horizontal lines show the mean value and whiskers show the overall range of the data. Columns represent the mean ± SEM of one independent experiment (n=5). Asterisks denote significant values as calculated by Two-way ANOVA when comparing WT and IL-17a/f$^{-/-}$ + SFB mice; **** $p < 0.0001$; *** $p < 0.001$; ** $p < 0.01$; * $p < 0.05$.

5.4.3. Influenza vaccine elicits Th17 dependent local antigen-specific IgA response

To investigate the impact of c-di-AMP-induced IL-17 secretion on the generation of antigen-specific humoral responses in a disease-relevant influence vaccine model, mice were i.n. immunized with PBS, inactivated NIBRG-14 (a H5N1 vaccine antigen) alone or co-administered with c-di-AMP. Additionally, mice were co-housed prior to immunization to exclude the observed impact of the microflora on the antigen-specific immune response. In an influenza vaccine model, IgG and neutralizing antibody responses are known to mediate protective immunity [176]. The analysis of sera derived from WT and IL-17a/f$^{-/-}$ mice immunized with NIBRG-14 co-administered with c-di-AMP revealed enhanced NIBRG-14-specific IgG titers as compared to mice immunized with PBS or NIBRG-14 alone (Figure 38A). No significant differences in IgG titers including IgG1 and IgG2c titers were detected in IL-17a/f$^{-/-}$ mice as compared to WT mice immunized with NIBRG-14 co-administered with c-di-AMP (Figure 38A and B). Additionally, neutralizing antibody titers in the sera of immunized mice were determined by performing hemagglutination inhibition (HAI) and microneutralization (MN) assays, determining the amount and the functionality of the antibodies. Sera derived from WT and IL-17a/f$^{-/-}$ mice immunized with NIBRG-14 co-administered with c-di-AMP showed enhanced HAI titers and H5-specific neutralizing antibody titers as compared to PBS and NIBRG-14 alone (Figure 38C and D). Significantly increased HAI titers and H5-specific neutralizing antibody titers were observed in IL-17a/f$^{-/-}$ mice immunized with NIBRG-14 co-administered with c-di-AMP as compared to correspondingly treated WT mice (Figure 38C and D). These data indicate that IL-17 secretion hampers the generation of neutralizing antibodies but not the overall IgG responses in this particular experimental model.

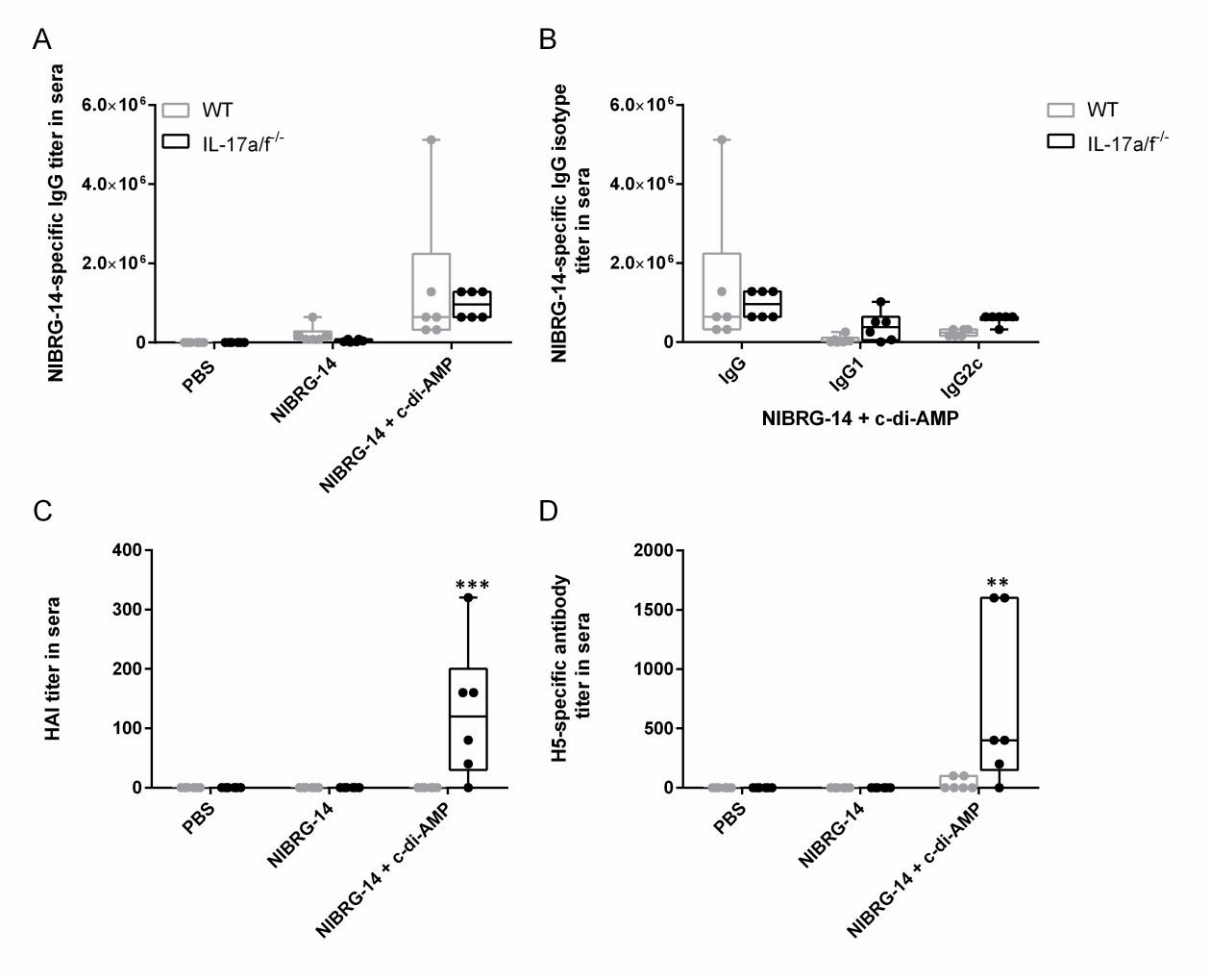

Figure 38: NIBRG-14-specific neutralizing antibody responses: WT and IL-17a/f$^{-/-}$ mice were i.n. immunized with PBS or NIBRG-14 alone (0.5 µg/dose) or NIBRG-14 co-administered with c-di-AMP (5 µg/dose). Sera samples of single animals were analyzed for the presence of antigen-specific IgG titers by ELISA and for neutralizing antibody titers by HAI and MN assay. NIBRG-14-specific serum titers of A) IgG, B) IgG, IgG1 and IgG2c, and neutralizing antibody titers assessed by C) HAI and D) MN assay are shown. Boxes represent the interquartile range, horizontal lines show the mean value and whiskers show the overall range of the data. Columns represent the mean ± SEM of one experiment (n=6). Shown is one representative out of two independent experiments. Asterisks denote significant values as calculated by Two-way ANOVA when comparing WT and IL-17a/f$^{-/-}$ mice; *** $p < 0.001$; ** $p < 0.01$.

Mucosal surfaces are persistently exposed to potentially harmful pathogens such as influenza. Therefore, they are protected by a first-line of defense that is mediated by sIgA amongst other factors [177-179]. Thus to investigate the impact of c-di-AMP-induced IL-17 secretion on mucosal immunity in the influenza vaccine model, the concentration of IgA, as well as the sIgA titers, were analyzed in nasal washes and lung lavage samples. In both, WT and IL-17a/f$^{-/-}$ mice, immunization with NIBRG-14 co-administered with c-di-AMP induced the secretion of NIBRG-14-specific IgA and

enhanced sIgA titers as compared to PBS and NIBRG-14 alone (Figure 39A and B). Interestingly, IL-17a/f$^{-/-}$ mice immunized with NIBRG-14 and c-di-AMP harbored a significantly reduced concentration of NIBRG-14-specific IgA and sIgA titers in nasal washes and lung lavage samples as compared to correspondingly immunized WT mice. This indicates that c-di-AMP-induced IL-17 secretion supports mucosal IgA responses.

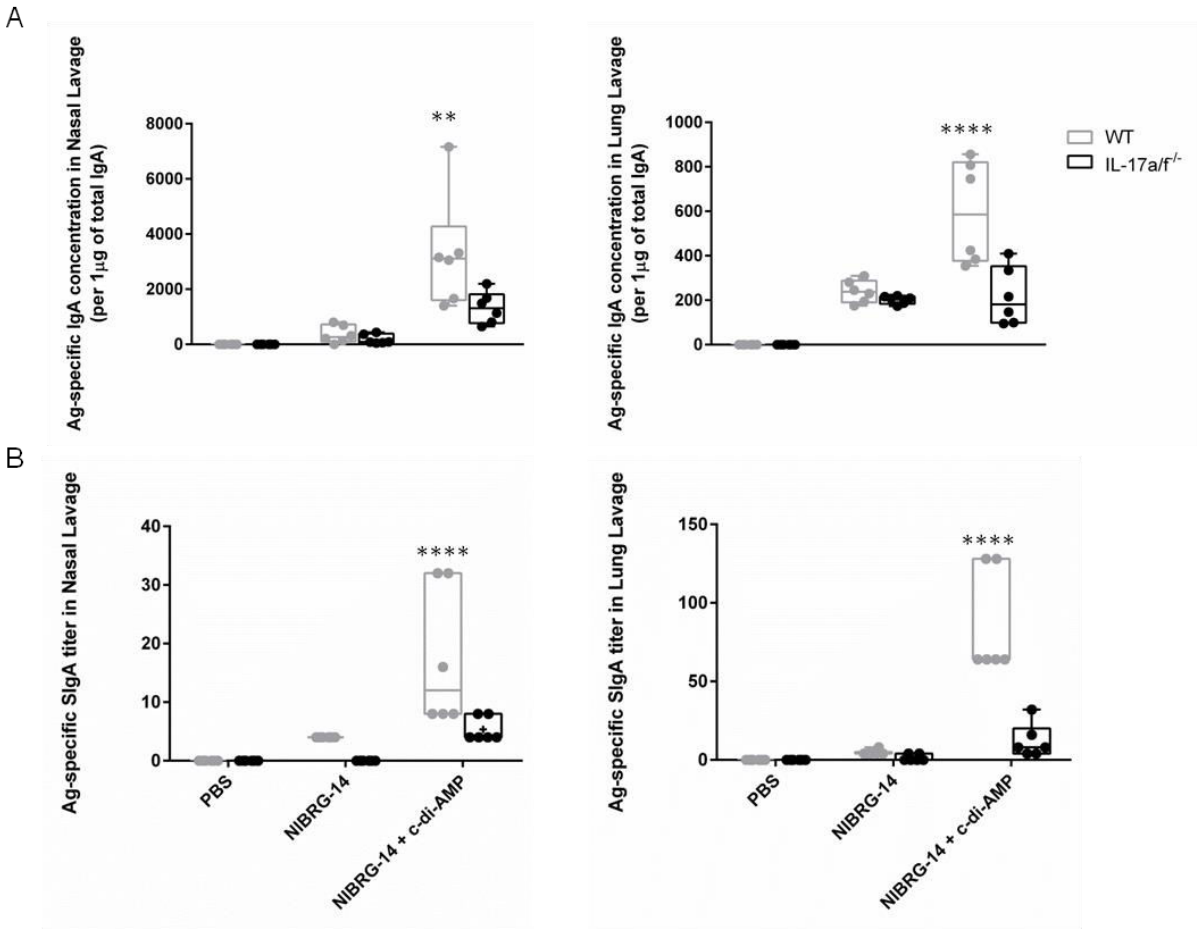

Figure 39: Mucosal IgA concentrations and sIgA titers upon immunization: WT and IL-17a/f$^{-/-}$ mice were i.n. immunized with PBS or NIBRG-14 alone (0.5 µg/dose) or NIBRG-14 co-administered with c-di-AMP (5 µg/dose). Nasal and lung lavage samples of single animals were analyzed for the level of antigen-specific IgA concentration in 1 µg of total IgA by ELISA. NIBRG-14-specific A) IgA concentrations and B) sIgA titers are shown. Boxes represent the interquartile range, horizontal lines show the mean value and whiskers show the overall range of the data. Columns represent the mean ± SEM of one experiment (n=6). Shown is one representative out of three independent experiments. Asterisks denote significant values as calculated by Two-way ANOVA when comparing WT and IL-17a/f$^{-/-}$ mice; **** $p < 0.0001$; ** $p < 0.01$

To further investigate the impact of c-di-AMP-induced IL-17 secretion on the generation of antigen-specific cellular responses in this disease-relevant influenza vaccine model, WT and IL-17a/f$^{-/-}$ mice were immunized i.n. with PBS, in-activated H5N1 NIBRG-14

alone or co-administered with c-di-AMP. Subsequently, the secretion of IL-17, IFNγ and IL-4 by splenocytes was assessed by ELISPOT following re-stimulation with NIBRG-14. The number of IL-17-producing cells was significantly enhanced in samples derived from WT animals immunized with NIBRG-14 co-administered with c-di-AMP as compared to samples derived from WT animals immunized with PBS or NIBRG-14 alone (Figure 40A). To confirm these results, splenic and lung lymphocytes were stimulated *ex vivo* with NIBRG-14 and analyzed by intracellular cytokine staining for $CD4^+$ T cells secreting IL-17. WT mice immunized with NIBRG-14 co-administered with c-di-AMP revealed significantly enhanced frequencies of splenic and lung IL-17-secreting $CD4^+$ T cells as compared to mice immunized with PBS or NIBRG-14 alone (Figure 40B and C). As expected, immunization of IL-17a/$f^{-/-}$ mice with NIBRG-14 co-administered with c-di-AMP did not induce any IL-17 secretion.

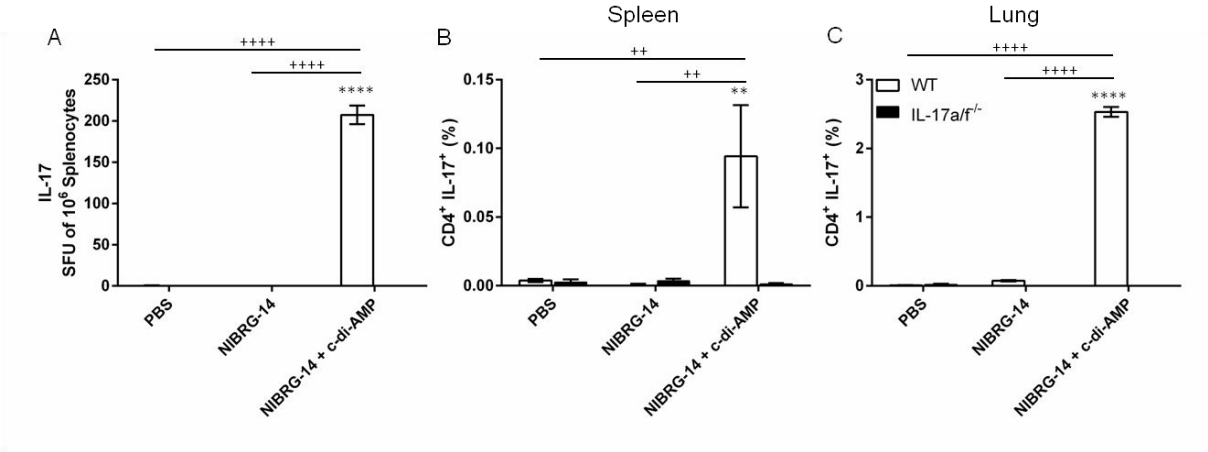

Figure 40: c-di-AMP-induced IL-17 secretion by $CD4^+$ T cells: WT and IL-17a/$f^{-/-}$ mice were i.n. immunized with PBS, NIBRG-14 alone (0.5 µg/dose) or NIBRG-14 co-administered with c-di-AMP (5 µg/dose). Splenocytes and lung lymphocytes were re-stimulated with NIBRG-14 (0.5µg/ml) overnight. The cells were incubated with brefeldin A (5 µg/ml) and monensin (6 µg/ml) for additional 4 h and were analyzed for A) IL-17secreting cells by ELISPOT (splenocytes) and frequencies of B) splenic and C) lung-derived IL-17-producing $CD4^+$ T cells by FACS. Results are expressed as subtracted background of unstimulated samples from stimulated samples. Columns represent the mean ± SEM of one experiment (n=6). Shown is one representative out of two independent experiments. Asterisks denote significant values as calculated by Two-way ANOVA when comparing WT and IL-17a/$f^{-/-}$ mice;**** $p < 0.0001$; ** $p < 0.01$. Plus denote significant values as calculated by Two-way ANOVA when comparing WT mice immunized with NIBRG-14 alone and with NIBRG-14 co-administered with c-di-AMP; ++++ $p < 0.0001$; ++ $p < 0.01$.

To understand the impact of c-di-AMP-induced IL-17 secretion on the NIBRG-14-specific Th1 response, splenocytes derived from immunized WT and IL-17a/$f^{-/-}$ mice were re-stimulated with NIBRG-14 and the number ofIFNγ producing splenic cells was

evaluated by ELISPOT. In both WT and IL-17a/f$^{-/-}$ mice the number of IFNγ-secreting splenic cells was significantly enhanced in the groups immunized with NIBRG-14 co-administered with c-di-AMP as compared to NIBRG-14 and PBS alone. Interestingly, IL-17a/f$^{-/-}$ mice immunized with NIBRG-14 co-administered with c-di-AMP displayed a higher number of CD4^{+}IFNγ-secreting cells as compared to WT mice (Figure 41A). These findings are confirmed by FACS analysis of NIBRG-14 re-stimulated splenic and lung lymphocytes. In both organs, WT and IL-17a/f$^{-/-}$ mice immunized with NIBRG-14 co-administered with c-di-AMP harbored enhanced frequencies of CD4^{+}IFNγ^{+} cells as compared to mice immunized with PBS or NIBRG-14 alone (Figure 41B and C). The comparison of WT and IL-17a/f$^{-/-}$ mice immunized with NIBRG-14 co-administered with c-di-AMP revealed elevated frequencies of CD4^{+}IFNγ-secreting cells in both organs derived from IL-17a/f$^{-/-}$ mice immunized with NIBRG-14 co-administered with c-di-AMP as compared to WT mice (Figure 41B and C). These data indicate that immunization with c-di-AMP induces Th1 responses that are more profound in the absence of IL-17 signaling.

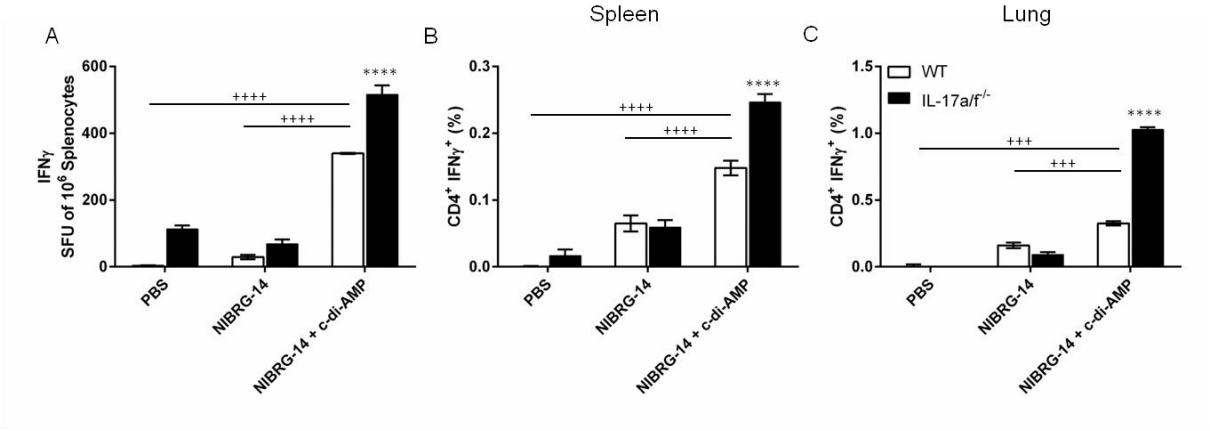

Figure 41: Impact of c-di-AMP-induced IL-17 secretion on NIBRG-14-specific Th1 responses: WT and IL-17a/f$^{-/-}$ mice were i.n. immunized with PBS, NIBRG-14 alone (0.5 µg/dose) or NIBRG-14 co-administered with c-di-AMP (5 µg/dose). Splenocytes and lung lymphocytes were re-stimulated with NIBRG-14 (0.5µg/ml) overnight. The cells were incubated with brefeldin A (5 µg/ml) and monensin (6 µg/ml) for additional 4 h and were analyzed for A) IFNγ-secreting cells by ELISPOT (splenocytes) and frequencies of B) splenic and C) lung-derived IFNγ-producing CD4^{+} T cells by FACS. Results are expressed as subtracted background of unstimulated samples from stimulated samples. Columns represent the mean ± SEM ofone experiment (n=6). Shown is one representative out of two independent experiments. Asterisks denote significant values as calculated by Two-way ANOVA when comparing WT and IL-17a/f$^{-/-}$ mice;**** $p < 0.0001$. Plus denote significant values as calculated by Two-way ANOVA when comparing WT mice immunized with NIBRG-14 alone and with NIBRG-14 co-administered with c-di-AMP; ++++ $p < 0.0001$; +++ $p < 0.001$.

To understand the impact of c-di-AMP-induced IL-17 secretion on the NIBRG-14-specific Th2 response, splenocytes derived from immunized WT and IL-17a/f$^{-/-}$ mice were re-stimulated with NIBRG-14 and the number of IL-4 producing splenic cells was evaluated by ELISPOT. In both, WT and IL-17a/f$^{-/-}$ mice, the number of IL-4-secreting splenic cells was significantly enhanced in the groups immunized with NIBRG-14 co-administered with c-di-AMP as compared to NIBRG-14 and PBS alone. IL-17a/f$^{-/-}$ mice immunized with NIBRG-14 co-administered with c-di-AMP displayed a reduced number of CD4^{+} IL-4-secreting cells as compared to WT mice (Figure 42A). These findings were confirmed by FACS analysis of NIBRG-14 re-stimulated splenic and lung lymphocytes. In both organs, WT and IL-17a/f$^{-/-}$ mice immunized with NIBRG-14 co-administered with c-di-AMP harbored enhanced frequencies of CD4^{+} IL-4^{+} cells as compared to mice immunized with PBS or NIBRG-14 alone (Figure 42B and C). The comparison of WT and IL-17a/f$^{-/-}$ mice immunized with NIBRG-14 co-administered with c-di-AMP revealed reduced frequencies of CD4^{+} IL-4-secreting cells in both organs derived from IL-17a/f$^{-/-}$ mice immunized with NIBRG-14 co-administered with c-di-AMP as compared to WT mice (Figure 42B and C). These data demonstrate that c-di-AMP-induced IL-17 secretion drives Th2 response stimulation.

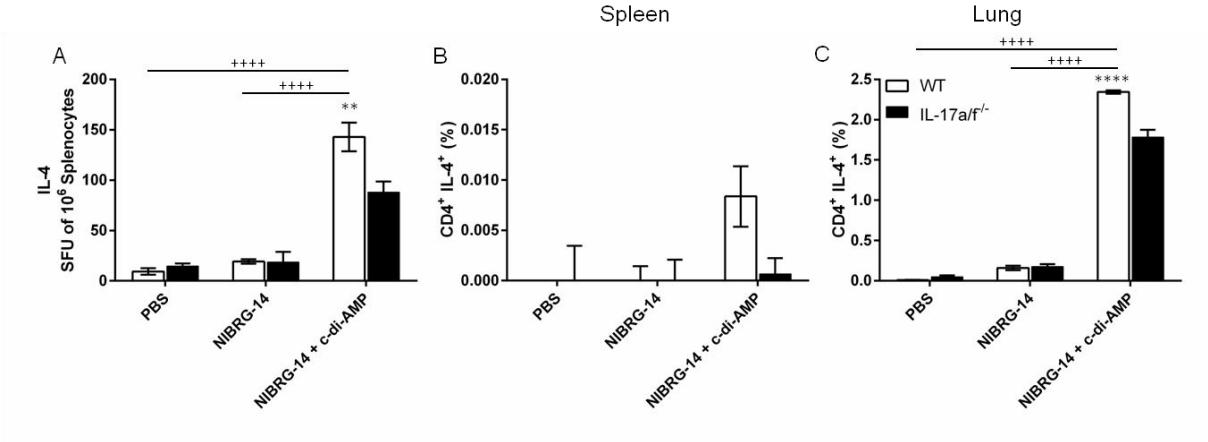

Figure 42: Impact of c-di-AMP-induced IL-17 secretion on NIBRG-14-specific Th2 responses: WT and IL-17a/f$^{-/-}$ mice were i.n. immunized with PBS, NIBRG-14 alone (0.5 µg/dose) or NIBRG-14 co-administered with c-di-AMP (5 µg/dose). Splenocytes and lung lymphocytes were re-stimulated with NIBRG-14 (0.5 µg/ml) overnight. The cells were incubated with brefeldin A (5 µg/ml) and monensin (6 µg/ml) for additional 4 h and were analyzed for A) IL-4 secreting cells by ELISPOT (splenocytes) and frequencies of B) splenic and C) lung-derived IL-4-producing CD4^{+} T cells by FACS. Columns represent the mean ± SEM of one experiment (n=6). Shown is one representative out of two independent experiments. Asterisks denote significant values as calculated by Two-way ANOVA when comparing WT and IL-17a/f$^{-/-}$ mice; **** $p < 0.0001$;** $p < 0.01$. Plus denote significant values as calculated by Two-way ANOVA when comparing WT mice immunized with NIBRG-14 alone and with NIBRG-14 co-administered with c-di-AMP; ++++ $p < 0.0001$.

5.4.4. Mechanisms favoring c-di-AMP-induced mucosal IgA response in an influenza vaccine model

The c-di-AMP-induced secretion of IL-17 seems to support antigen-specific IgA responses. Therefore, the factors favoring IgA secretion were subsequently evaluated upon immunization with NIBRG-14 and c-di-AMP. Two different mechanisms are described to play a central role for IgA-dependent mucosal immune responses: The activation of high-affinity IgA producing plasma B cells and modulation of the expression level of pIgR (polymeric Ig receptor) by epithelial cells responsible for sIgA transport [180, 181]. To investigate the impact of c-di-AMP-induced IL-17 secretion on plasma cell differentiation, the formation of germinal centers was assessed with respect to the interaction of GC B cells and T_{FH} cells. In addition, the expression level of pIgR by lung epithelial cells upon immunization was determined.

5.4.4.1. c-di-AMP-induced IL-17 secretion results in the co-localization of T_{FH} cells and GC B cells in GCs thereby promoting plasma B cell differentiation

GCs provide a microenvironment that promotes and regulates the interaction of B cells with T_{FH} cells, which provide the cognate help required for the generation of high-affinity, antibody-producing plasma B cells [44]. To investigate the role of c-di-AMP-induced IL-17 secretion in the context of plasma B cell generation in an influenza vaccination model, the interaction of GC B cells with T_{FH} cells was assessed. Histological analysis was performed 12 days post immunization (6 day post 1st boost) with PBS, NIBRG-14 alone or NIBRG-14 co-administered with c-di-AMP to determine the interaction of GC B cells with T_{FH} cells in context to plasma B cell differentiation. WT mice immunized with PBS or NIBRG-14 alone showed disseminated T_{FH} cells and GC B cells (Figure 43A and B upper panel). In contrast, WT mice immunized with NIBRG-14 co-administered with c-di-AMP showed co-localization of GC B cells and T_{FH} cells, hence favoring the environment for generation of plasma B cells (Figure 43C upper plots). In IL-17a/f$^{-/-}$ mice the GC B cells and T_{FH} cells were disseminated under all treatment conditions (Figure 43C lower plots). The histological scoring revealed a significant increase in co-localization of GC B cells and T_{FH} cells in WT mice immunized with NIBRG-14 co-administered with c-di-AMP as compared to mice immunized with PBS alone (Figure 43D). A significantly reduced co-localization of GC B cells and T_{FH} cells was observed in IL-17a/f$^{-/-}$ mice immunized with NIBRG-14 co-administered with c-di-AMP as compared to the corresponding WT group. These data indicate that

NIBRG-14 and c-di-AMP-induced IL-17 secretion is required for optimal GC responses with respect to the generation of plasma B cells.

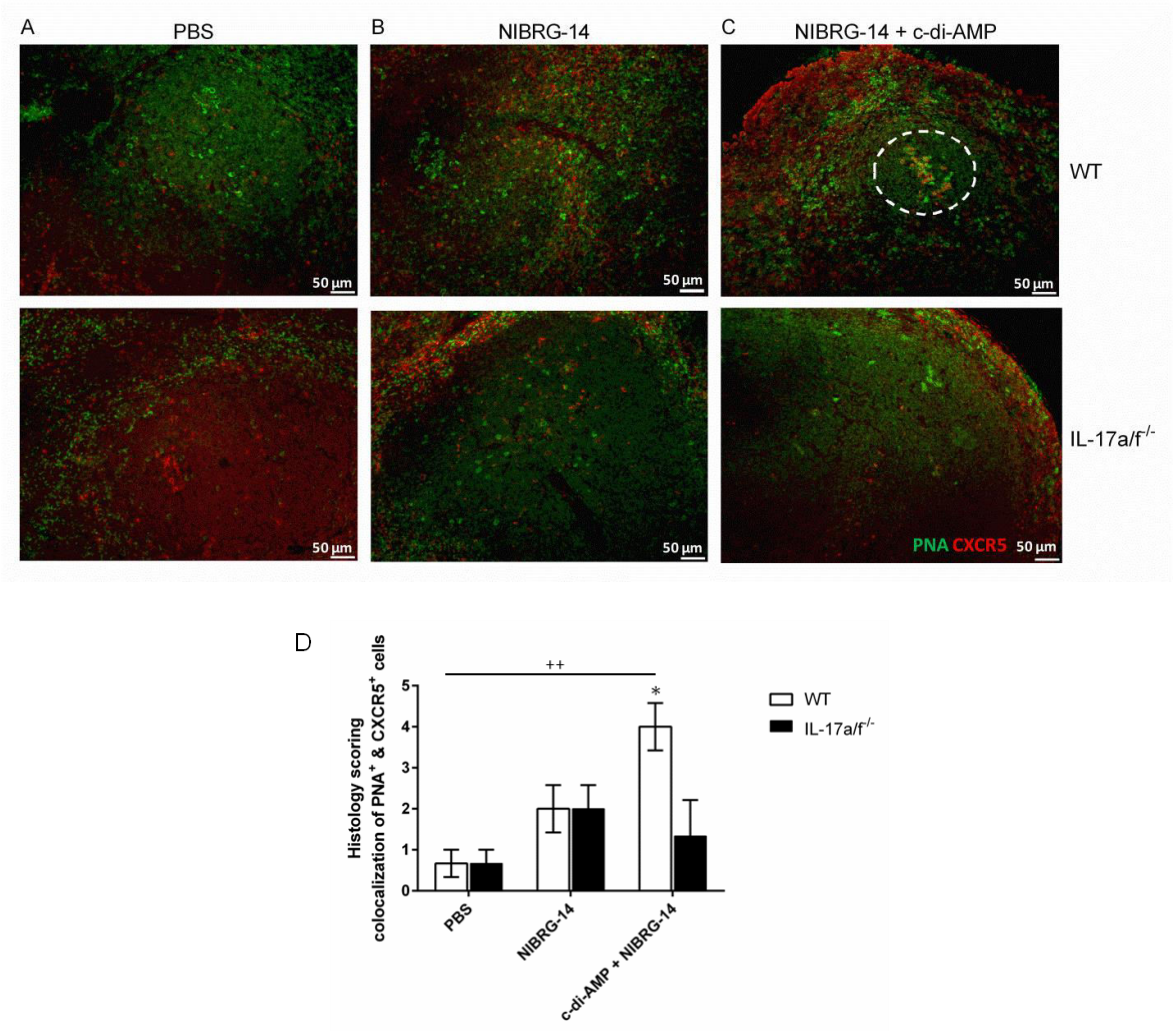

Figure 43: Co-localization of T_{FH} cells and GC B cells mediated by c-di-AMP-induced IL-17 secretion: WT (upper panel) and IL-17a/f$^{-/-}$ (lower panel) mice were i.n. immunized with PBS or NIBRG-14 alone (0.5 µg/dose) or NIBRG-14 co-administered with c-di-AMP (5 µg/dose). The animals were sacrificed on day 12 post immunization. Spleen tissues were stained for GC B cells (CD19^{+}PNA^{+}, green) and T_{FH} cells (CD3^{+}CXCR5^{+}, red) and fluorescent imaging was performed to assess for the cell distribution. The analysis was performed at 20x magnification. Localization of GC B cells and T_{FH} cells in mice immunized with A) PBS, B) NIBRG-14 and C) NIBRG-14 co-administered with c-di-AMP. D) Histology scoring of co-localization of GC B cells (PNA^{+}) and T_{FH} cells (CXCR5^{+}) was determined. Columns represent the mean ± SEM of one independent experiment (n=9). Asterisks denote significant values as calculated by Two-way ANOVA comparing WT and IL-17a/f$^{-/-}$ mice; * $p < 0.05$. Plus denote significant values as calculated by Two-way ANOVA when comparing WT mice immunized with PBS alone and with OVA co-administered with c-di-AMP; ++ $p < 0.01$.

To further confirm these *in vivo* observations *in vitro* co-culture studies were performed.To this end, sorted T_{FH} cells ($CD4^+CXCR5^+$) and GC B cells ($CD19^+PNA^+$) obtained from cLNs and spleens of naïve WT and IL-17a/f$^{-/-}$ mice were co-cultured for 6 days in the presence of NIBRG-14 or c-di-AMP alone or in combination. Controls were left untreated. A significantly increased frequency of plasma B cells ($CD19^+CD138^+$) was detected in co-cultures supplemented with both NIBRG-14 and c-di-AMP as compared to NIBRG-14 alone. Furthermore,a significantly lower frequency of plasma B cells was observed in wells containing cells isolated from IL-17a/f$^{-/-}$ mice cultured with NIBRG-14 and c-di-AMP as compared to corresponding WT co-cultures (Figure 44A). The addition of rIL-17A to the IL-17a/f$^{-/-}$ co-cultures significantly increased the differentiation of plasma B cells to the level found in co-cultures containing cells isolated from WT mice. The analysis of plasma B cell subclasses showed that c-di-AMP-induced IL-17 secretion supports IgA subclass differentiation (Figure 44B).This indicates that IL-17 plays a direct role for the differentiation of plasma B cells.

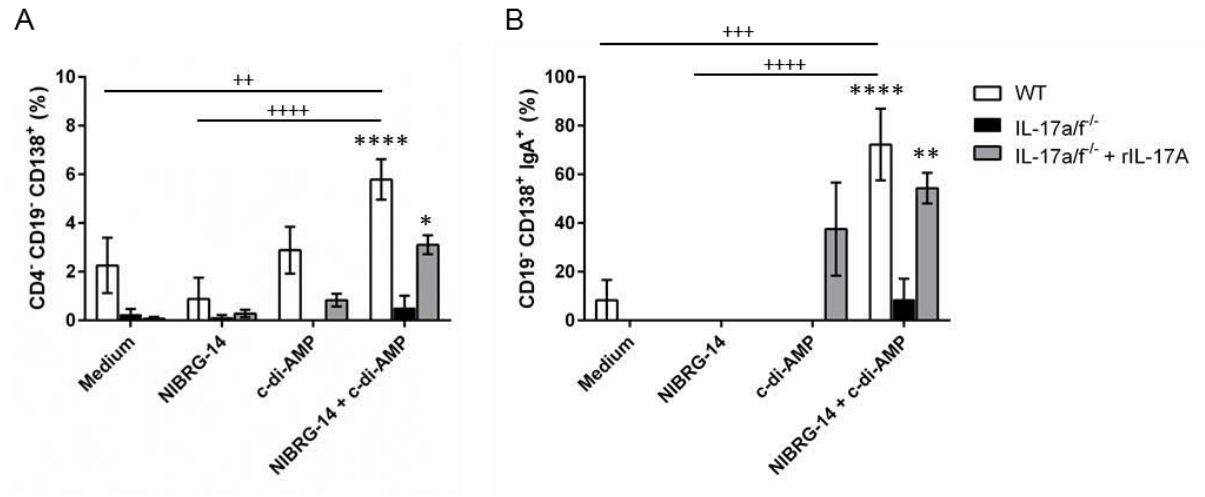

Figure 44: c-di-AMP-induced plasma B cell differentiation: Sorted GC B cells and T_{FH} cells derived from cLNs and spleens of WT and IL-17a/f$^{-/-}$ mice were left untreated or treated with NIBRG-14 alone (1 µg/ml) or c-di-AMP alone (5 µg/ml) or in combination for 6 days. rIL-17A was added to IL-17a/f$^{-/-}$ culture conditions as indicated. The cells were incubated with brefeldin A (5 µg/ml) and monensin (6 µg/ml) for additional 4 h, subsequently stained with cell population specific markers and analyzed by flow cytometry. Frequencies of A) plasma B cells ($CD19^-CD138^+$) and B) IgA^+ plasma B cells ($CD19^-CD138^+IgA^+$) were determined. Columns represent the mean ± SEM of one independent experiment (n=3). Asterisks denote significant values as calculated by Two-way ANOVA when comparing WT and IL-17a/f$^{-/-}$ cultures; **** $p < 0.0001$; ** $p < 0.01$; * $p < 0.05$. Plus denote significant value between different treatment groups of NIBRG-14 co-administered with c-di-AMP as calculated by Two-way ANOVA; ++++ $p < 0.0001$; +++ $p < 0.001$ ++ $p < 0.01$.

IgA class switching is known to be impacted by T cell-derived cytokines including TGFβ1, IL-4, IL-6 and IL-10 [182]. Thus, the analysis of the specific cytokine milieu induced upon immunization can provide insights into the immune processes initiated by c-di-AMP treatment leading to IgA^+ plasma B cell generation. Therefore, to gain insights into the cytokines contributing to IgA class-switch, the c-di-AMP-induced cytokine environment was evaluated. To this end, splenic cells obtained from immunized mice were stimulated *ex vivo* with NIBRG-14 for 72 h and the supernatant was assessed to gain an in depth insight into the cytokine profile. Splenic cells obtained from WT and IL-17a/f$^{-/-}$ mice immunized with NIBRG-14 co-administered with c-di-AMP displayed elevated levels of IFNγ, IL-2, TNFα, IL-4, IL-6, IL-10, IL-17 and IL-22 as compared to PBS and NIBRG-14 alone (Figure 45A, B, C and D). Furthermore, a significantly reduced secretion of IL-4, IL-6 and IL-10, cytokines known to favor IgA class-switch, was observed in IL-17a/f$^{-/-}$ mice immunized with NIBRG-14 co-administered with c-di-AMP as compared to WT mice (Figure 45B and D). Therefore, the obtained results suggest that the *in vivo* induction of c-di-AMP-induced IL-17 secretion might favor a cytokine environment that promotes IgA class-switch.

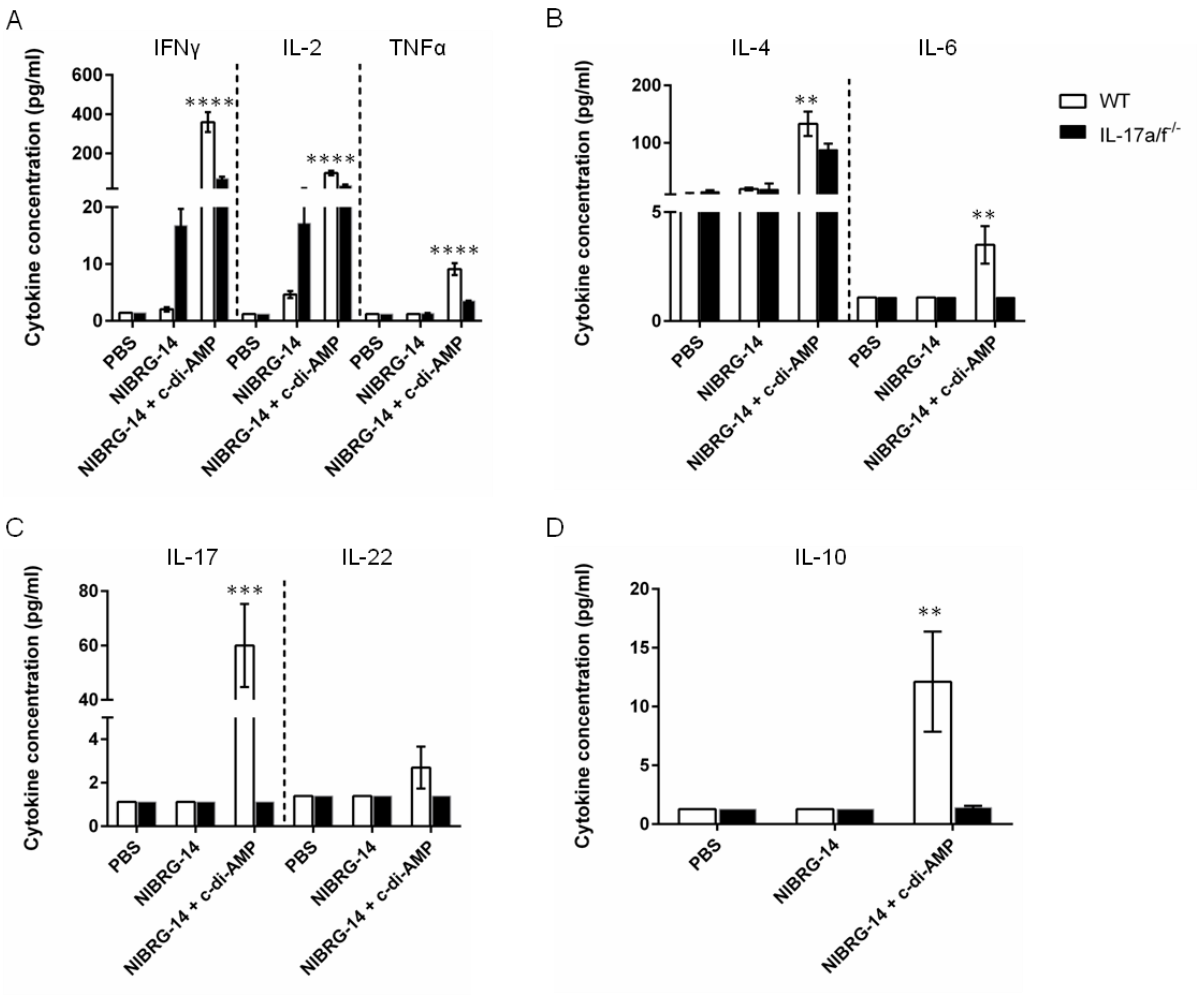

Figure 45: Immunization-induced serum cytokine pattern: Splenic cells obtained from WT and IL-17a/f$^{-/-}$ mice immunized with PBS, NIBRG-14 alone (0.5 µg/dose) or NIBRG-14 co-administered with c-di-AMP (5 µg/dose) were re-stimulated *ex vivo* with NIBRG-14 (2 µg) for 72 h and the supernatant was collected and stored at -20°C. The cytokine profiles resulting from A) Th1 B) Th2 C) Th17 and D) T_{reg} cytokine secretion were analyzed by CBA. Columns represent the mean ± SEM of one experiment (n=3). Asterisks denote significant values as calculated by Two-way ANOVA when comparing WT and IL-17a/f$^{-/-}$ mice; **** $p < 0.0001$; *** $p < 0.001$; ** $p < 0.01$.

5.4.4.2. Impact of c-di-AMP-induced mucosal IL-17 secretion on pIgR expression by lung epithelium

Besides the generation of plasma B cells, pIgR is known to play a central role in mucosal immunity by mediating the delivery of polymeric IgA to the apical surface of epithelial cells via transcytosis [183]. The pIgR is typically expressed by mucous and ciliated epithelial cells in the bronchi [184]. Therefore, to assess the role of pIgR for the c-di-AMP-induced IL-17-mediated IgA responses a kinetic experiment was performed.

Mice were i.n. immunized and subsequently boosted once 14 days after immunization with PBS, NIBRG-14 alone or NIBRG-14 co-administered with c-di-AMP. On day 1, day 6 and day 11 post boost the level of pIgR expression was determined by performing RTPCR using RNA obtained from lung tissue. Although not statistically significant, there is a clear trend for slightly increased expression levels of pIgR in WT mice on day 15 and day 20 after the immunization as compared to WT mice immunized with PBS alone. On the other hand, on day 25 a significant induction of pIgR expression in WT mice immunized with NIBRG-14 co-administered with c-di-AMP as compared to WT mice immunized with PBS or NIBRG-14 alone was observed. Furthermore, samples derived from IL-17a/f$^{-/-}$ mice immunized with NIBRG-14 co-administered with c-di-AMP showed a significantly reduced pIgR expression as compared to correspondingly immunized WT mice (Figure 46). These findings show that c-di-AMP-induced IL-17 secretion mediates the upregulation of pIgR expression on lung epithelial cells, thereby representing a possible mechanism for the observed enhanced sIgA secretion.

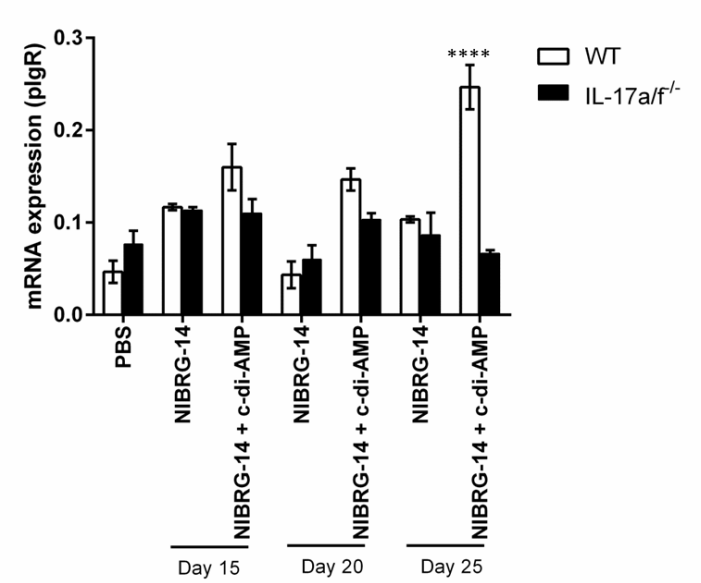

Figure 46: Impact of c-di-AMP-induced IL-17 secretion on pIgR expression by lung epithelial cells: WT and IL-17a/f$^{-/-}$ mice were i.n. immunized with PBS, NIBRG-14 alone (0.5 µg/dose) or NIBRG-14 co-administered with c-di-AMP (5 µg/dose). Animals were sacrificedon day 15, day 20 and day 25 after immunization and pIgR expression was determined. Columns represent the mean ± SEM of one independent experiment (n=3). Asterisks denote significant values as calculated by Two-way ANOVA when comparing WT and IL-17a/f$^{-/-}$ mice; **** $p < 0.0001$.

pIgR expression is induced by a range of factors including the cytokine microenvironment [42]. Therefore, the local cytokine profile in the lung was analyzed in order to obtain a mechanistic insight into the induction of pIgR expression by epithelial

cells upon i.n. immunization with NIBRG-14 co-administered with c-di-AMP. Thus, the cytokine profile in lung lavage samples obtained at day 15, 20 and 25 post immunization was analyzed with respect to cytokines known to up-regulate pIgR expression, including IFNγ, TNFα and IL-4. In addition, the concentration of IL-17A was assessed in order to confirm that the presence of IL-17A is responsible for the observed pIgR expression. On day 20 and 25 no cytokine secretion was detected. Whereas, on day 15 enhanced levels of IFNγ and TNFα were observed in lung lavage samples derived from WT and IL-17a/f$^{-/-}$ mice immunized with NIBRG-14 co-administered with c-di-AMP as compared to WT and IL-17a/f$^{-/-}$ mice immunized with PBS or NIBRG-14 alone (Figure 47). Furthermore, a significantly reduced concentration of IFNγ and TNFα was observed in IL-17a/f$^{-/-}$ mice immunized with NIBRG-14 and c-di-AMP as compared to WT mice immunized accordingly. Additionally, a significantly enhanced level of IL-17A was observed in WT mice immunized with NIBRG-14 and c-di-AMP as compared to WT mice immunized with PBS or NIBRG-14 alone. IL-4 was not detected in lung lavage samples. These data indicate that the enhanced pIgR expression by airway epithelial cells upon immunization with NIBRG-14 and c-di-AMP might be modulated by increased secretion of IFNγ and TNFα dependent on IL-17 signaling.

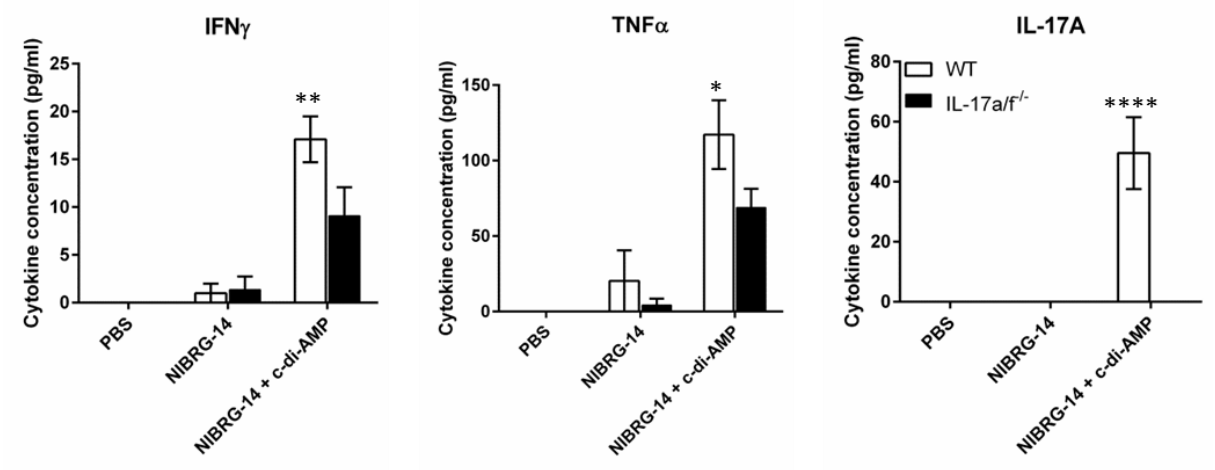

Figure 47: c-di-AMP-induced IFNγ and TNFα secretion in the airways: WT and IL-17a/f$^{-/-}$ mice were immunized with PBS, NIBRG-14 alone (0.5 µg/dose) or NIBRG-14 co-administered with c-di-AMP (5 µg/dose). Lung lavage samples were collected at day 15 after immunization and analyzed for the indicated cytokines by CBA. Columns represent the mean ± SEM of one experiment (n=3). Asterisks denote significant values as calculated by Two-way ANOVA when comparing WT and IL-17a/f$^{-/-}$ BAL samples; **** $p < 0.0001$; ** $p < 0.01$; * $p < 0.05$.

5.5. Assessment of c-di-AMP-induced protective immune responses in an acute influenza challenge

The presented data provide evidence that c-di-AMP-induced IL-17 secretion mediates strong antigen-specific cellular (Th2 and Th17) and humoral (IgA) responses upon i.n. administration. However, the protective efficacy of c-di-AMP-induced antigen-specific Th17 responses in the course of viral infections still remains elusive. Therefore, to explore the protective potential of c-di-AMP-induced Th17 responses WT and IL-17a/f$^{-/-}$ mice were immunized i.n. with PBS, NIBRG-14 alone or co-administered with c-di-AMP according to the prime boost schedule and subsequently challenged with a sub-lethal dose of 2.5x10^4 ffu H5N1 influenza virus. The body weight and health status of the animals were monitored daily. Animals immunized with PBS lost more than 20% of their starting weight at day 6 in WT mice and day 7 in IL-17a/f$^{-/-}$ mice after infection and were thus sacrificed (Figure 48). WT mice immunized with NIBRG-14 alone displayed ~8% of weight reduction at day 4 post infection and started to recover their weight at day 5 post infection. In contrast, IL-17a/f$^{-/-}$ mice immunized with NIBRG-14 alone displayed negligible (~2%) weight loss at day 4 post infection as compared to corresponding WT mice. WT mice vaccinated with NIBRG-14 co-administered with c-di-AMP exhibited a strong resistance to influenza challenge with less than 5% of weight reduction at day 2 post infection, and showed a rapid recovery of their starting weight at day 3 post infection. No significant difference in the weight reduction was observed when comparing WT and IL-17a/f$^{-/-}$ mice immunized with NIBRG-14 co-administered with c-di-AMP (Figure 48B).

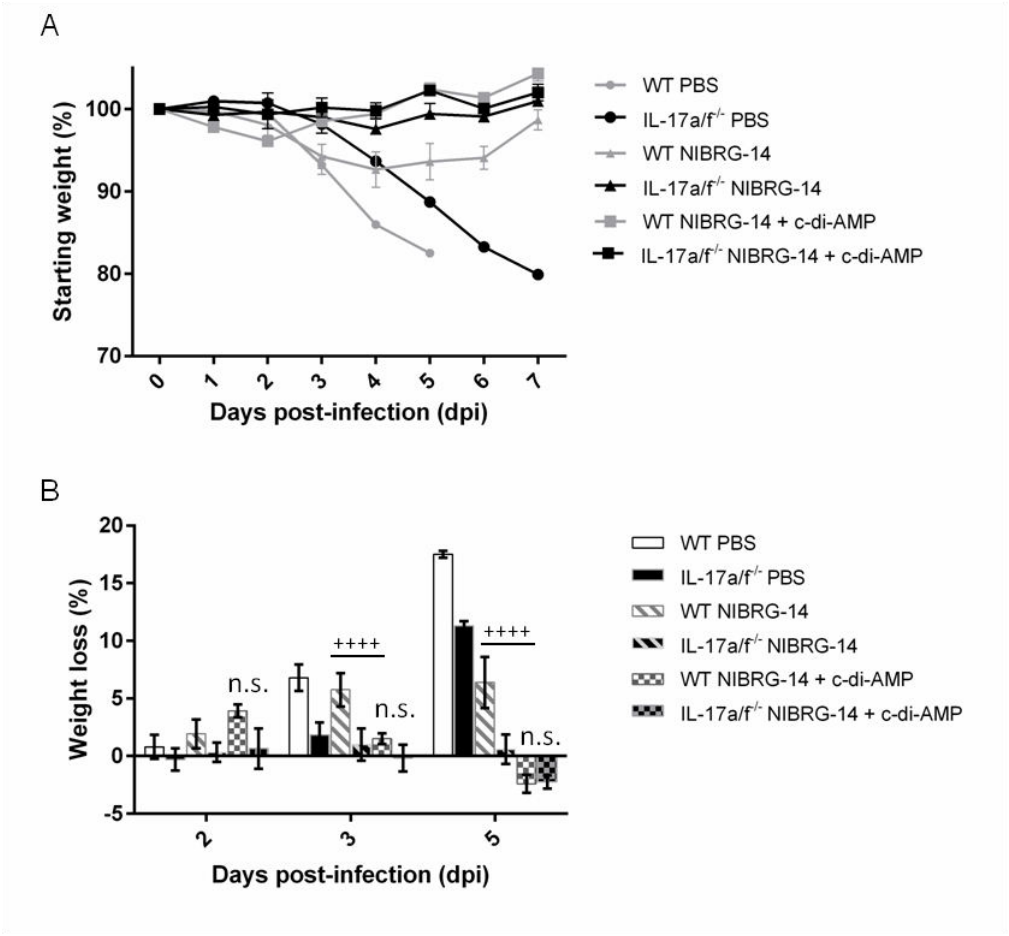

Figure 48: Weight development of immunized mice after i.n. H5N1 virus challenge: WT and IL-17a/f$^{-/-}$ mice were i.n. immunized with PBS, NIBRG-14 alone (0.5 µg/dose) or NIBRG-14 co-administered with c-di-AMP (5 µg/dose). Subsequently, immunized mice were i.n. challenged with a sub-lethal dose of $2.5x10^4$ ffu of the H5N1 virus strain. Animals were sacrificed when they showed weight loss > 20% of their starting weight. A) Starting weight and B) weight loss at day 2, 3 and 5 post infection. Columns represent the mean ± SEM of one independent experiment (n=6). Plus denote significant value comparing WT mice immunized with NIBRG-14 alone and with NIBRG-14 co-administered with c-di-AMP as calculated by Two-way ANOVA; ++++ $p < 0.0001$; n.s. = not significant.

6. Discussion and Outlook

The crucial role of IL-17-secreting cells in combating bacterial and fungal mucosal infections has been well described. In this line, it was shown that IL-17 regulates anti-fungal immunity against *C. albicans* by upregulating proinflammatory cytokines like IL-6, as well as by recruiting neutrophils at thesite of infection [185, 186]. Recent studies have further described the role of Th17 cells in promoting pIgR-mediated delivery of sIgA into the airway lumen and intestines [187, 188]. This is likely to support defense against respiratory and gastro-enteric pathogens, and contribute to intestinal homeostasis. The versatile functions of Th17 cells including the initiation of humoral immunity by regulating GC formation in response to acute viral myocarditis and augmenting other T helper subsets in response to infections (*e.g. M. tuberculosis*) additionally highlight the potential of Th17 cells as targets for mucosal vaccination strategies [189, 190]. However, the exploitation of their potential as targets for prophylactic and therapeutic applications requires an in-depth understanding of the mechanisms underlying Th17 differentiation as well as their role in inducing antigen-specific immune responses. Therefore, this thesis aimed at elucidating the impact of Th17 responses for the outcome of vaccination strategies.

The c-di-AMP, a bacterial secondary messenger, has been reported as a potent systemic and mucosal vaccine adjuvant [97]. It is able to promote the elicitation of Th17 responses; however, its specific impact on Th17-differentiation and vaccine-induced antigen-specific Th17 responses still needs to be elucidated. Thus, c-di-AMP was applied as a tool to understand the cellular mechanisms inducing antigen-specific Th17 responses upon i.n. immunization. The specific impact of IL-17-secreting cells for viral control and vaccine-induced protective immune responses were assessed using IL-17a/f$^{-/-}$ mice. These approaches represent an important step towards understanding Th17-mediated immune responses, their regulation and their subsequent exploitation for the development of innovative immunization strategies.

Aiming at revealing the mechanisms underlying Th17 differentiation, *in vitro* treatment of WT-derived BMDCs with c-di-AMP resulted in a strong maturation with an enhanced surface expression of MHC I and CD86. This up-regulation of MHC I and CD86 are consistent with previous studies identifying BMDCs and macrophages as the target cell populations activated upon *in vitro* treatment with c-di-AMP [96, 112]. However, the additional observation of an increased surface expression of IL-17RA and TNFα is not completely in line with its described STING-dependent activation of theTBK3-IRF3

pathway resulting in type 1 IFN production *in vitro* [110, 191, 192]. These findings hint towards an alternative c-di-AMP-activated signaling pathway downstream of STING via NF-κB signaling subsequently resulting in TNFα production. This hypothesis is supported by previous studies in IFNAR$^{-/-}$ mice demonstrating that type 1 IFNs are dispensable for CDN-induced antigen-specific generation of IgG and IgA, in which a non-canonical STING-dependent TNF activation pathway has been proposed [193]. The side-by-side comparison of BMDCs derived from WT and IL-17a/f$^{-/-}$ mice upon stimulation with c-di-AMP *in vitro* revealed an impaired surface expression of MHC I and CD86 by IL-17a/f$^{-/-}$ BMDCs as compared to those derived from WT mice. This suggests a reduction in their ability to evoke effector immune responses. The findings also show that IL-17 seems to be required for c-di-AMP-induced BMDC maturation, which in turn facilitates the stimulation of an adaptive immune response.

WT-derived CD4$^+$ T cells co-cultured with c-di-AMP-primed IL-17a/f$^{-/-}$-derived BMDCs exhibited impaired expression of IL-17 as well as RORγt as compared to WT-derived CD4$^+$ T cells co-cultured with WT-derived BMDCs. As expected, these results confirm the inability of IL-17a/f$^{-/-}$ BMDCs to drive Th17 differentiation. *In vitro* stimulation of naïve CD4$^+$ T cells with exogenous addition of IL-6, TGF-β, IL-1β and IL-23 were shown to contribute to Th17 differentiation [194-196]. Therefore, to thoroughly understand the mechanism underlying the observed defective Th17 differentiation, the effects of different cytokines secreted following *in vitro* treatment of BMDCs with c-di-AMP were considered. The analysis of supernatants derived from c-di-AMP treated WT BMDCs revealed increased levels of IL-6 as compared to IL-17a/f$^{-/-}$ BMDCs. IL-6 is a pleiotropic cytokine secreted by DCs, macrophages and CD4$^+$ T cells [165]. Besides its importance for Th17 differentiation IL-6 also inhibits the TGF-β-induced T_{reg} differentiation [197]. Thus, c-di-AMP-induced IL-6 secretion might inhibit the functionality of T_{reg} cells thus enabling the induction of Th17 response in WT settings. In IL-17a/f$^{-/-}$ mice, the reduced IL-6 response might result in a higher functionality of T_{reg} cells, thus suppressing Th17 induction. This hypothesis is supported by a study showing that *in vivo* immunization of IL-6$^{-/-}$ (gp130$^{-/-}$) mice with myelin oligodendrocyte glycoprotein (MOG35-55) in complete Freund's adjuvant (CFA) resulted in enhancedT_{reg} response [198]. While IL-23 was not detectable in the supernatant of c-di-AMP-treated BMDCs, the flow cytometry analysis of IL-12/IL-23p40-expressing BMDCs upon *in vitro* stimulation with c-di-AMP revealed an enhanced expression of IL-12/IL-23p40 by BMDCs derived from WT mice as compared to those derived from IL-17a/f$^{-/-}$ mice. Several reports showed that Th17 cells can be generated *in vitro* using either IL-23 alone or co-stimulation with TGF-β and IL-6 [194, 195, 199]. In addition, stimulation of naïve T cells with IL-23 was shown to induce

the generation and expansion of pathogenic Th17 cells [168]. However, *in vitro* experiments in the presence of antibodies blocking IL-6 and/or IL-23 signaling revealed that IL-6 but not IL-23 is required for the observed c-di-AMP-induced Th17 differentiation. This is supported by previous studies showing the differentiation of naïve $CD4^+$ T cells into Th17 cells upon co-culture with LPS-stimulated DCs *in vitro* in the presence of IL-23 blocking antibodies, as long as IL-6 and TGFβ are present [194, 200]. Since TGFβ levels were not affected by c-di-AMP stimulation, the obtained results strongly support that c-di-AMP-induced IL-6 secretion by BMDCs induces Th17 differentiation while IL-23 is dispensable for this commitment. However, an IL-23-dependent homeostasis of Th17 cells cannot be excluded, since IL-23 has been reported to maintain the Th17 phenotype *in vitro* [201]. To address this role of IL-23, *in vitro* co-culture experiments applying the stepwise blocking or addition of IL-6 and or IL-23 could provide crucial insights.

In order to explore the role of c-di-AMP-induced Th17 responses in evoking antigen-specific immunity, immunization experiments using OVA as model antigen co-administered with c-di-AMP as adjuvant were conducted comparing the immune responses in WT and IL-17a/$f^{-/-}$ mice. Previous studies performed in WT mice showed that co-administration of c-di-AMP as a mucosal vaccine adjuvant results in improved antigen-specific cellular and humoral responses [97]. The present study revealed that c-di-AMP-induced IL-17 secretion supports antigen-specific Th2 immunity, as detected by an enhanced IL-4 secretion. IL-17a/$f^{-/-}$ mice showed an impaired Th2 response upon vaccination, as indicated by a reduced IL-4 secretion compared to what observed in WT mice. Th1 responses were found to be enhanced in IL-17a/$f^{-/-}$ mice as compared to WT mice, as demonstrated by a higher IFNγ secretion. While there is no direct evidence linking IL-17 secretion and Th2 responses, the repressive effect of IL-17 on Th1 responses has been reported in mice treated *in vivo* with anti-IL-17, which showed an increased number of IFNγ-producing cells in response to a *C.albicans* infection as compared to untreated controls [202]. IL-17A has further been shown to inhibit Th1 cell development by suppressing Th1 associated gene expression, such as T-bet, osteopontin and IL-12β2, in a colitis model [203]. In addition to Th cells, mice lacking IL-17a/f revealed an increased cytotoxic capacity as compared to WT mice. Combined with the observed enhanced Th1 response in IL-17a/$f^{-/-}$ mice, this finding is consistent with the described importance of Th1 cells for the generation of CTL-mediated immunity. Mice immunized with DCs pulsed with a Th1 polarizing antigen, displayed a higher magnitude of IFNγ-producing CTLs. This effect was abrogated upon depletion of

CD4 cells [204, 205]. IL-17a/f$^{-/-}$ mice immunized with OVA co-administered with c-di-AMP further exhibited an impaired OVA-specific humoral immune response with regard to the secretion of IgA, IgG and IgG1. This is in line with a study describing that the adoptive transfer of Th17 cells derived from 2D2 MOG_{35-55}-specific TCR transgenic mice into WT mice resulted in a significantly enhanced MOG-specific IgG1 response as compared to mice that did not receive Th17 cells [206]. Another study described that adoptive transfer of DO11.10 CD4^{+} Th17 cells and subsequent exposure to OVA aerosols resulted in enhanced IgA levels in the broncho-alveolar lavage fluid (BAL) of Th17 recipient BALB/c mice [187]. These data indicate that c-di-AMP-induced IL-17 supports the humoral immune response both at the systemic (IgG1) as well as the mucosal (IgA) level.

The production of IgA is a hallmark of adaptive mucosal immunity and its ability to prevent colonization of pathogens at the mucosal surfaces contributes to the prevention of infections [73, 207, 208]. Several factors such as cytokines including IL-4, IL-5 and IL-6 derived from interacting B and T cells are described to modulate mucosal humoral responses [209]. In this regard, Th2 cell-derived IL-5 has been shown to increase the IgA production of LPS-activated murine B cells *in vivo* [210]. Thus, the reduced IL-5 secretion observed in *ex vivo* stimulated splenic cells obtained from immunized IL-17a/f$^{-/-}$ mice as compared to WT mice might explain the reduced IgA levels detected in the absence of IL-17. The analysis of *in vivo* intraperitoneal administered rIL-5 and rIL-17 alone or in-combination (1 day prior to immunization and boosting) confirmed the requirement of IL-5 for the induction of IgA secretion. Thus, the obtained data suggest that c-di-AMP-induced Th17 responses favor antigen-specific Th2 responses, thereby contributing to antigen-specific humoral immune responses.

Experiments comparing the immune response of co-housed and non-co-housed mice showed a significant increase in OVA-specific IgG and IgG2c titers in IL-17a/f$^{-/-}$ mice upon co-housing with WT mice as compared to non-co-housed IL-17a/f$^{-/-}$ mice. These findings are in line with recent publications highlighting the strong influence of the microbiota on the immune system and vaccine efficacy [173, 211]. Colonization of germ-free mice with microbiota obtained from WT mice contributes to the generation of Th17 cell immune responses [212]. In addition, germ-free mice displayed a reduced trivalent inactivated influenza vaccine-specific IgG response as compared to WT mice 7 days post vaccination, thereby highlighting the role of microbiota for vaccine efficacy [213]. Thus, the generated data indicate that the microbiota strongly influences c-di-AMP-induced systemic humoral immune responses. In contrast, OVA-specific IgA

titers were not impacted by changes in the microbiota upon co-housing. This suggests that the observed IgA response is solely dependent on the c-di-AMP-induced Th17 response. The comparison of 16s rRNA isolated from feces of naïve WT and IL-17a/f$^{-/-}$ mice showed a huge variability in the composition of the microbiota which was paralleled by a low relative abundance of the SFB microbial community in IL-17a/f$^{-/-}$ mice. SFB has been reported to promote the accumulation of Th17 cells in the small intestine, thereby driving the production of IgA [214]. This represents a possible mechanism accounting for the observed reduction of antigen-specific IgA response in IL-17a/f$^{-/-}$ mice as compared to WT mice. Thus, the observed altered systemic humoral response due to co-housing and simultaneous differences in the SFB microbial community support a direct correlation of microbiota and humoral responses in the presented experimental setting. This hypothesis is supported by a previous publication showing that secondary colonization of germ-free mice that were already mono-associated with SFB with *Morganella morganii* resulted in increased GC reaction, thereby favoring antibody production [215, 216]. In addition, upon colonization of germ-free mice with SFB, 95% of all IL-17 producing cells in the lamina propria lymphocytes of the small intestine were identified as Th17 cells (CD4^{+}TCRαβ^{+} lymphocytes) [217, 218]. This report supports the finding of a higher abundance of SFB microbial community in correlation with the c-di-AMP-induced expansion of CD3^{+}CD4^{+} cells as the main IL-17 secreting population in WT mice. Interestingly, colonization of IL-17a/f$^{-/-}$ mice with feces obtained from mice monocolonized with SFB showed no significant difference in IgG immune responses upon immunization. In contrast, in lung lavage samples IgA concentrations were slightly increased in IL-17a/f$^{-/-}$ mice monocolonized with SFB when compared to non-colonized IL-17a/f$^{-/-}$ mice. Thus, it is likely that SFB alone is not responsible for the altered humoral immunization-induced immune response. Other factors such as the complex interplay of other microbial communities can be responsible for the altered c-di-AMP induced systemic humoral response in IL-17a/f$^{-/-}$ mice upon co-housing.

The role of c-di-AMP-induced IL-17 responses in mediating adaptive immunity and the generation of protective immune responses was further assessed in an influenza vaccination model. IL-17a/f$^{-/-}$ mice immunized with the inactivated NIBRG-14 strain co-administered with c-di-AMP exhibited enhanced neutralizing antibody responses as compared to WT mice. However, no significant differences in the IgG titers were observed in the two mouse strains. This finding is in contrast to a study showing that mice immunized with HA-DNA displayed high IgG1 levels which were associated with

enhanced titers of neutralizing antibodies that positively correlate to vaccine-induced protective immunity against sublethal challenge with 3 minimum lethal doses (MLD_{50}) of HK/Syd which consists of A/Sydney/5/97 (H3N2) strain and A/Puerto Rico/8/34 (H1N1) strain. In the same study, IgG2c titers were correlated with protection and viral clearance after a lethal influenza challenge [219]. Individuals vaccinated with LAIV and TIV vaccines displayed increased anti-influenza neutralizing antibody responses with an increased salivary homotypic IgG concentration but displayed no IgA response [220]. This in line with findings where IL-17a/f$^{-/-}$ mice exhibited enhanced titers of NIBRG14-specific neutralizing antibodies but reduced IgA responses. Furthermore, reduced NIBRG-14-specific IgA and sIgA titers were observed in IL-17a/f$^{-/-}$ mice when compared to WT mice. These findings are in line with a report stating that mice vaccinated with the Th17-inducing adjuvant Cationic Adjuvant Formulation no.1 promoted substantial IgA levels but not IgG in the lungs. This effect was abrogated upon depletion of IL-17A [221]. The importance of IgA is further supported by studies showing its potential to prevent influenza infection better than IgG [222]. The induction of mucosal immunity in terms of sIgA production acts as an important first line of defense against pathogens such as influenza [223]. Although, IgG is the major systemic antibody class, more than 80% of human and mouse plasma cells located at the gastrointestinal and respiratory tracts produce IgA with incorporated J chain, thus being committed to sIgA generation [224]. These data suggest that c-di-AMP-induced Th17-mediated NIBRG-14-specific IgA might be an essential defense mechanism needed for protection against influenza infection upon immunization using a c-di-AMP-adjuvanted vaccine.

Following the *ex vivo* re-stimulation of splenic cells isolated from WT mice immunized with NIBRG-14 and c-di-AMP, elevated concentrations of IL-4, IL-6 and IL-10 were detected in supernatant fluids. This cytokine environment has been reported to promote an IgA class-switch [182]. This is supported by the finding that the stimulation of LPS-activated B cells with TGFβ1, IL-4 and IL-6 supports the secretion of IgA [225]. Therefore, the obtained results hint that the induction of Th17 responses by c-di-AMP *in vivo* triggers IgA class-switching possibly by impacting the micro environment.

The histological analysis of splenic T_{FH} cells and GC B cells 12 day post immunization showed their co-localization in follicles upon immunization with NIBRG-14 and c-di-AMP in WT but not IL-17a/f$^{-/-}$ mice. This is consistent with recently published studies showing that IL-17RA-IL-17 signaling regulates the localization of T_{FH} cells in GC light zone. In the presence of IL-17, T_{FH} cells upregulate the expression of regulator of G-protein signaling (Rgs16), thereby promoting GC development and high-affinity antibody

production [226]. The observed importance of c-di-AMP-induced IL-17 for the differentiation of plasma cells is further supported by the finding that the co-culture of T_{FH} cells and GC B cells derived from WT mice, but not IL-17a/f$^{-/-}$ mice, supplemented with c-di-AMP resulted in the differentiation of GC B cells to plasma B cells. The need of IL-17 for this effect was confirmed by IL-17A supplementation, which resulted in a restored plasma B cell differentiation of cells derived from IL-17a/f$^{-/-}$ mice. The cytokine profile analysis of the supernatant derived from the IL-17A-supplemented co-culture of cells derived from IL-17a/f$^{-/-}$ mice revealed enhanced concentrations of IL-4 and IL-21 as compared to non-supplemented conditions. Besides other factors, IL-4 and IL-21 are known to be essential for the proliferation and survival of B cells in GCs [227, 228]. This suggests that IL-17-induced IL-21 and IL-4 secretion promotes the observed plasma B cell differentiation. Furthermore, a considerable degree of plasticity between T_{FH} cells and Th17 cells favored by the microenvironment of the Peyer's patches has been reported [229]. In this regard, it was reported that the conversion of Th17 cells into T_{FH} cells is needed for the generation of antigen-specific IgA responses in the gut mucosa [230]. In order to assess the extent of this plasticity upon treatment with c-di-AMP, experiments conducted in IL-17 fate-reporter mice should be included in future studies. IL-17 fate reporter (Il17a^{Cre}R26R^{eYFP}) mice enable to identify and visualize fate mapping of Th17cells *in vivo.* The fluorescent reporter would permanently label Il17Cre cells, thus allowing identification of cells that switched on the IL-17 program.This could provide crucial information regarding whether c-di-AMP-induced Th17 cells deviate towards a T_{FH} cell-like phenotype, thereby contributing to the observed NIBRG-14-specific IgA response.

The absence of IL-17 signaling further resulted in significantly lower pIgR expression levels on lung epithelial cells upon immunization with NIBRG-14 co-administered with c-di-AMP as compared to WT mice. This indicates a role of c-di-AMP-induced IL-17 in the induction of pIgR expression. The pIgR is an integral component of the airway and intestinal mucosal immunity that mediates the delivery of polymeric IgA and IgM to the apical surface of epithelial cells via transcytosis [73, 231]. It has been reported that adoptive transfer of polarized DO11.10 CD4$^+$ Th17 cells mediates the influx of CD19$^+$ B cells into the lungs resulting in elevated IgA levels in the BAL [187]. Furthermore, the i.n. administration of IL-17 promoted pIgR-mediated delivery of sIgA into the airway lumen, thus contributing to airway immunity [157, 232]. In addition, lower levels of pIgR and IgA have been reported in the fecal content of IL-17R$^{-/-}$ mice as compared to WT mice, resulting in severe colitis upon treatment with dextran sodium sulfate [158]. These

data support the crucial role of IL-17 for an efficient mucosal immunity mediated via pIgR. The analysis of the lung lavage cytokine profile showed an elevated concentration of IFNγ, TNFα and IL-17 in WT but not IL-17a/f$^{-/-}$ mice after immunization with NIBRG-14 co-administered with c-di-AMP. The expression level of pIgR is known to be regulated by a range of factors including IFNγ, TNFα and IL-4 [233]. Therefore, the obtained results strongly support the assumption that the c-di-AMP-induced IL-17 secretion mediates upregulation of pIgR expression on lung epithelial cells, supposedly via the activation of IFNγ and TNFα, thereby representing a potential mechanism contributing to the observed enhanced sIgA secretion.

The role of IL-17A during influenza virus infections remains controversial, since it has been reported as playing both pathogenic and protective roles [234-237]. Similar to these reports, higher weight loss and viral loads were observed in lungs of naïve WT mice as compared to naïve IL-17a/f$^{-/-}$ mice 5 days post infection with the H5N1 influenza strain. While WT mice eventually succumbed to infection, IL-17a/f$^{-/-}$ mice recovered their weight. In addition, an increase in the frequency of neutrophils and NK cell populations was observed in the lungs of infected WT mice. Th17 cells are known to have profound effects on neutrophil recruitment and activation through the release of IL-6, G-CSF, KC, MIP-2 by tissue epithelial and endothelial cells, thus contributing to increased inflammation during influenza infection [238]. Apart from their role in viral clearance, NK cells are also described to contribute to exacerbated pathology during influenza virus infection, as shown by NK cell depletion studies [239]. These findings suggest a direct correlation between the IL-17-neutrophil-NK cell network and immunopathology during influenza infection, resulting in the death of infected mice. However, further studies such as *in vitro* infection experiments and *in vivo* depletion studies need to be performed to support this hypothesis.

Upon challenge of immunized mice with a sub-lethal dose of the H5N1 influenza strain, no significant differences in weight loss post challenge were observed comparing WT and IL-17a/f$^{-/-}$ mice immunized with NIBRG-14 co-administered with c-di-AMP. Hence, c-di-AMP-induced NIBRG-14-specific responses seem to mediate protective immunity against influenza virus independently of the IL-17-mediated response. This finding contradicts previously described challenge studies using mucosal adjuvants such as CRX-601, a TLR4 agonist, and CT. In these experiments an exacerbated, Th17-dependent, morbidity of vaccinated mice was observed. This effect was shown to be dependent on an enhanced Th17-dependent neutrophil recruitment to the lung [160,

240]. However, c-di-AMP-primed NIBRG-14-specific Th17 cells seem not to be detrimental in the presented H5N1 influenza infection model.

The results presented here disclose specific key mechanisms responsible for c-di-AMP-induced Th17 differentiation as well as Th17-mediated antigen-specific immune responses. However, in order to get comprehensive insights into c-di-AMP-induced mechanisms impacting IL-17-secreting cells, several aspects still need to be addressed. One of these aspects includes the identification of factors responsible for a defective Th17 differentiation driven by IL-17a/f$^{-/-}$-derived BMDCs. In this context, an enhanced Th1 response was observed in immunized IL-17a/f$^{-/-}$ mice as compared to WT mice. Thus, a shift towards the secretion of Th1 driving cytokines by IL-17a/f$^{-/-}$-derived BMDCs might be the reason for the defective Th17 differentiation of co-cultured WT-derived CD4^{+} T cells. In order to confirm this hypothesis, *in vitro* studies using antibodies that block Th1 polarizing cytokine signaling, *e.g*. IL-12 and IL-2 could be performed. Furthermore, the assessment of signaling pathways contributing to the migration of c-di-AMP-stimulated plasma B cells from the lymph nodes to the lung as effector site should be addressed, since defective migration might contribute to hamper immune responses. The migration capacity can be addressed by performing migration assays using trans-well systems in the presence of different chemokines, such as CXCL12 and CXCL13. These chemokines are described to induce the migration of plasma cells expressing mucosal homing receptors such as CXCR10, CXCR9 or CXCR4 [241]. IL-17 has further been shown to contribute to CXCL12 – CXCR4 signaling, which has been demonstrated to be essential for the appropriate maturation of B cell follicles in *P. aeruginosa*-induced BALT formation [242]. Additionally, *C.albicans*-specific Th17 cells isolated from humans have been shown to express CXCL13, thus promoting B cell chemotaxis [243]. The suggested trans-well experiments would thus provide crucial information regarding the contribution of IL-17 induced chemokines which are responsible for the migration of plasma B cells from the lymph nodes to the lungs in the stimulation of local IgA responses. Another aspect that will need to be addressed is the stimulation of antigen-specific memory responses. Advanced multi-color flow cytometry panels can be used for the analysis of different memory cell populations and their effector functions to elucidate the effect of c-di-AMP-induced IL-17 responses on memory cell subpopulations. The resulting data could provide insights into the role of IL-17 signaling for the long-term maintenance of protective immune response. In addition, an adoptive transfer of c-di-AMP-induced Th17 cells into IL-17a/f$^{-/-}$ mice prior to viral challenge

represent a valid approach to address the importance of this Th17 subset for viral clearance upon challenge with the H5N1 influenza strain.

In conclusion, the results presented in this thesis reveal essential mechanisms mediated by c-di-AMP-induced Th17 cells and their importance for the generation of antigen-specific immunity. The findings draw attention to the need for a more thorough characterization of Th17-mediated immune responses. In contrast to what has been shown so far, the findings demonstrate that c-di-AMP-induced Th17 cells are not detrimental but facilitate effective immune responses that mediate protection against the sub-lethal H5N1 challenge. Therefore, the results depicted in this thesis highlight the potential of using Th17 inducing adjuvants such as c-di-AMP for the development of safe mucosal vaccines with the ability to promote effective local immunity against infectious agents.

7. Summary

Respiratory infections caused by influenza virus represent a major health problem worldwide causing annual epidemics leading to 250,000 to 500,000 deaths yearly. Vaccination has proven to be an effective tool in controlling and eradicating many viral infections but due to inadequate protection elicited by current vaccines foster the search for improved or new immune interventions. In this regard, highly accepted needle-free vaccination strategies are urgently needed. Among them, mucosal vaccines appeal as a very promising approach. Current use of subunit vaccines and purified antigens are often very poorly immunogenic when delivered by mucosal route. Therefore implementation of adjuvants represents a key approach to improve immunogenicity thereby improving vaccine efficacy. One of the striking features of mucosal vaccines is the induction of IL-17 responses since IL-17 secreting cells predominantly reside at the mucosal surfaces. Therefore, IL-17 secreting cells represent interesting targets for mucosal vaccination strategies. The role of IL-17 secreting cells in the fight against mucosa associated bacterial and fungal infections have been emphasized. However, their role in combating viral infections and their significance for mucosal vaccine design remains elusive. Bis-(3',5')-cyclic dimeric adenosine monophosphate (c-di-AMP), a potent IL-17 inducer, was investigated for its potential to induce IL-17-mediated antigen-specific immune responses. The c-di-AMP treated BMDCs derived from IL-17a/f$^{-/-}$ mice displayed reduced expression of activation markers MHC I and CD86, thereby suggesting a reduction in their ability to evoke effector immune response. Furthermore, *in vitro* blocking experiments suggested that IL-6 but not IL-23 secreted by c-di-AMP-primed BMDCs seems to be the crucial mediator for c-di-AMP-induced Th17 differentiation. The i.n. immunization with OVA or NIBRG-14 adjuvanted with c-di-AMP resulted in impaired Th2 responses and IgA concentrations, but enhanced Th1 response in mice lacking IL-17. In addition, in an influenza infection model the histological evaluation revealed that c-di-AMP induced IL-17 is required for the co-localization of T_{FH} cells and GC B cells, thus favoring the generation of plasma B cells. Further *in vitro* co-culture studies of T_{FH} cells and GC B cells obtained from mice lacking IL-17 showed abrogated plasma cell differentiation, which could be restored by supplementation of rIL-17A. In addition, elevated concentrations of IL-4, IL-6 and IL-10 detected following re-stimulation of splenic cells obtained from immunized WT mice, indicating a cytokine environment promoting IgA class-switch. In this regard, the absence of IL-17 signaling resulted in a significantly lower pIgR expression level on lung epithelial cells in mice immunized with the inactivated H5N1 NIBRG-14 strain co-

administered with c-di-AMP. This indicates a role of c-di-AMP induced IL-17 for the induction of pIgR and thus the delivery of polymeric IgA to the apical surface of epithelial cells. Furthermore, the analysis of the cytokine milieu in lung lavage samples derived from immunized WT mice showed an elevated concentration of IFNγ and TNFα, which are required for regulating pIgR expression. Taken together this data demonstrates that c-di-AMP-induced Th17-mediated mucosal immunity is regulated via two different mechanisms (i) increased production of high-affinity plasma B cells and (ii) enhanced expression of pIgR by lung epithelial cells which in turn favors sIgA export. Interestingly, upon influenza virus challenge with the H5N1 strain, mice immunized with NIBRG-14 and c-di-AMP displayed strong resistance to infection with no significant differences between WT and IL-17a/f$^{-/-}$ mice. Differences in the microbiota impacted c-di-AMP-induced IL-17 mediated antigen-specific Th1 and IgG responses, but showed no significant influence on the IgA responses. The findings presented in this thesis reveal mechanisms underlying c-di-AMP mediated Th17 cell differentiation as well as the impact of c-di-AMP triggered IL-17 responses on the generation of antigen-specific mucosal immune responses (Figure 49). A better understanding of the mechanisms involved in the induction of vaccine-induced IL-17 responses and their contribution towards the generation of antigen-specific immunity will substantially facilitate the rational design of novel mucosal vaccines against infectious diseases.

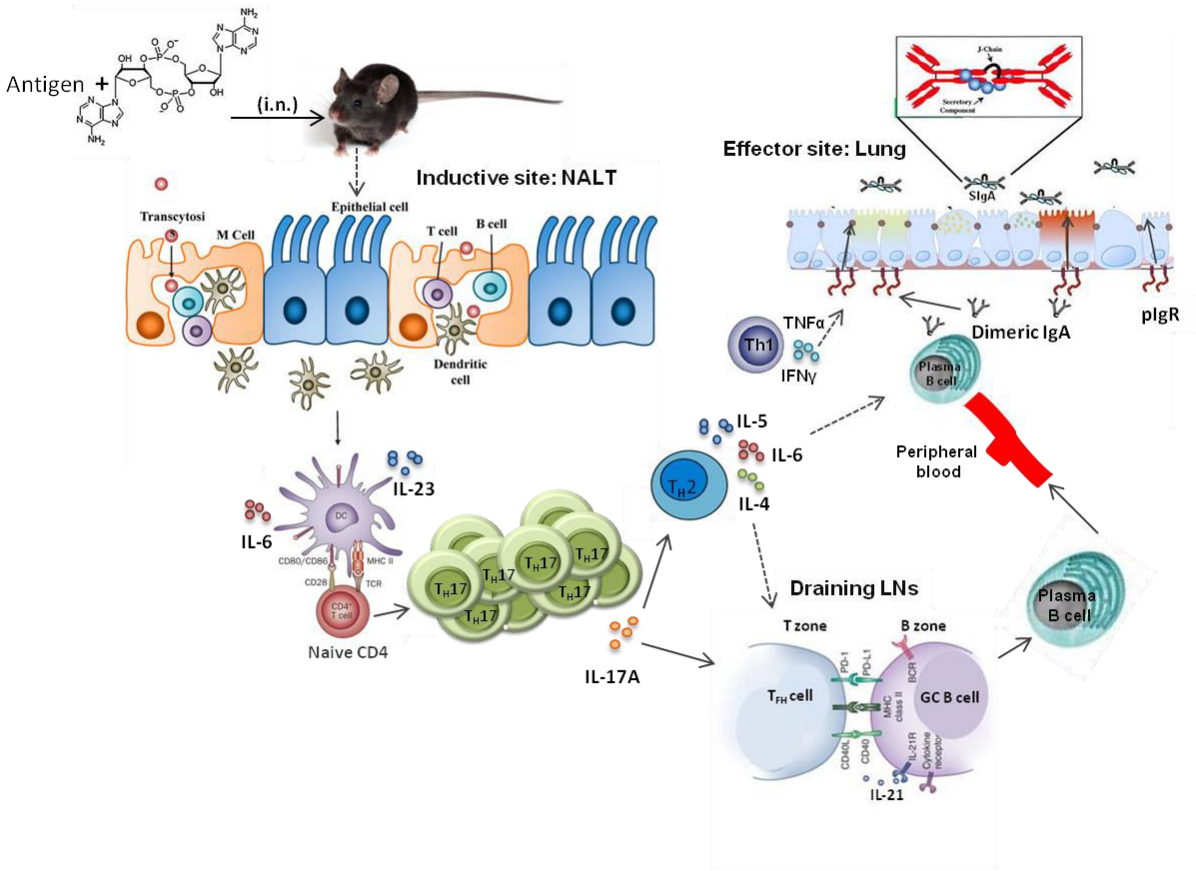

Figure 49: Schematic overview illustrating the potential mechanism of c-di-AMP-induced Th17-mediated responses contributing to the generation of antigen-specific mucosal IgA response post vaccination

Reference

1. Chaplin, D.D., *Overview of the immune response.* J Allergy Clin Immunol, 2010. 125(2 Suppl 2): p. S3-23.
2. McCullough, K.C. and Summerfield, A., *Basic concepts of immune response and defense development.* Ilar j, 2005. 46(3): p. 230-240.
3. Murphy K, T.P., Walport M, *Janeway's Immuno Biology 8th edition*. 2008: Garland Science.
4. Dranoff, G., *Cytokines in cancer pathogenesis and cancer therapy.* Nat Rev Cancer, 2004. 4(1): p. 11-22.
5. Sjoberg, A.P., Trouw, L.A., and Blom, A.M., *Complement activation and inhibition: a delicate balance.* Trends Immunol, 2009. 30(2): p. 83-90.
6. Unanue, E.R. and Askonas, B.A., *The immune response of mice to antigen in macrophages.* Immunology, 1968. 15(2): p. 287-296.
7. Guerra, K.P. and Delgado, R., *Homo-and heterodinuclear complexes of the tris(catecholamide) derivative of a tetraazamacrocycle with Fe3+, Cu2+ and Zn2+ metal ions.* Dalton Trans, 2008(4): p. 539-550.
8. Dutton, R.W., *In vitro studies of immunological responses of lymphoid cells.* Adv Immunol, 1967. 6: p. 253-336.
9. Wykes, M., et al., *Dendritic cells interact directly with naive B lymphocytes to transfer antigen and initiate class switching in a primary T-dependent response.* J Immunol, 1998. 161(3): p. 1313-1319.
10. Batista, F.D., Iber, D., and Neuberger, M.S., *B cells acquire antigen from target cells after synapse formation.* Nature, 2001. 411(6836): p. 489-494.
11. Underhill, D.M. and Ozinsky, A., *Toll-like receptors: key mediators of microbe detection.* Curr Opin Immunol, 2002. 14(1): p. 103-110.
12. Vasselon, T. and Detmers, P.A., *Toll receptors: a central element in innate immune responses.* Infect Immun, 2002. 70(3): p. 1033-1041.
13. Akira, S., Uematsu, S., and Takeuchi, O., *Pathogen recognition and innate immunity.* Cell, 2006. 124(4): p. 783-801.
14. Creagh, E.M. and O'Neill, L.A., *TLRs, NLRs and RLRs: a trinity of pathogen sensors that co-operate in innate immunity.* Trends Immunol, 2006. 27(8): p. 352-357.
15. Medzhitov, R., *Recognition of microorganisms and activation of the immune response.* Nature, 2007. 449(7164): p. 819-826.
16. Paul, William E., *Bridging Innate and Adaptive Immunity.* Cell. 147(6): p. 1212-1215.
17. Zuniga-Pflucker, J.C., *T-cell development made simple.* Nat Rev Immunol, 2004. 4(1): p. 67-72.
18. Broere, F., et al., *A2 T cell subsets and T cell-mediated immunity.* 2011: p. 15-27.

19. Lafferty, K.J. and Cunningham, A.J., *A new analysis of allogeneic interactions.* Aust J Exp Biol Med Sci, 1975. 53(1): p. 27-42.

20. Acuto, O. and Michel, F., *CD28-mediated co-stimulation: a quantitative support for TCR signalling.* Nat Rev Immunol, 2003. 3(12): p. 939-951.

21. McMaster, W.G., et al., *Inflammation, immunity, and hypertensive end-organ damage.* Circ Res, 2015. 116(6): p. 1022-1033.

22. Zhu, J., Yamane, H., and Paul, W.E., *Differentiation of Effector CD4 T Cell Populations.* Annu Rev Immunol, 2010. 28: p. 445-489.

23. Russ, B.E., et al., *T cell immunity as a tool for studying epigenetic regulation of cellular differentiation.* Front Genet, 2013. 4: p. 218.

24. Li, Z., Zhang, Y., and Sun, B., *Current understanding of Th2 cell differentiation and function.* Protein & Cell, 2011. 2(8): p. 604-611.

25. Song, X., Gao, H., and Qian, Y., *Th17 differentiation and their pro-inflammation function.* Adv Exp Med Biol, 2014. 841: p. 99-151.

26. Dong, C., *Differentiation and function of pro-inflammatory Th17 cells.* Microbes Infect, 2009. 11(5): p. 584-588.

27. Zhu, J., Yamane, H., and Paul, W.E., *Differentiation of effector CD4 T cell populations (*).* Annu Rev Immunol, 2010. 28: p. 445-489.

28. Crotty, S., *Follicular helper CD4 T cells (TFH).* Annu Rev Immunol, 2011. 29: p. 621-663.

29. Zhu, J., Yamane, H., and Paul, W.E., *Differentiation of Effector CD4 T Cell Populations.* Annu Rev Immunol, 2010. 28: p. 445-489.

30. Miceli, M.C. and Parnes, J.R., *The roles of CD4 and CD8 in T cell activation.* Semin Immunol, 1991. 3(3): p. 133-141.

31. Brincks, E.L., et al., *CD8 T cells utilize TNF-related apoptosis-inducing ligand (TRAIL) to control influenza virus infection.* Journal of immunology (Baltimore, Md. : 1950), 2008. 181(7): p. 4918-4925.

32. Volpe, E., et al., *Fas–Fas Ligand: Checkpoint of T Cell Functions in Multiple Sclerosis.* Front Immunol, 2016. 7: p. 382.

33. Masopust, D. and Schenkel, J.M., *The integration of T cell migration, differentiation and function.* Nat Rev Immunol, 2013. 13(5): p. 309-320.

34. Mueller, S.N., et al., *Memory T cell subsets, migration patterns, and tissue residence.* Annu Rev Immunol, 2013. 31: p. 137-161.

35. LeBien, T.W. and Tedder, T.F., *B lymphocytes: how they develop and function.* Blood, 2008. 112(5): p. 1570-1580.

36. Alberts B, J.A., Lewis J, *B cell and Antibodies*. Molecular Biology of the Cell. 4th edition. 2002, New York: Garland Science.

37. Cambier, J.C., Pleiman, C.M., and Clark, M.R., *Signal transduction by the B cell antigen receptor and its coreceptors.* Annu Rev Immunol, 1994. 12: p. 457-486.

38. Platts-Mills, T.A., *The role of immunoglobulin E in allergy and asthma.* Am J Respir Crit Care Med, 2001. 164(8 Pt 2): p. S1-5.

39. Galli, S.J. and Tsai, M., *IgE and mast cells in allergic disease.* Nat Med. 18(5): p. 693-704.

40. Halpern, M.S. and Koshland, M.E., *Novel Subunit in Secretory IgA.* Nature, 1970. 228(5278): p. 1276-1278.

41. Mestecky, J., Zikan, J., and Butler, W.T., *Immunoglobulin M and secretory immunoglobulin A: presence of a common polypeptide chain different from light chains.* Science, 1971. 171(3976): p. 1163-1165.

42. Johansen, F.E. and Kaetzel, C.S., *Regulation of the polymeric immunoglobulin receptor and IgA transport: new advances in environmental factors that stimulate pIgR expression and its role in mucosal immunity.* Mucosal Immunol, 2011. 4(6): p. 598-602.

43. Crotty, S., *A brief history of T cell help to B cells.* Nat Rev Immunol, 2015. 15(3): p. 185-189.

44. MacLennan, I.C., *Germinal centers.* Annu Rev Immunol, 1994. 12: p. 117-139.

45. De Silva, N.S. and Klein, U., *Dynamics of B cells in germinal centres.* Nat Rev Immunol, 2015. 15(3): p. 137-148.

46. Shinnakasu, R., et al., *Regulated selection of germinal-center cells into the memory B cell compartment.* Nat Immunol, 2016. 17(7): p. 861-869.

47. Pissani, F. and Streeck, H., *Emerging concepts on T follicular helper cell dynamics in HIV infection.* Trends Immunol, 2014. 35(6): p. 278-286.

48. Erkoreka, A., *Origins of the Spanish Influenza pandemic (1918–1920) and its relation to the First World War.* J Mol Genet Med, 2009. 3(2): p. 190-194.

49. *Global Health Observatory (GHO) data*. 2015.

50. KG Nicholson, R.W., AJ Hay *Structure of influenza A, B and C viruses*. Textbook of Influenza. 1998: Blackwell Science.

51. García-Sastre, A., *Influenza A virus subtype H1N2*. 2009: ScienceDirect.

52. *Influenza seasonal fact sheet*. 2014.

53. La Gruta, N.L., et al., *A question of self-preservation: immunopathology in influenza virus infection.* Immunol Cell Biol, 2007. 85(2): p. 85-92.

54. Taubenberger, J.K. and Morens, D.M., *The pathology of influenza virus infections.* Annu Rev Pathol, 2008. 3: p. 499-522.

55. Iwasaki, A. and Pillai, P.S., *Innate immunity to influenza virus infection.* Nat Rev Immunol, 2014. 14(5): p. 315-328.

56. Kreijtz, J.H., Fouchier, R.A., and Rimmelzwaan, G.F., *Immune responses to influenza virus infection.* Virus Res, 2011. 162(1-2): p. 19-30.

57. Narasaraju, T., et al., *Excessive Neutrophils and Neutrophil Extracellular Traps Contribute to Acute Lung Injury of Influenza Pneumonitis.* Am J Pathol, 2011. 179(1): p. 199-210.

58. Gregory, D.J. and Kobzik, L., *Influenza lung injury: mechanisms and therapeutic opportunities.* Am J Physiol Lung Cell Mol Physiol, 2015. 309(10): p. L1041-1046.

59. Braciale, T.J., Sun, J., and Kim, T.S., *Regulating the adaptive immune response to respiratory virus infection.* Nat Rev Immunol, 2012. 12(4): p. 295-305.

60. Yuki, Y. and Kiyono, H., *Mucosal vaccines: novel advances in technology and delivery.* Expert Rev Vaccines, 2009. 8(8): p. 1083-1097.

61. Coelingh, K.L., et al., *Development of live attenuated influenza vaccines against pandemic influenza strains.* Expert Rev Vaccines, 2014. 13(7): p. 855-871.

62. Cox, M.M.J., et al., *Safety, efficacy, and immunogenicity of Flublok in the prevention of seasonal influenza in adults.* Therapeutic Advances in Vaccines, 2015. 3(4): p. 97-108.

63. Houser, K. and Subbarao, K., *Influenza Vaccines: Challenges and Solutions.* Cell Host Microbe, 2015. 17(3): p. 295-300.

64. Lycke, N., *Recent progress in mucosal vaccine development: potential and limitations.* Nat Rev Immunol, 2012. 12(8): p. 592-605.

65. Yuki, Y. and Kiyono, H., *Mucosal vaccines: novel advances in technology and delivery.* Expert Review of Vaccines, 2009. 8(8): p. 1083-1097.

66. Riese, P., et al., *Intranasal formulations: promising strategy to deliver vaccines.* Expert Opin Drug Deliv, 2014. 11(10): p. 1619-1634.

67. Lamichhane, A., Azegamia, T., and Kiyonoa, H., *The mucosal immune system for vaccine development.* Vaccine, 2014. 32(49): p. 6711-6723.

68. Janeway CA, T.P., *The immune system in health and diseases 5th Edition*. Immunobiology. 2001, New York: Garland Science.

69. McGhee, J.R. and Fujihashi, K., *Inside the mucosal immune system.* PLoS Biol, 2012. 10(9): p. e1001397.

70. Parker, D. and Prince, A., *Innate Immunity in the Respiratory Epithelium.* Am J Respir Cell Mol Biol, 2011. 45(2): p. 189-201.

71. Martin, T.R. and Frevert, C.W., *Innate Immunity in the Lungs.* Proc Am Thorac Soc, 2005. 2(5): p. 403-411.

72. Grzela, K., Zagórska, W., and Grzela, T., *Mechanisms of the innate immunity in the respiratory system.* Central European Journal of Immunology, 2012. 3: p. 280-285.

73. Mantis, N.J., Rol, N., and Corthesy, B., *Secretory IgA's complex roles in immunity and mucosal homeostasis in the gut.* Mucosal Immunol, 2011. 4(6): p. 603-611.

74. Corthésy, B., *Multi-Faceted Functions of Secretory IgA at Mucosal Surfaces.* Front Immunol, 2013. 4.

75. Neutra, M.R. and Kozlowski, P.A., *Mucosal vaccines: the promise and the challenge.* Nat Rev Immunol, 2006. 6(2): p. 148-158.

76. Oster, G., et al., *Benefits and risks of live attenuated influenza vaccine in young children.* Am J Manag Care, 2010. 16(9): p. e235-244.

77. Birkhoff, M., Leitz, M., and Marx, D., *Advantages of Intranasal Vaccination and Considerations on Device Selection.* Indian J Pharm Sci, 2009. 71(6): p. 729-731.

78. Kiyono, H. and Fukuyama, S., *NALT- versus PEYER'S-patch-mediated mucosal immunity.* Nat Rev Immunol, 2004. 4(9): p. 699-710.

79. Wu, H.Y., Nguyen, H.H., and Russell, M.W., *Nasal lymphoid tissue (NALT) as a mucosal immune inductive site.* Scand J Immunol, 1997. 46(5): p. 506-513.

80. Chao, W.-W. and Lin, B.-F., *Isolation and identification of bioactive compounds in Andrographis paniculata (Chuanxinlian).* Chin Med, 2010. 5: p. 17-17.

81. Goodrich, M.E. and McGee, D.W., *Regulation of mucosal B cell immunoglobulin secretion by intestinal epithelial cell-derived cytokines.* Cytokine, 1998. 10(12): p. 948-955.

82. Kim, S.-H. and Jang, Y.-S., *The development of mucosal vaccines for both mucosal and systemic immune induction and the roles played by adjuvants.* Clinical and Experimental Vaccine Research, 2017. 6(1): p. 15-21.

83. Xu, Y., Yuen, P.W., and Lam, J.K., *Intranasal DNA Vaccine for Protection against Respiratory Infectious Diseases: The Delivery Perspectives.* Pharmaceutics, 2014. 6(3): p. 378-415.

84. Gray, D., *A role for antigen in the maintenance of immunological memory.* Nat Rev Immunol, 2002. 2(1): p. 60-65.

85. Azegami, T., Yuki, Y., and Kiyono, H., *Challenges in mucosal vaccines for the control of infectious diseases.* Int Immunol, 2014. 26(9): p. 517-528.

86. Rhee, J.H., Lee, S.E., and Kim, S.Y., *Mucosal vaccine adjuvants update.* Clin Exp Vaccine Res, 2012. 1(1): p. 50-63.

87. Shahiwala, A., Vyas, T.K., and Amiji, M.M., *Nanocarriers for systemic and mucosal vaccine delivery.* Recent Pat Drug Deliv Formul, 2007. 1(1): p. 1-9.

88. Zeng, L., *Mucosal adjuvants: Opportunities and challenges.* Human Vaccines & Immunotherapeutics, 2016. 12(9): p. 2456-2458.

89. Chen, W., et al., *Recent advances in the development of novel mucosal adjuvants and antigen delivery systems.* Hum Vaccin, 2010. 6(9).

90. Savelkoul, H.F., et al., *Choice and Design of Adjuvants for Parenteral and Mucosal Vaccines.* Vaccines (Basel), 2015. 3(1): p. 148-171.

91. Riese, P., et al., *Vaccine adjuvants: key tools for innovative vaccine design.* Curr Top Med Chem, 2013. 13(20): p. 2562-2580.

92. Rappuoli, R., et al., *Vaccines for the twenty-first century society.* Nat Rev Immunol, 2011. 11(12): p. 865-872.

93. Stevceva, L. and Ferrari, M.G., *Mucosal adjuvants.* Curr Pharm Des, 2005. 11(6): p. 801-811.

94. Mutsch, M., et al., *Use of the inactivated intranasal influenza vaccine and the risk of Bell's palsy in Switzerland.* N Engl J Med, 2004. 350(9): p. 896-903.

95. Maroof, A., et al., *Intranasal vaccination promotes detrimental Th17-mediated immunity against influenza infection.* PLoS Pathog, 2014. 10(1): p. e1003875.

96. Skrnjug, I., et al., *The mucosal adjuvant cyclic di-AMP exerts immune stimulatory effects on dendritic cells and macrophages.* PLoS One, 2014. 9(4): p. e95728.

97. Ebensen, T., et al., *Bis-(3',5')-cyclic dimeric adenosine monophosphate: strong Th1/Th2/Th17 promoting mucosal adjuvant.* Vaccine, 2011. 29(32): p. 5210-5220.

98. Ebensen, T., et al., *A Pegylated Derivative of -Galactosylceramide Exhibits Improved Biological Properties.* The Journal of Immunology, 2007. 179(4): p. 2065-2073.

99. Danilchanka, O. and Mekalanos, J.J., *Cyclic Dinucleotides and the Innate Immune Response.* Cell, 2013. 154(5): p. 962-970.

100. Danilchanka, O. and Mekalanos, John J., *Cyclic Dinucleotides and the Innate Immune Response.* Cell. 154(5): p. 962-970.

101. Chen, L.H., et al., *Cyclic di-GMP-dependent signaling pathways in the pathogenic Firmicute Listeria monocytogenes.* PLoS Pathog, 2014. 10(8): p. e1004301.

102. Hong, Y., et al., *Cyclic di-GMP mediates Mycobacterium tuberculosis dormancy and pathogenecity.* Tuberculosis (Edinb), 2013. 93(6): p. 625-634.

103. Tamayo, R., et al., *Role of cyclic Di-GMP during el tor biotype Vibrio cholerae infection: characterization of the in vivo-induced cyclic Di-GMP phosphodiesterase CdpA.* Infect Immun, 2008. 76(4): p. 1617-1627.

104. Corrigan, R.M., et al., *c-di-AMP is a new second messenger in Staphylococcus aureus with a role in controlling cell size and envelope stress.* PLoS Pathog, 2011. 7(9): p. e1002217.

105. Du, B., et al., *Functional analysis of c-di-AMP phosphodiesterase, GdpP, in Streptococcus suis serotype 2.* Microbiol Res, 2014. 169(9-10): p. 749-758.

106. Schaap, P., *CYCLIC DI-NUCLEOTIDE SIGNALLING ENTERS THE EUKARYOTE DOMAIN.* IUBMB life, 2013. 65(11): p. 897-903.

107. Burdette, D.L., et al., *STING is a direct innate immune sensor of cyclic di-GMP.* Nature, 2011. 478(7370): p. 515-518.

108. Sauer, J.D., et al., *The N-ethyl-N-nitrosourea-induced Goldenticket mouse mutant reveals an essential function of Sting in the in vivo interferon response to Listeria monocytogenes and cyclic dinucleotides.* Infect Immun, 2011. 79(2): p. 688-694.

109. Jin, L., et al., *MPYS is required for IFN response factor 3 activation and type I IFN production in the response of cultured phagocytes to bacterial second messengers cyclic-di-AMP and cyclic-di-GMP.* J Immunol, 2011. 187(5): p. 2595-2601.

110. Parvatiyar, K., et al., *The helicase DDX41 recognizes the bacterial secondary messengers cyclic di-GMP and cyclic di-AMP to activate a type I interferon immune response.* Nat Immunol, 2012. 13(12): p. 1155-1161.

111. Lolicato, M., et al., *Cyclic dinucleotides bind the C-linker of HCN4 to control channel cAMP responsiveness.* Nat Chem Biol, 2014. 10(6): p. 457-462.

112. Libanova, R., Becker, P.D., and Guzman, C.A., *Cyclic di-nucleotides: new era for small molecules as adjuvants.* Microb Biotechnol, 2012. 5(2): p. 168-176.

113. Karaolis, D.K., et al., *Bacterial c-di-GMP is an immunostimulatory molecule.* J Immunol, 2007. 178(4): p. 2171-2181.

114. Ebensen, T., et al., *The bacterial second messenger cdiGMP exhibits promising activity as a mucosal adjuvant.* Clin Vaccine Immunol, 2007. 14(8): p. 952-958.

115. Libanova, R., et al., *The member of the cyclic di-nucleotide family bis-(3', 5')-cyclic dimeric inosine monophosphate exerts potent activity as mucosal adjuvant.* Vaccine, 2010. 28(10): p. 2249-2258.

116. Skrnjug, I., Guzman, C.A., and Rueckert, C., *Cyclic GMP-AMP displays mucosal adjuvant activity in mice.* PLoS One, 2014. 9(10): p. e110150.

117. Sanchez, M.V., et al., *Intranasal delivery of influenza rNP adjuvanted with c-di-AMP induces strong humoral and cellular immune responses and provides protection against virus challenge.* PLoS One, 2014. 9(8): p. e104824.

118. Gaffen, S.L., *Structure and signalling in the IL-17 receptor superfamily.* Nat Rev Immunol, 2009. 9(8): p. 556.

119. Jin, W. and Dong, C., *IL-17 cytokines in immunity and inflammation.* Emerg Microbes Infect, 2013. 2(9): p. e60-.

120. Pappu, R., Rutz, S., and Ouyang, W., *Regulation of epithelial immunity by IL-17 family cytokines.* Trends Immunol, 2012. 33(7): p. 343-349.

121. Cua, D.J. and Tato, C.M., *Innate IL-17-producing cells: the sentinels of the immune system.* Nat Rev Immunol, 2010. 10(7): p. 479-489.

122. Zheng, Y., et al., *Interleukin-22 mediates early host defense against attaching and effacing bacterial pathogens.* Nat Med, 2008. 14(3): p. 282-289.

123. Cash, H.L., et al., *Symbiotic bacteria direct expression of an intestinal bactericidal lectin.* Science, 2006. 313(5790): p. 1126-1130.

124. Aujla, S.J., et al., *IL-22 mediates mucosal host defense against Gram-negative bacterial pneumonia.* Nat Med, 2008. 14(3): p. 275-281.

125. Chan, Y.R., et al., *Lipocalin 2 is required for pulmonary host defense against Klebsiella infection.* J Immunol, 2009. 182(8): p. 4947-4956.

126. Happel, K.I., et al., *Cutting edge: roles of Toll-like receptor 4 and IL-23 in IL-17 expression in response to Klebsiella pneumoniae infection.* J Immunol, 2003. 170(9): p. 4432-4436.

127. Curtis, M.M. and Way, S.S., *Interleukin-17 in host defence against bacterial, mycobacterial and fungal pathogens.* Immunology, 2009. 126(2): p. 177-185.

128. Iwakura, Y., et al., *The roles of IL-17A in inflammatory immune responses and host defense against pathogens.* Immunol Rev, 2008. 226: p. 57-79.

129. Kolls, J.K. and Linden, A., *Interleukin-17 family members and inflammation.* Immunity, 2004. 21(4): p. 467-476.

130. Korn, T., et al., *IL-17 and Th17 Cells.* Annu Rev Immunol, 2009. 27: p. 485-517.

131. Bermejo, D.A., et al., *Trypanosoma cruzi trans-sialidase initiates an ROR-γt–AHR-independent program leading to IL-17 production by activated B cells.* Nat Immunol, 2013. 14(5): p. 514-522.

132. Zuniga, L.A., et al., *Th17 cell development: from the cradle to the grave.* Immunol Rev, 2013. 252(1): p. 78-88.

133. Harrington, L.E., et al., *Interleukin 17-producing CD4+ effector T cells develop via a lineage distinct from the T helper type 1 and 2 lineages.* Nat Immunol, 2005. 6(11): p. 1123-1132.

134. Dong, C., *TH17 cells in development: an updated view of their molecular identity and genetic programming.* Nat Rev Immunol, 2008. 8(5): p. 337-348.

135. Ito, Y., et al., *Gamma/delta T cells are the predominant source of interleukin-17 in affected joints in collagen-induced arthritis, but not in rheumatoid arthritis.* Arthritis Rheum, 2009. 60(8): p. 2294-2303.

136. Ouyang, W., Kolls, J.K., and Zheng, Y., *The Biological Functions of T Helper 17 Cell Effector Cytokines in Inflammation.* Immunity, 2008. 28(4): p. 454-467.

137. Hou, W., Kang, H.S., and Kim, B.S., *Th17 cells enhance viral persistence and inhibit T cell cytotoxicity in a model of chronic virus infection.* The Journal of Experimental Medicine, 2009. 206(2): p. 313-328.

138. Lock, C., et al., *Gene-microarray analysis of multiple sclerosis lesions yields new targets validated in autoimmune encephalomyelitis.* Nat Med, 2002. 8(5): p. 500-508.

139. Komiyama, Y., et al., *IL-17 Plays an Important Role in the Development of Experimental Autoimmune Encephalomyelitis.* The Journal of Immunology, 2006. 177(1): p. 566-573.

140. Tzartos, J.S., et al., *Interleukin-17 production in central nervous system-infiltrating T cells and glial cells is associated with active disease in multiple sclerosis.* Am J Pathol, 2008. 172(1): p. 146-155.

141. Lubberts, E., *The role of IL-17 and family members in the pathogenesis of arthritis.* Curr Opin Investig Drugs, 2003. 4(5): p. 572-577.

142. Hsu, H.C., et al., *Interleukin 17-producing T helper cells and interleukin 17 orchestrate autoreactive germinal center development in autoimmune BXD2 mice.* Nat Immunol, 2008. 9(2): p. 166-175.

143. Gordon, K.B., et al., *Phase 3 Trials of Ixekizumab in Moderate-to-Severe Plaque Psoriasis.* N Engl J Med, 2016. 375(4): p. 345-356.

144. Leonardi, C., et al., *Anti-interleukin-17 monoclonal antibody ixekizumab in chronic plaque psoriasis.* N Engl J Med, 2012. 366(13): p. 1190-1199.

145. Genovese, M.C., et al., *LY2439821, a humanized anti-interleukin-17 monoclonal antibody, in the treatment of patients with rheumatoid arthritis: A phase I randomized, double-blind, placebo-controlled, proof-of-concept study.* Arthritis Rheum, 2010. 62(4): p. 929-939.

146. Wei, M. and Duan, D., *Efficacy and safety of monoclonal antibodies targeting interleukin-17 pathway for inflammatory arthritis: a meta-analysis of randomized controlled clinical trials.* Drug Des Devel Ther, 2016. 10: p. 2771-2777.

147. Knier, B., Hemmer, B., and Korn, T., *Novel monoclonal antibodies for therapy of multiple sclerosis.* Expert Opin Biol Ther, 2014. 14(4): p. 503-513.

148. Luchtman, D.W., et al., *IL-17 and related cytokines involved in the pathology and immunotherapy of multiple sclerosis: Current and future developments.* Cytokine Growth Factor Rev, 2014. 25(4): p. 403-413.

149. Chen, K., et al., *Th17 cells mediate clade-specific, serotype-independent mucosal immunity.* Immunity, 2011. 35(6): p. 997-1009.

150. Conti, H.R., et al., *Th17 cells and IL-17 receptor signaling are essential for mucosal host defense against oral candidiasis.* J Exp Med, 2009. 206(2): p. 299-311.

151. Zhang, Z., Clarke, T.B., and Weiser, J.N., *Cellular effectors mediating Th17-dependent clearance of pneumococcal colonization in mice.* J Clin Invest, 2009. 119(7): p. 1899-1909.

152. Wu, W., et al., *Th17-stimulating protein vaccines confer protection against Pseudomonas aeruginosa pneumonia.* Am J Respir Crit Care Med, 2012. 186(5): p. 420-427.

153. Khader, S.A., et al., *IL-23 and IL-17 in the establishment of protective pulmonary CD4+ T cell responses after vaccination and during Mycobacterium tuberculosis challenge.* Nat Immunol, 2007. 8(4): p. 369-377.

154. Priebe, G.P., et al., *IL-17 is a critical component of vaccine-induced protection against lung infection by lipopolysaccharide-heterologous strains of Pseudomonas aeruginosa.* J Immunol, 2008. 181(7): p. 4965-4975.

155. Doreau, A., et al., *Interleukin 17 acts in synergy with B cell-activating factor to influence B cell biology and the pathophysiology of systemic lupus erythematosus.* Nat Immunol, 2009. 10(7): p. 778-785.

156. Mitsdoerffer, M., et al., *Proinflammatory T helper type 17 cells are effective B-cell helpers.* Proc Natl Acad Sci U S A, 2010. 107(32): p. 14292-14297.

157. Jaffar, Z., et al., *Cutting edge: lung mucosal Th17-mediated responses induce polymeric Ig receptor expression by the airway epithelium and elevate secretory IgA levels.* J Immunol, 2009. 182(8): p. 4507-4511.

158. Cao, A.T., et al., *Th17 cells upregulate polymeric Ig receptor and intestinal IgA and contribute to intestinal homeostasis.* J Immunol, 2012. 189(9): p. 4666-4673.

159. McKinstry, K.K., et al., *IL-10 deficiency unleashes an influenza-specific Th17 response and enhances survival against high-dose challenge.* J Immunol, 2009. 182(12): p. 7353-7363.

160. Gopal, R., et al., *Mucosal Pre-Exposure to Th17-Inducing Adjuvants Exacerbates Pathology after Influenza Infection.* Am J Pathol, 2014. 184(1): p. 55-63.

161. Haas, J.D., et al., *Development of interleukin-17-producing gammadelta T cells is restricted to a functional embryonic wave.* Immunity, 2012. 37(1): p. 48-59.

162. Ozaras, R., et al., *N-acetylcysteine attenuates alcohol-induced oxidative stress in the rat.* World J Gastroenterol, 2003. 9(1): p. 125-128.

163. Zygmunt, B.M., Weissmann, S.F., and Guzman, C.A., *NKT Cell Stimulation with α-Galactosylceramide Results in a Block of Th17 Differentiation after Intranasal Immunization in Mice.* PLoS One, 2012. 7(1): p. e30382.

164. Bedoya, S.K., et al., *Isolation and th17 differentiation of naive CD4 T lymphocytes.* J Vis Exp, 2013(79): p. e50765.

165. Kimura, A. and Kishimoto, T., *IL-6: regulator of Treg/Th17 balance.* Eur J Immunol, 2010. 40(7): p. 1830-1835.

166. Zhou, L., et al., *IL-6 programs TH-17 cell differentiation by promoting sequential engagement of the IL-21 and IL-23 pathways.* Nat Immunol, 2007. 8(9): p. 967-974.

167. Stritesky, G.L., Yeh, N., and Kaplan, M.H., *IL-23 Promotes Maintenance but Not Commitment to the Th17 Lineage.* The Journal of Immunology, 2008. 181(9): p. 5948-5955.

168. McGeachy, M.J. and Cua, D.J., *Th17 cell differentiation: the long and winding road.* Immunity, 2008. 28(4): p. 445-453.

169. Moon, B.g., et al., *The Role of IL-5 for Mature B-1 Cells in Homeostatic Proliferation, Cell Survival, and Ig Production.* The Journal of Immunology, 2004. 172(10): p. 6020-6029.

170. Vinuesa, C.G., et al., *Follicular B helper T cells in antibody responses and autoimmunity.* Nat Rev Immunol, 2005. 5(11): p. 853-865.

171. Ma, C.S., et al., *The origins, function, and regulation of T follicular helper cells.* The Journal of Experimental Medicine, 2012. 209(7): p. 1241-1253.

172. Borsutzky, S., et al., *The mucosal adjuvant macrophage-activating lipopeptide-2 directly stimulates B lymphocytes via the TLR2 without the need of accessory cells.* J Immunol, 2005. 174(10): p. 6308-6313.

173. Valdez, Y., Brown, E.M., and Finlay, B.B., *Influence of the microbiota on vaccine effectiveness.* Trends in Immunology. 35(11): p. 526-537.

174. Farkas, A.M., et al., *Induction of Th17 cells by segmented filamentous bacteria in the murine intestine.* J Immunol Methods, 2015. 421: p. 104-111.

175. Yang, Y., et al., *Focused specificity of intestinal TH17 cells towards commensal bacterial antigens.* Nature, 2014. 510(7503): p. 152-156.

176. Erkoreka, A., *Origins of the Spanish Influenza pandemic (1918–1920) and its relation to the First World War.* Journal of Molecular and Genetic Medicine : An International Journal of Biomedical Research, 2009. 3(2): p. 190-194.

177. Mantis, N.J., Rol, N., and Corthésy, B., *Secretory IgA's Complex Roles in Immunity and Mucosal Homeostasis in the Gut.* Mucosal Immunol, 2011. 4(6): p. 603-611.

178. Corthesy, B., *Multi-Faceted Functions of Secretory IgA at Mucosal Surfaces.* Frontiers in Immunology, 2013. 4(185).

179. Brandtzaeg, P., *Secretory IgA: Designed for Anti-Microbial Defense.* Frontiers in Immunology, 2013. 4(222).

180. Johansen, F.-E. and Brandtzaeg, P., *Transcriptional regulation of the mucosal IgA system.* Trends in Immunology. 25(3): p. 150-157.

181. Pilette, C., et al., *Lung mucosal immunity: immunoglobulin-A revisited.* European Respiratory Journal, 2001. 18(3): p. 571-588.

182. Cerutti, A., *The regulation of IgA class switching.* Nat Rev Immunol, 2008. 8(6): p. 421-434.

183. Kaetzel, C.S., *The Polymeric Immunoglobulin Receptor.* Mucosal Immunity, 2013.

184. Jaffar, Z., et al., *Cutting Edge: Lung mucosal Th17-mediated responses induce polymeric immunoglobulin receptor expression by the airway epithelium and elevate secretory IgA levels.* J Immunol, 2009. 182(8): p. 4507-4511.

185. Conti, H.R. and Gaffen, S.L., *IL-17-mediated immunity to the opportunistic fungal pathogen Candida albicans.* Journal of immunology (Baltimore, Md. : 1950), 2015. 195(3): p. 780-788.

186. Curtis, M.M. and Way, S.S., *Interleukin-17 in host defence against bacterial, mycobacterial and fungal pathogens.* Immunology, 2009. 126(2): p. 177-185.

187. Jaffar, Z., et al., *Cutting Edge: Lung mucosal Th17-mediated responses induce polymeric immunoglobulin receptor expression by the airway epithelium and elevate secretory IgA levels.* Journal of immunology (Baltimore, Md. : 1950), 2009. 182(8): p. 4507-4511.

188. Cao, A.T., et al., *Th17 cells upregulate polymeric Ig receptor and intestinal IgA and contribute to intestinal homeostasis.* Journal of immunology (Baltimore, Md. : 1950), 2012. 189(9): p. 4666-4673.

189. Kumar, P., Chen, K., and Kolls, J.K., *Th17 cell based vaccines in mucosal immunity.* Curr Opin Immunol, 2013. 25(3): p. 373-380.

190. Yuan, J., et al., *Th17 cells facilitate the humoral immune response in patients with acute viral myocarditis.* J Clin Immunol, 2010. 30(2): p. 226-234.

191. Barker, J.R., et al., *STING-dependent recognition of cyclic di-AMP mediates type I interferon responses during Chlamydia trachomatis infection.* MBio, 2013. 4(3): p. e00018-00013.

192. Bowie, A.G., *Innate sensing of bacterial cyclic dinucleotides: more than just STING.* Nat Immunol, 2012. 13(12): p. 1137-1139.

193. Blaauboer, S.M., Gabrielle, V.D., and Jin, L., *MPYS/STING-mediated TNF-alpha, not type I IFN, is essential for the mucosal adjuvant activity of (3'-5')-cyclic-di-guanosine-monophosphate in vivo.* J Immunol, 2014. 192(1): p. 492-502.

194. Bedoya, S.K., et al., *Isolation and Th17 Differentiation of Naïve CD4 T Lymphocytes.* Journal of Visualized Experiments : JoVE, 2013(79): p. 50765.

195. Sekiya, T. and Yoshimura, A., *In Vitro Th Differentiation Protocol.* Methods Mol Biol, 2016. 1344: p. 183-191.

196. Zheng, S.G., *Regulatory T cells vs Th17: differentiation of Th17 versus Treg, are the mutually exclusive?* American journal of clinical and experimental immunology, 2013. 2(1): p. 94-106.

197. Tanaka, T., Narazaki, M., and Kishimoto, T., *IL-6 in Inflammation, Immunity, and Disease.* Cold Spring Harbor Perspectives in Biology, 2014. 6(10): p. a016295.

198. Korn, T., et al., *IL-6 controls Th17 immunity in vivo by inhibiting the conversion of conventional T cells into Foxp3+ regulatory T cells.* Proc Natl Acad Sci U S A, 2008. 105(47): p. 18460-18465.

199. Stockinger, B. and Veldhoen, M., *Differentiation and function of Th17 T cells.* Curr Opin Immunol, 2007. 19(3): p. 281-286.

200. Veldhoen, M., et al., *TGFbeta in the context of an inflammatory cytokine milieu supports de novo differentiation of IL-17-producing T cells.* Immunity, 2006. 24(2): p. 179-189.

201. Stritesky, G.L., Yeh, N., and Kaplan, M.H., *IL-23 promotes maintenance but not commitment to the Th17 lineage.* Journal of immunology (Baltimore, Md. : 1950), 2008. 181(9): p. 5948-5955.

202. Zelante, T., et al., *IL-23 and the Th17 pathway promote inflammation and impair antifungal immune resistance.* Eur J Immunol, 2007. 37(10): p. 2695-2706.

203. Awasthi, A. and Kuchroo, V.K., *IL-17A directly inhibits TH1 cells and thereby suppresses development of intestinal inflammation.* Nat Immunol, 2009. 10(6): p. 568-570.

204. Huang, H., et al., *CD4(+) Th1 cells promote CD8(+) Tc1 cell survival, memory response, tumor localization and therapy by targeted delivery of interleukin 2 via acquired pMHC I complexes.* Immunology, 2007. 120(2): p. 148-159.

205. Ekkens, M.J., et al., *Th1 and Th2 Cells Help CD8 T-Cell Responses.* Infection and Immunity, 2007. 75(5): p. 2291-2296.

206. Mitsdoerffer, M., et al., *Proinflammatory T helper type 17 cells are effective B-cell helpers.* Proceedings of the National Academy of Sciences, 2010. 107(32): p. 14292-14297.

207. Corthésy, B., *Roundtrip Ticket for Secretory IgA: Role in Mucosal Homeostasis?* The Journal of Immunology, 2007. 178(1): p. 27-32.

208. Lamm, M.E., *The IgA mucosal immune system.* Am J Kidney Dis, 1988. 12(5): p. 384-387.

209. Takatsu, K., *Cytokines involved in B-cell differentiation and their sites of action.* Proc Soc Exp Biol Med, 1997. 215(2): p. 121-133.

210. Harriman, G.R., et al., *The role of IL-5 in IgA B cell differentiation.* J Immunol, 1988. 140(9): p. 3033-3039.

211. Andoh, A., et al., *Interleukin (IL)-4 and IL-17 synergistically stimulate IL-6 secretion in human colonic myofibroblasts.* Int J Mol Med, 2002. 10(5): p. 631-634.

212. Gaboriau-Routhiau, V., et al., *The Key Role of Segmented Filamentous Bacteria in the Coordinated Maturation of Gut Helper T Cell Responses.* Immunity. 31(4): p. 677-689.

213. Minton, K., *Microbiota: A 'natural' vaccine adjuvant.* Nat Rev Immunol, 2014. 14(10): p. 650-651.

214. Umesaki, Y., et al., *Differential roles of segmented filamentous bacteria and clostridia in development of the intestinal immune system.* Infect Immun, 1999. 67(7): p. 3504-3511.

215. Klaasen, H.L., et al., *Apathogenic, intestinal, segmented, filamentous bacteria stimulate the mucosal immune system of mice.* Infect Immun, 1993. 61(1): p. 303-306.

216. Talham, G.L., et al., *Segmented filamentous bacteria are potent stimuli of a physiologically normal state of the murine gut mucosal immune system.* Infect Immun, 1999. 67(4): p. 1992-2000.

217. Ivanov, II, et al., *Induction of intestinal Th17 cells by segmented filamentous bacteria.* Cell, 2009. 139(3): p. 485-498.

218. Gaboriau-Routhiau, V., et al., *The key role of segmented filamentous bacteria in the coordinated maturation of gut helper T cell responses.* Immunity, 2009. 31(4): p. 677-689.

219. Huber, V.C., et al., *Distinct contributions of vaccine-induced immunoglobulin G1 (IgG1) and IgG2a antibodies to protective immunity against influenza.* Clin Vaccine Immunol, 2006. 13(9): p. 981-990.

220. Weinberg, A., et al., *Anti-Influenza Serum and Mucosal Antibody Responses after Administration of Live Attenuated or Inactivated Influenza Vaccines to HIV-Infected Children.* Journal of Acquired Immune Deficiency Syndromes (1999), 2010. 55(2): p. 189-196.

221. Christensen, D., et al., *Vaccine-induced Th17 cells are established as resident memory cells in the lung and promote local IgA responses.* Mucosal Immunol, 2017. 10(1): p. 260-270.

222. Muramatsu, M., et al., *Comparison of Antiviral Activity between IgA and IgG Specific to Influenza Virus Hemagglutinin: Increased Potential of IgA for Heterosubtypic Immunity.* PLOS ONE, 2014. 9(1): p. e85582.

223. van Riet, E., et al., *Mucosal IgA responses in influenza virus infections; thoughts for vaccine design.* Vaccine, 2012. 30(40): p. 5893-5900.

224. Brandtzaeg, P., et al., *The B-cell system of human mucosae and exocrine glands.* Immunol Rev, 1999. 171: p. 45-87.

225. McIntyre, T.M., Kehry, M.R., and Snapper, C.M., *Novel in vitro model for high-rate IgA class switching.* J Immunol, 1995. 154(7): p. 3156-3161.

226. Ding, Y., et al., *IL-17-induced Rgs16 expression is essential for follicular T helper cell localization in the germinal centers of autoimmune BXD2 mice (123.44).* The Journal of Immunology, 2012. 188(1 Supplement): p. 123.144-123.144.

227. Crotty, S., *Follicular Helper CD4 T Cells (TFH).* Annual Review of Immunology, 2011. 29(1): p. 621-663.

228. Linterman, M.A., et al., *IL-21 acts directly on B cells to regulate Bcl-6 expression and germinal center responses.* The Journal of Experimental Medicine, 2010. 207(2): p. 353-363.

229. Hirota, K., et al., *Plasticity of Th17 cells in Peyer's patches is responsible for the induction of T cell-dependent IgA responses.* Nat Immunol, 2013. 14(4): p. 372-379.

230. Milpied, P.J. and McHeyzer-Williams, M.G., *High-affinity IgA needs TH17 cell functional plasticity.* Nat Immunol, 2013. 14(4): p. 313-315.

231. Corthésy, B., *Multi-Faceted Functions of Secretory IgA at Mucosal Surfaces.* Frontiers in Immunology, 2013. 4: p. 185.

232. Jaffar, Z., et al., *Antigen-specific Treg regulate Th17-mediated lung neutrophilic inflammation, B-cell recruitment and polymeric IgA and IgM levels in the airways.* Eur J Immunol, 2009. 39(12): p. 3307-3314.

233. Johansen, F.-E. and Kaetzel, C., *Regulation of the polymeric immunoglobulin receptor and IgA transport: New advances in environmental factors that stimulate pIgR expression and its role in mucosal immunity.* Mucosal Immunol, 2011. 4(6): p. 598-602.

234. Crowe, C.R., et al., *Critical role of IL-17RA in immunopathology of influenza infection.* J Immunol, 2009. 183(8): p. 5301-5310.

235. Li, C., et al., *IL-17 response mediates acute lung injury induced by the 2009 Pandemic Influenza A (H1N1) Virus.* Cell Res, 2012. 22(3): p. 528-538.

236. Hamada, H., et al., *Tc17, a Unique Subset of CD8 T Cells That Can Protect against Lethal Influenza Challenge.* The Journal of Immunology, 2009. 182(6): p. 3469-3481.

237. McKinstry, K.K., et al., *IL-10 Deficiency Unleashes an Influenza-Specific Th17 Response and Enhances Survival against High-Dose Challenge.* The Journal of Immunology, 2009. 182(12): p. 7353-7363.

238. Kimizuka, Y., et al., *Roles of Interleukin-17 in an Experimental Legionella pneumophila Pneumonia Model.* Infect Immun, 2012. 80(3): p. 1121-1127.

239. Zhou, G., Juang, S.W., and Kane, K.P., *NK cells exacerbate the pathology of influenza virus infection in mice.* Eur J Immunol, 2013. 43(4): p. 929-938.

240. Subbarao, K., et al., *Intranasal Vaccination Promotes Detrimental Th17-Mediated Immunity against Influenza Infection.* PLoS Pathogens, 2014. 10(1): p. e1003875.

241. Kunkel, E.J. and Butcher, E.C., *Plasma-cell homing.* Nat Rev Immunol, 2003. 3(10): p. 822-829.

242. Fleige, H., et al., *IL-17-induced CXCL12 recruits B cells and induces follicle formation in BALT in the absence of differentiated FDCs.* J Exp Med, 2014. 211(4): p. 643-651.

243. Takagi, R., et al., *B cell chemoattractant CXCL13 is preferentially expressed by human Th17 cell clones.* J Immunol, 2008. 181(1): p. 186-189.